Development of a Customised, Self Powered Data Logger for Monitoring Farm Fence Energizers

A thesis
submitted in partial fulfilment
of the requirements for the Degree
of
Masters of Engineering
at the
University of Waikato
By

Elliot Gabriel Jethro Finn

THE UNIVERSITY OF
WAIKATO
Te Whare Wānanga o Waikato

ABSTRACT

For gathering information on the performance of energizer products in the field, Gallagher Group Limited had a well out-dated data-logger which periodically monitored the voltage of the fence and transmitted the data back to base over a GSM network. However the existing data-logger had very limited capability and a new one was needed that could monitor the environment inside and around the energizer, and hopefully provide some information on why an energiser might be failing.

The ideal data-logger was self powered, could last years in the field without needing to be serviced, and could collect data on the energizer without affecting it in any way. It would also collect data on as many environmental parameters as possible, such as temperature, humidity, ambient light level, lightening strikes and pressure. Ideally it would also be able to monitor the energizer voltage using a contactless measuring system.

The data-logger was designed for Gallagher Animal Management Systems, the part of Gallagher Group Limited that specialises in farming equipment. The design project arose from the need for a data-logger that could monitor both the fence voltage and the environment around the fence, so that a critical explanation of why an energizer failed in the field could be found, leading to better product design in the future. It was jointly funded by Gallagher Group Limited and the Foundation of Research Science and Technology (FoRST).

ACKNOWLEDGEMENTS

I would like to dedicate this Thesis to my parents Greg and Penny, for the love and support they have given me for all 23 years of my life, both mentally and financially, and the excellent job they both did in raising me. Both my parents are very understanding and have backed all the decisions I have made so far in my life, especially going to university to study Electronic Engineering. Thank you both, a lot.

There are several other parties I would like to thank for the research. Firstly, my academic supervisor, Nihal Kularatna, who helped me through my research at every step, giving me fuel for thought all the way through and helping me stay interested in the project. He was a great influence in finding and choosing this project for my Masters of Engineering.

Secondly I would like to thank my industry supervisor, Hayden Goble, and the team at Gallagher Group Limited, for their continued support during the project, giving me ideas along the way and helping me find things that I have needed to achieve the final project outcome. Without their support I could not have come so far in project to this date.

I would also like the thank both Gallagher Group Limited and the Foundation of Research Science and Technology for making the project possible through the project funding and living expenses throughout the year, without which I would never have been able to complete the project.

Lastly, I would like to thank my wife, Alona, for her love, care and support over the last year, our first year as a married couple, throughout which she was also completing her Masters of Science at the University of Waikato. She helped me research and write this thesis, even while needing to complete her own, and was extremely understanding and helpful throughout the whole time I was doing my project. Thank you, and I love you.

TABLE OF CONTENTS

LIST OF TABLES

LIST OF FIGURES

CHAPTER ONE: INTRODUCTION

1.1 Scope

The project to develop the farm fence energizer monitoring system was undertaken in conjunction with Gallagher Group Limited, who design and produce animal management systems and security management systems, and under various other daughter companies produce tooling, custom engineering products and injection moulded plastics, and contract manufacturing to a broad range of industries.

The project was partially funded by a Technology in Industry Fellowship (TIF) funding from the Foundation of Research, Science and Technology (FoRST), a Crown Agent formed in 1990 to support and fund the development of both individuals and companies doing research towards the good of the public and the environment in New Zealand.

Gallagher Group Limited are constantly designing new and improving existing products and systems. Previously they have had very little they can use in the way of testing their latest developments, and needed a new way to properly test their products in the environments they would be used in. The goal of the project was to develop a self powered data-logger which could monitor as many environmental factors as possible, and report them back to base while remaining in the field logging data. Because there was currently nothing similar to this data logger on the market, there was high potential for what it could be used for.

1.2 Company Overview

The first animal management system, developed by Bill Gallagher in the early 1930's, as stated in the website (Gallagher Group Ltd, 2007), was not to contain animals in a paddock, but to break a horse's habit of using the family car as a scratching post. In 1937, Bill Gallagher read that people in America were using electrified wire to contain stock; which lead him to develop the first Gallagher electric fence.

Figure 1.1: Photo of an old Gallagher energizer (Gallagher Ltd, 2007)

Gallagher Group Limited was established in 1938, according to the website (Gallagher Animal Management Systems, 2007), for the purpose of marketing and selling the animal control systems, and today, in 2008, are known and trusted in many countries throughout the world, and are among the global leaders in farm management systems.

Figure 1.2: Gallagher Group Limited Company Logo

Gallagher Group Limited have become a well-established global business group, expanding their product range outside just animal management systems, and have become a major competitor in security management systems, and have incorporated a broad range of companies, such as:

- PEC – contract manufacturing and fuel pump specialists.
- Gallagher Plastics – plastic injection moulding.
- Sunplas Engineering – Toolmakers and custom engineering projects.
- Franklin – farm fencing and gate systems.
- Grayson Gates – Farm gates and gate hardware.

Currently Gallagher Group Headquarters are situated in Hamilton, New Zealand, with distribution networks, including regional offices, joint ventures and distribution agents, in over 130 countries, and employ over 650 staff within New Zealand and a further 300 internationally.

Gallagher Group Limited received their first international awards for innovation at the Australian Orange Field Days, and the New Zealand field days in the 1970's and have sustained their success, continuing to receive world-class awards for their constantly updated products.

1.3 Animal Management Systems

Gallagher Animal Management Systems include ranges such as electric fence energizers and components, fence monitors and fault finders, Electronic Identification (EID), animal weigh scales, and more.

The products are often designed to work together, for example the EID products help with the weigh scales to identify which animal is being weighed, making it one step closer to a fully automated system. However most products can be used in multiple situations, for example the EID can also be used to make sure a particular animal goes into the correct paddock or holding cell, or for helping the farmer find out what treatments or conditions the animal may need or have, provided it is paired up with the right equipment that can enable that feature.

There are a large range of energizers with varying energy output, from 0.09 joules to 57 joules, each powered from a different power source, either mains electricity powered, battery powered, or solar powered with a rechargeable battery for power storage (Gallagher Ltd, 2007). Most of the energizers are designed to output an approximate ten kilo-volt pulse ranging from 50 microseconds (μs) to 150 micro-seconds but due to various conditions, for example, when there is a short on the fence line, this is not always possible.

The fence monitors and fault finders can be used to help identify when or where (respectively) there is a fault with the fence. The fence monitors simply monitor the voltage of each pulse and record, or alert the user, when there is a fault, and the fault finder can then be used to find the fault.

1.4 Industrial Project Requirements

The project was to develop a Data Logger that was capable of monitoring a battery-powered, portable energizer, including the fence voltage and the environment around and inside the energiser.

While the SmartWatch, a solar powered fence voltage monitor with a GSM Module, could monitor the fence voltage and report back to base, there was nothing available on the market that could monitor the fence voltage along with

other environmental effects that could be used to do full data-logging for testing new fences, like what the project was set to deliver.

The final product had to meet the following specifications:

- Monitor fence voltage 0-20 kilo-volts.
- Monitor energiser battery voltage 0-20 volts.
- Monitor ambient temperature -20°C to +80°C.
- Monitor energizer internal case temperature -20°C to +80°C.
- Store up to twelve months of data logs.
- Logging rate of one hour to twelve hours.
- Solar powered.
- Waterproof enclosure
- Remote interrogation from New Zealand to overseas.

The design could be based on the SmartWatch, and the systems it used, but must measure the temperature (as stated above), along with any other environmental effect that could be easily and accurately measured.

1.5 Thesis Structure

Chapter One: Introduction, gives an outline of the project, including the scope of the project and how it was funded, the company and more specifically the division the project was done for, Gallagher Animal Management Systems, and the requirements for the outcome of the project.

Chapter Two: Background, some background knowledge is given into the electric fence energizer products the project has been designed for, and some of the features of these energizers, then goes on to introducing data loggers, what they do and the existing data logger for monitoring the fence voltage. It gives a background into ultra-capacitors including a brief history, and developments currently underway in ultra-capacitor technology. It then gives a brief overview of energy harvesting and some types that are readily available in most places, and then gives an introduction into power management systems and why they are needed in technology in the future.

Chapter Three: Hardware – Preliminary Implementation, gives a brief description of the hardware in the existing data logger. It then goes on to describe in some detail how the first revision of the hardware developed by the student for the project was meant to work, and how various parts of the unit were programmed to test the rest of the circuit. It also discusses some of the mistakes that were made which forced a second revision to be designed before field testing the unit.

Chapter Four: Energy/Power Management System using Ultra-Capacitors, details the research and testing that was undertaken during the project. This included researching and testing some of the characteristics of ultra-capacitors such as charging and discharging, testing for equivalent series resistance, and researching into voltage balancing techniques for ultra-capacitors in series. Also included in chapter four are research and efficiency tests on low drop-out regulators and step down switch mode power supplies, to compare possibilities for the data-logger and for energy storage using ultra-capacitors.

Chapter Five: Final Implementation including Power Management System, gives an in depth description of the hardware in the second revision. It includes a block diagram for the full system and sample circuit diagrams for individual parts of the system to help explain how these parts work. Various parts of the system had to be designed on separate daughter boards so they could be placed outside the main enclosure, so these printed circuit boards are detailed individually with the details of their circuitry. The main printed circuit board is also discussed, along with placements of all the groups of circuitry and the overall size of the board.

Chapter Six: Conclusion, discusses the project overview, the results of the tests and how they impacted the second design revision of the data-logger. It includes changes that had to be made to the design to make it work more efficiently with the power storage system, whether it was a battery or an ultra-capacitor bank. It also discusses future improvements that can be made to the design of the data logger system and work that can be done on energy harvesting and ultra-capacitor storage, and the efficiency of the power supplies; including a recommendation for what type of power management system would be ideal for the data-logger application. It then finishes by giving a final overview of the project, with a few comments how well the project went, and discusses the project outcome.

CHAPTER TWO: BACKGROUND

2.1 Energizers

Gallagher Group Limited have two ranges of energizers currently on the market in the animal management sector, the SmartPower range and the PowerPlus range, to cover as many requirements as possible. While most energizers are designed for farming, some can be used in the equine industry for horse enclosures.

2.1.1 SmartPower

The SmartPower range was designed to enable the farmer to manage the farm fence system in the easiest, most efficient way possible. With just three models ranging from 15 to 75 joules of stored energy, it is the smaller of the two ranges, but also has the largest energizer, and the whole range has been designed with many extra features to make the fence and energizer easier to manage. Some of these features are a remote turn off function to turn the energizer output off from anywhere along the fence line, a display to show the stored energy, output voltage and earth/ground voltage, and the patented 'Adaptive Control' intelligence, which adjusts the energy output to what the fence needs to maintain the required voltage.

SmartPower MX7500

This is the largest energizer from Gallagher Animal Management Systems, with a stored energy capability of 75 Joules, and output energy of 57 Joules. It can energize up to 160 kilometres of multi wire[1] fence[2] (recommended for 40 kilometres), or a property size of 750 acres (300 hectares).

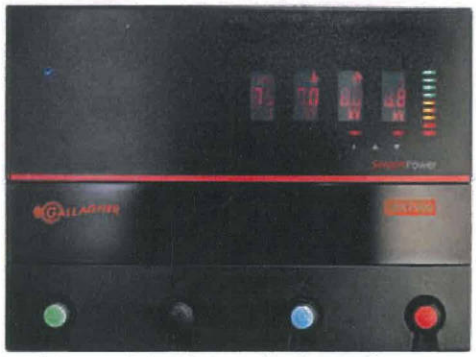

Figure 2.1: Photo of a SmartPower MX7500 Energizer (Gallagher Ltd, 2007)

The SmartPower MX7500 is powered only by the mains, and comes with a SmartPac remote, which has fault finding abilities, to make it easier to find a fault, and switch the energizer off remotely along the fence line so the user can fix the fence without returning to the energizer to turn it off. It also has a changeable output voltage which can be adjusted between five kilovolts and nine kilovolts.

[1] Multi wire fence is where the fence is made of three parallel wires all energised on the same line.
[2] Length of a single wire fence is up to three times that of a multi wire fence.

SmartPower MBX

The next model down in the SmartPower range, the MBX2500 has a stored energy capability of 25 Joules and output energy of 15 Joules. It is capable of energizing a multi wire fence up to 80 kilometres in length (20 kilometres recommended), or a property size of up to 250 acres (100 hectares).

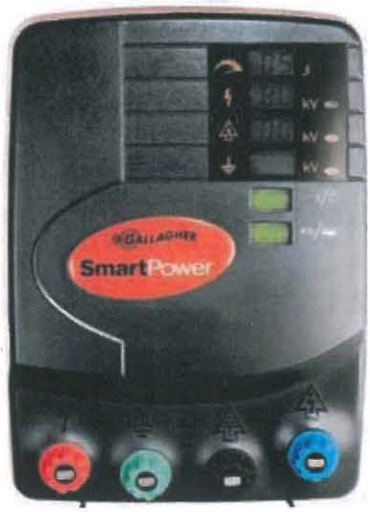

Figure 2.2: Photo of a SmartPower MBX Energiser (Gallagher Ltd, 2007)

The smallest of the SmartPower range is the MBX1500, with just 15 Joules of stored energy and 10 Joules output energy, capable of energizing 60 kilometres of multi wire fence (15 kilometres recommended), or a property size of up to 150 acres (60 hectares).

The SmartPower MBX products are mains powered with battery backup to keep the fence energized even during mains disturbances, and have the option to be solar powered. Each one comes with an XR1 remote control for switching off the fence from anywhere along the fence line.

SmartPower Summary

Table 2.1: Summary of the SmartPower energizer range

Energiser	Energy	Length of multi wire fence	Additional information
MX7500	• Stored: 75 Joules • Output: 57 Joules	• Capable: 160 kilometres • Recommended: 40 kilometres	• Mains Powered only • Comes with SmartPac remote control and faultfinder • Easy to read LED displays • Adjustable output voltage • Adaptive control intelligence
MBX2500	• Stored: 25 Joules • Output: 15 Joules	• Capable: 80 kilometres • Recommended: 20 kilometres	• Mains Powered with battery backup • Comes with XR1 remote control • Easy to read LCD Displays • Solar power option • Adaptive control intelligence
MBX1500	• Stored: 15 Joules • Output: 10 Joules	• Capable: 60 kilometres • Recommended: 15 kilometres	• Mains Powered with battery backup • Comes with XR1 remote control • Easy to read LCD Displays • Solar power option • Adaptive control intelligence • Equine industry option

2.1.2 PowerPlus

The PowerPlus range is designed for value and performance, with 21 different models ranging in output power from 0.09 Joules up to 60 Joules. While some of the PowerPlus Energizers have got features from the SmartPower range, they are generally less expensive energisers. They can be mains powered, battery powered, solar powered, or portable, with some having the option of doing either battery or solar powered.

PowerPlus MR

The top of the PowerPlus range, each of these three energisers are solely mains powered, but can still be turned off by remote on the fence line, just like the SmartPower range. All of the PowerPlus MR products have a bar graph indicator for displaying the output voltage of the energizer.

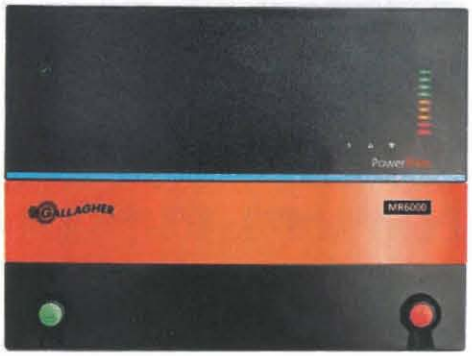

Figure 2.3: Photo of the PowerPlus MR6000 (Gallagher Ltd, 2007)

The PowerPlus MR6000 is the second largest energizer made by Gallagher Animal Management Systems, with a stored energy of 60 Joules and output energy of 48 Joules. Capable of energizing up to 140 kilometres of multi wire fence (35 kilometres recommended), or a property size of up to 600 acres (240 hectares), it also has the Adaptive control intelligence of the SmartPower range to help minimise power usage and still maintain the required voltage.

The PowerPlus MR5000 has a stored energy of 50 Joules and output energy of 32 Joules, and is capable of energizing multi wire fences up to 120 kilometres long (30 kilometres recommended), or property sizes of up to 500 acres (200 hectares). With Automatic Turbo mode, which operates in a similar way to the Adaptive control intelligence, but with only two stored energy ranges, it helps minimise power usage when it is not required.

The PowerPlus MR2500 has the same features of the MR5000, but with half the stored energy and output energy, which is rated for this model at 25 Joules and 16

Joules respectively. It can energize up to 80 kilometres of multi wire fence (20 kilometres recommended), or a property size of up to 250 acres (100 hectares).

Table 2.2: Summary table of the PowerPlus MR Energizers

Energiser	Energy	Length of multi wire fence	Additional information
MR6000	• Stored: 60 Joules • Output: 48 Joules	• Capable: 140 kilometres • Recommended: 35 kilometres	• Mains Powered only • SmartPac remote control and faultfinder capable • Bar graph display • Adjustable output voltage • Adaptive control intelligence
MR5000	• Stored: 50 Joules • Output: 32 Joules	• Capable: 120 kilometres • Recommended: 30 kilometres	• Mains Powered only • XR1 Remote control capable • Bar graph display • Automatic Turbo mode
MR2500	• Stored: 25 Joules • Output: 16 Joules	• Capable: 60 kilometres • Recommended: 15 kilometres	• Mains Powered only • XR1 Remote control capable • Bar graph display

PowerPlus M

The PowerPlus M series is the most basic of mains energizers, powered only off the mains supply, with only a bar graph indicator to show the output voltage of the energizer. The series consists of 5 energizers with output energies ranging from 1.2 Joules up to 18 Joules, and, model dependant, are capable of energizing up to 65 kilometres of multi wire fencing (16 kilometres recommended), or a property size of up to 180 acres (72 hectares).

Figure 2.4: Photo of the PowerPlus M1200 Energizer (Gallagher Ltd, 2007)

PowerPlus B

The PowerPlus B series are all primarily battery powered, with the option of going solar powered on the B700 and B1600 models by connecting a solar panel, or being completely portable like the B40 or B11. They are the best option on a large property with no access to the mains supply, only requiring a battery for power.

Figure 2.5: Photo of the PowerPlus B1600 Energiser (Gallagher Ltd, 2007)

Table 2.3: Summary table of the PowerPlus M Energizers

Energiser	Energy	Length of multi wire fence	Additional information
M1800	• Stored: 18 Joules • Output: 11 Joules	• Capable: 75 kilometres • Recommended: 16 kilometres	• Mains Powered only • Fence OK indicator LED shows fence condition
M1200	• Stored: 12 Joules • Output: 8.5 Joules	• Capable: 48 kilometres • Recommended: 12 kilometres	• Mains Powered only • Bar graph display shows fence voltage • Equine industry option
M600	• Stored: 6.0 Joules • Output: 4.5 Joules	• Capable: 35 kilometres • Recommended: 9.0 kilometres	• Mains Powered only • Bar graph display shows fence voltage
M300	• Stored: 3.0 Joules • Output: 2.5 Joules	• Capable: 25 kilometres • Recommended: 6.0 kilometres	• Mains Powered only • Bar graph display shows fence voltage • Equine industry option
M150	• Stored: 1.5 Joules • Output: 1.0 Joules	• Capable: 13 kilometres • Recommended: 3.0 kilometres	• Mains Powered only • Bar graph display shows fence voltage

The PowerPlus B series ranges in stored energy from 0.11 Joules up to 16 Joules, and output energy from 0.09 Joules up to 10.5 Joules. The largest of the series is capable of energizing up to 60 kilometres of multi wire fence (recommended for 15 kilometres), and can be used on a property of up to 160 acres (64 hectares).

Most of the models in the series have various power usage options, like full power, where the pulse operates at normal voltage and the pulse interval is normal, or night mode, where the pulse interval is dropped back during the night to preserve power, or random pulse mode, where the pulse interval is varied randomly from normal length to a much longer length, saving power with longer pulse intervals.

Figure 2.6 Photo of the PowerPlus B100 energizer (Gallagher Ltd, 2007)

For more detailed information on the PowerPlus B series please refer to the PowerPlus summary table (Table 2.4).

Table 2.4: Summary of the PowerPlus B energizers

Energiser	Energy	Length of multi wire fence	Additional information
B1600	• Stored: 16 Joules • Output: 10.6 Joules	• Capable: 60 kilometres • Recommended: 15 kilometres	• Battery Powered only • Multiple power modes
B700	• Stored: 7 Joules • Output: 5.6 Joules	• Capable: 40 kilometres • Recommended: 10 kilometres	• Battery Powered only • Multiple power modes
B280	• Stored: 2.8 Joules • Output: 2.1 Joules	• Capable: 35 kilometres • Recommended: 8.0 kilometres	• Battery Powered only • Bar graph display • Multiple power modes • Battery check mode • Equine industry option
B180	• Stored: 1.8 Joules • Output: 1.25 Joules	• Capable: 25 kilometres • Recommended: 6.0 kilometres	• Battery Powered only • Bar graph display • Multiple power modes • Battery check mode
B80	• Stored: 0.8 Joules • Output: 0.63 Joules	• Capable: 12 kilometres • Recommended: 4.0 kilometres	• Battery Powered only • Bar graph display • Battery check mode
B300	• Stored: 2.6 Joules • Output: 2.0 Joules	• Capable: 30 kilometres • Recommended: 6.0 kilometres	• Battery Powered only • Fully portable • Multiple power modes • Multiple Pulse modes
B200	• Stored: 1.45 Joules • Output: 1.1 Joules	• Capable: 20 kilometres • Recommended: 4.0 kilometres	• Battery Powered only • Fully portable • Multiple power modes • Multiple Pulse modes
B100	• Stored: 0.8 Joules • Output: 0.55 Joules	• Capable: 11 kilometres • Recommended: 2.5 kilometres	• Battery Powered only • Fully portable • Multiple power modes • Multiple Pulse modes
B40	• Stored: 0.38 Joules • Output: 0.28 Joules	• Capable: 6.0 kilometres • Recommended: 1.5 kilometres	• Battery Powered • Fully portable • Multiple power modes • Equine industry option
B11	• Stored: 0.11 Joules • Output: 0.09 Joules	• Capable: 1.0 kilometres • Recommended: 0.5 kilometres	• Battery Powered • Fully portable • Multiple power modes • Equine industry option

PowerPlus Solar

The solar powered PowerPlus products come with the option of being fully portable or permanent, without any modifications to the product. While they are not the only solar powered energizers, they are the only energizers with solar panel built into the casing. Both the S50 and the S17 automatically use night mode to preserve power during the night, preserving battery life.

Figure 2.7: Photo of the PowerPlus S50 Energizer (Gallagher Ltd, 2007)

The PowerPlus S50 has a stored energy rating of 0.5 Joules, with an output energy rated at 0.35 joules, and is capable of energizing up to 8 kilometres of multi wire fence (2 kilometres recommended), and is suitable for a property size of up to 5 acres (1.25 hectares).

The S17 Solar Energizer has a stored energy rating of 0.17 Joules, with and output energy rated at 0.11 Joules, and is capable of up to 1.5 kilometres of multi wire fence (1 kilometre recommended), suitable for a property size of up to 2 acres (0.8 hectares).

Figure 2.8: Photo of the S17 Solar Energizer (Gallagher Ltd, 2007)

Table 2.5: Summary of the PowerPlus Solar Energizers

Energiser	Energy	Length of multi wire fence	Additional information
PowerPlus S50	• Stored: 0.5 Joules • Output: 0.35 Joules	• Capable: 2 kilometres • Recommended: 8 kilometres	• Solar Powered only • Portable or Permanent • Automatic night mode • Equine industry option
S17	• Stored: 0.17 Joules • Output: 0.11 Joules	• Capable: 1.5 kilometres • Recommended: 1 kilometres	• Solar Powered only • Portable or Permanent • Automatic night mode • Equine industry option

More information about farm fence energizers can be found in (Gallagher Ltd, 2007).

2.2 Data-loggers

Data-loggers are used around the world as a means to test products, environmental parameters, human responses, and any other varying effect or system that needs to be measured over a long period of time, or where many measurements have to be made to test what is happening over a set period of time. Their main function is to log data about what the target system is doing and how it is changing, which could be from a slight change in temperature or humidity, to a physical movement or total system collapse.

Gallagher Group Limited has a Data logger that monitors the voltage on the fence at the peak of a pulse called the SmartWatch Monitoring System, that has the ability of remote interrogation via an on board Global System for Mobile communications (GSM) module, which enables the user to find out about how the fence is performing from anywhere in the world, provided the GSM module can make contact with a cellular network. Unfortunately this data-logger only measures the fence voltage, and no other parameters, environmental or otherwise.

Figure 2.9: Photo of the SmartWatch monitoring system (Gallagher Ltd, 2007)

2.2.1 High Voltage Pulse Monitoring

One of the main challenges for developing a data-logger for an electric fence is the ability to measure the voltage of the fence to a reasonable degree of accuracy. Because most Analog to Digital Converters (ADCs) operate at a relatively low voltage, normally around two volts up to five volts, and take time in the order of nanoseconds up to hundreds of microseconds depending which type of ADC is used, so it can be quite difficult to get an accurate and reproducible result.

Fortunately, because a data-logger to monitor the fence voltage already existed in Gallagher Animal Management Systems, most of the work in designing that area was already done, however some of the design would have to be revised to suit a

new method of taking the measurement, as it needed to be changed in order to try to save more energy between fence pulses.

2.2.2 Environmental Measurements

It is important when testing a new product to know what the environment is like at each given point, so that the designer can determine whether a glitch or failure was caused by something that happened in the environment that affected the hardware, or if it was just a general hardware fault.

Some environmental faults could be moisture being absorbed into the edges of the Printed Circuit Board (PCB) causing shorts between tracks, or the Temperature could be above 80 Degrees Celsius, causing some of the components properties to change and in some cases even destroying the component, or even if a solar panel isn't getting enough light and can't provide enough power for the system to run. Faults like these can easily be tracked using a data-logger by adding on temperature sensors, humidity sensors, light level sensors, and any other sensor that could be related to the possible cause of a failure.

2.2.3 Remote Interrogation

For a company like Gallagher Group Limited the ability to remotely interrogate the data-logger is a necessity, as they could be placed almost anywhere in the world, and to recover the data without remote interrogation could be very time consuming and expensive. Therefore a reliable system for recovering the data without needing to physically connect to the data-logger is a must.

In the existing data-logger the way this was achieved was using a GSM Module to send the information back to base via text message, or during a data call. This is particularly useful because most countries around the world use GSM networks for mobile phones, therefore making the data-logger usable in almost every country in the world, provided it has a link to a GSM network.

2.3 Ultra-capacitors/Super-capacitors

Over the last decade Ultra-capacitors, otherwise known as Super-capacitors or Electric Double-Layer Capacitors (EDLCs), have been becoming a common circuit element. This is due research being done to increase the storage capacity per volume, a substantial drop in price, and life times of up to 100 times as many charge/discharge cycles as batteries with no significant drop in performance or electrical characteristics, making them seem a better than electro-chemical batteries.

The first known patent for an ultra-capacitor design was granted to General Electric engineer Howard I. Becker (Becker, 1957); where the document stated that although the mechanism for the technology was unknown, an electrolytic capacitor can be made using two porous carbon electrodes separated by Pyrex glass wool, which had a much larger capacitance than a standard capacitor, but with a breakdown voltage of just 2.5 volts, much lower than that of a standard capacitor. Not too long afterwards research was done, by the company Standard Oil, into fuel cells, when they inadvertently rediscovered a similar technique; which they patented in 1966. Standard Oil licensed the technology to Nippon Electric Company, limited, (renamed NEC in 1983) who commercialised it and marketed the result as super-capacitors.

Currently ultra-capacitors are still made in the same general way, but with improvements in technology and resources the techniques have been developed and refined; increasingly so over the last decade as the drive for alternative, environmentally friendly energy sources and storage, and the potential for high current density applications like regenerative breaking, have driven developers to making cost effective, high energy density ultra-capacitors.

Comparing the current ultra-capacitors in the market with electrochemical batteries in the market, the energy densities of ultra-capacitors are still a long way away from matching that of an electrochemical battery. The gravimetric energy density of a BOOSTCAP 3000 farad ultra-capacitor from Maxwell Technologies is 5.52 watt hours per kilo-gram; whereas the gravimetric energy density of a lead

acid battery can be up to 40 watt hours per kilogram[3]. For a lithium ion battery the gravimetric energy density can be up to 150 watt hours per kilo-gram, and up to nearly 1000 watt hours per kilo-gram for fuel cells.

However, one major advantage of ultra-capacitors is that they have over ten times the power density of a lithium battery, its closest electrochemical competitor, and are almost equivalent to that of an electrolytic capacitor. Power density is the measure of how many watts a storage device can supply (or store) per kilogram. It is because of this high power density that ultra-capacitors have the ability to charge in minutes or even seconds, rather than the hours it takes to charge a battery of the same weight.

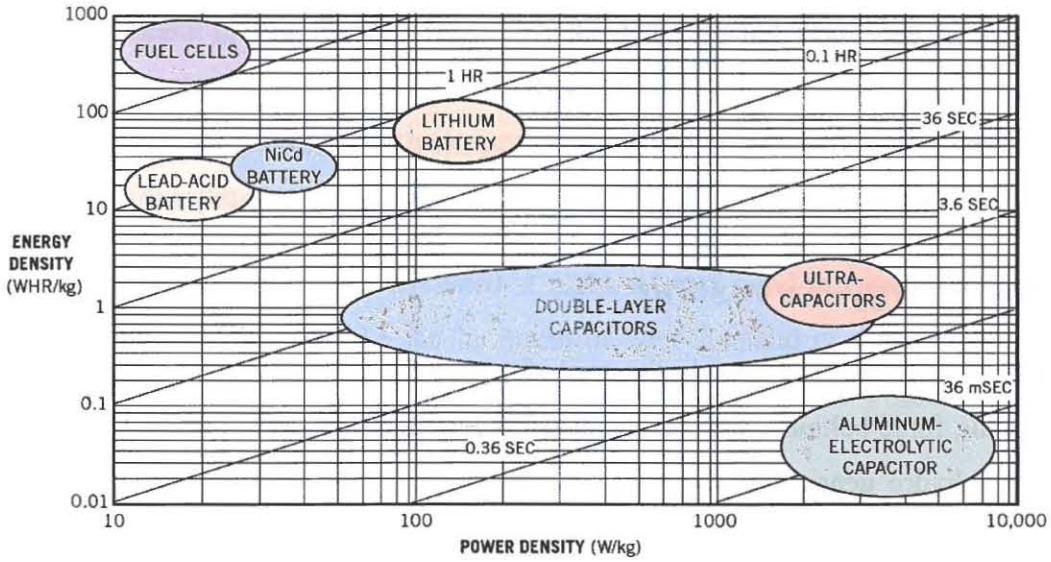

Figure 2.10: Graph of energy density vs. power density for common storage devices (Prophet, 2003)

Article (Halber, 2006) states that researchers from Massachusetts Institute of Technology's Laboratory for Electromagnetic and Electronic Systems (LEES) have discovered that using carbon nanotubes instead of activated carbon as electrodes increases porosity, giving a more uniform pore size and a much larger overall surface area, and therefore increasing the overall capacitance and energy density of the ultra-capacitor. As stated by the article (Schindall, 2007), LEES researchers hope to increase the energy density of ultra-capacitors up to as much as 50 percent of the energy density of an electrochemical battery of a similar weight.

[3] Note that the value for energy density in batteries and ultra-capacitors vary with the source, so these values are for a rough comparison only.

EEstor, Inc. has gone in a completely different direction, focusing on using a different dielectric or insulator between the electrodes. The United States Patent issued to EEstor, inc. (Weir et al., 2006), claims that by using a barium titanate based dielectric the Electrical energy storage units (EESUs), as they call them, can safely sustain a voltage of up to 3500 Volts with a dielectric thickness of just 12.76 micrometres. It also claims that an EESU can have a capacitance of 31 Farads, and can be safely charged to a voltage of 3500 volts, therefore storing over 52 kilo-watt-hours of power, and discharge at a rate of just 0.1% over a 30 day period, and also that it "*can be rapidly charged without damaging the material or reducing its life*" (Weir and Nelson, 2006).

With these advancements in ultra-capacitor technology, along with the promise that ultra-capacitors have a much longer lifetime, can charge in a fraction of the time it takes to recharge a battery of the same capacity, and have a lot less environmental toxins than that of electrochemical batteries, the possibility of ultra capacitors one day completely replacing batteries seems ultimately achievable.

2.4 Energy Harvesting

Throughout the past decade the push for alternative energy sources has been a driving force behind the development of solar panels, wind turbines (wind mills), micro-hydro generators and even tidal generators to be developed as a means to generate power for small scale electricity supplies for houses, and large scale generation for national electricity supplies.

During this time the cost of such energy sources has dropped dramatically, making it a viable option to power stand alone electronic devices; thus making it a great option for powering a data-logger which could be left in the field for years on end without needing to recharge or replace the batteries.

2.4.1 Solar

Solar power is a simple but effective source of electricity, requiring only a solar panel and a battery to provide power all day round. The solar panel provides power to the system and charges the battery during daytime, the battery powers the system during the night when the solar panel cannot provide enough power.

Due to the demand for alternative energy solar panels have also become common, easy to find, and most importantly, cheap. They are available in a range of output voltages, most commonly six volts or twelve volts, and because there are no moving parts there is virtually no need to service the solar panel during its lifetime.

For these reasons it an ideal form of energy harvesting, particularly for a data-logger which could be on the back outskirts of a farm, where it is difficult to get to for repairs, servicing or recharging.

2.4.2 Wind

Wind energy has been used for centuries in the farming environment, early uses including making flour from wheat. Recently however research has gone into using wind to generate electricity, because it is renewable and relatively easily acquired, and can generate electricity even during the night when solar panels are effectively useless.

Because wind energy can be harvested at night, a small wind generator would be extremely useful in areas like the far south of New Zealand or the Netherlands where there are very few hours of daylight during winter; which would severely limit the amount of power a solar panel could provide.

Another place where wind turbine could be useful is on farms near the ocean, where salt is a major problem and can settle on a solar panel, degrading the amount of light the solar panel actually gets. A wind turbine, while it would still get the salt build up, could be designed to cope with the salt. Another advantage of using a wind turbine in coastal areas in that even when there is no wind, there is often a sea-breeze, so a good wind turbine would be able to power the unit almost all day.

However because a wind generator has moving parts there is always the possibility of needing to be serviced, making it inadvisable to use for farm fence data-loggers in normal daylight conditions where a solar panel can be used.

2.4.3 Hybrid Solar and Wind Harvesting

Because both solar panels and wind generators are intermittent, i.e. when there is no sunlight for solar panels or no wind for the wind generator, one way to get a more constant inflow of power is to combine the two into one hybrid system as shown in Figure 2.11.

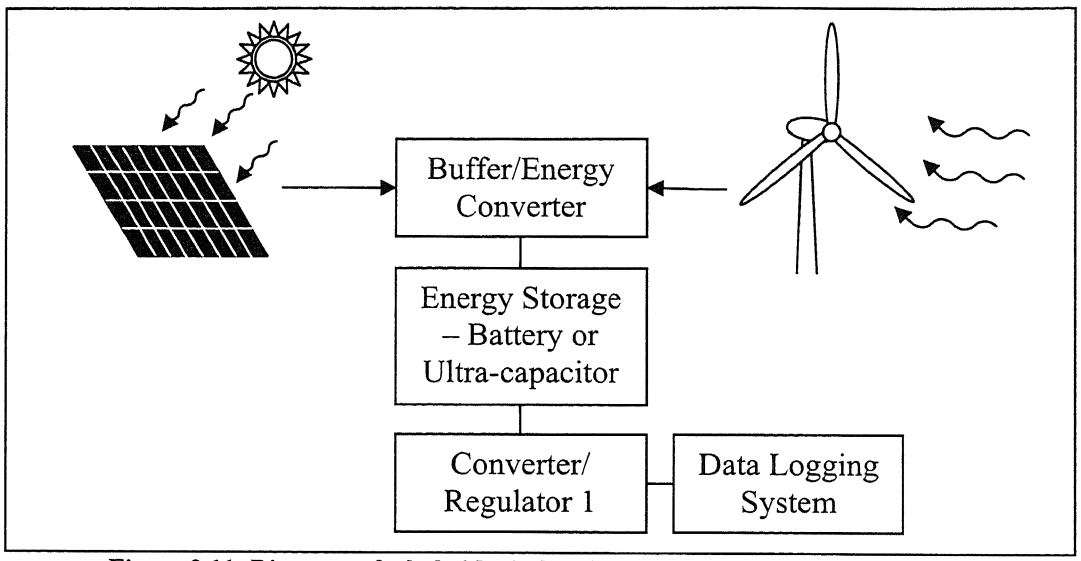

Figure 2.11: Diagram of a hybrid wind and solar energy harvesting system

The two different generator types compliment and reinforce each other, maximising on time and reducing the need for a large battery or ultra-capacitor bank for backup power. The reason for this is that during the night when the solar panel can not harvest any energy the wind generator could harvest energy from the wind, provided that there is wind, and during the day when there is no wind to harvest the solar panel could harvest all the energy needed for the system.

The only time when no energy could be harvested from the environment and a small battery would be necessary to keep the system running, is during a still night, when there is no wind and no sunlight.

2.5 Power Management Systems

The efficiency of a power supply has always been a largely targeted area in analog design, with new types of power supplies such as charge pumps, Low Drop-out regulators (LDOs), and switching regulators such as Switch Mode Power Supplies (SMPSs), and Single Ended Primary Inductor Converters (SEPICs) being created over the past few decades. Power management systems were once just a means to

get a better line efficiency from a system by combining power supply techniques and making a more efficient power supply. As technology has improved, individual power supplies have been developed and refined to become increasingly efficient, with many current power supplies achieving an efficiency of greater than 93 percent, and some achieving up to 95 percent or even higher. A summary of the types of converters and regulators, and some of their properties is provided in Figure 2.6.

Table 2.6: Summary of converter and regulator types and properties (Kularatna, 2008)

Feature	LDOs (and VLDOs)	Charge Pump Converters	Switching Regulators
Design complexity	Low	Moderate	Moderate to high
Cost	Low	Moderate	Moderate
Noise	Lowest	Low	Low to moderate
Efficiency	Low to moderate	Moderate to high	High
Thermal management	Poor to moderate	Good	Best
Output current capability	Moderate	Low	High
Requirement of magnetic parts	No	No	Yes
Limitations	Cannot step up	V_{in}/V_{out} ratio	Layout considerations

However in an increasingly mobile world the drive for increased efficiency to provide extended battery life efficiency is needed more than ever; and although power supplies are up to 93 percent efficient, they are often only 93 percent efficient over a given output current range. For example, as taken from the data sheet (MAXIM Integrated Products, 2002), the efficiency of a MAX1953 SMPS can be up to 93 percent for an input voltage of 3.3 volts, an output voltage of 2.5 volts, and an output current of 1.5 amperes; but for an input current of 100 milli-amperes and an output voltage of 2.5 volts, the efficiency can be as low as 78 percent for an input voltage of 3.3 volts, or 58 percent for an input voltage of five volts.

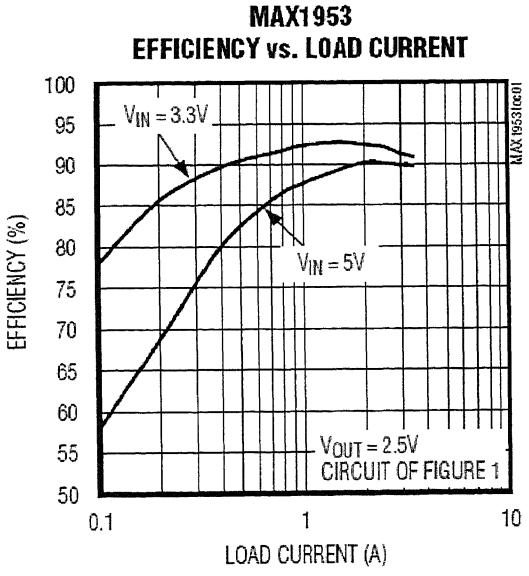

Figure 2.12: Graph of Efficiency vs. Load Current for the MAX1953 SMPS (MAXIM Integrated Products, 2002)

Because power supplies have this output current condition on the efficiency, where high efficiency is only achievable over a particular output current range, it can be necessary to use multiple power supplies to power the same rail. For this case each different power supply powers the rail for a particular current range, and either switches off or goes into sleep mode or shutdown mode when the current is out of its designated range. By using this method it can be possible to achieve an overall average efficiency of above 90 percent over a much larger output current range.

Modern power management systems are still directed towards higher efficiency, but are focussing on using different methods to get there. For example, to increase the overall efficiency a power management system supplies different voltage rails to various components, with the high speed components all running off a low voltage rail so it uses less power. Power management systems are gradually moving further and further away from power supply to improve efficiency, and closer to the rest of the circuit.

New power management techniques include powering down or completely turning off parts of the circuit that are not being used and using the lowest voltage for a sub-system that it can operate effectively and constantly on. Some of the later techniques include controlling the input rail to the power supplies, for example, using an isolated bus converter that can convert a high voltage input, either DC or mains AC, and converting it down to a low voltage isolated input for the power supplies that regulate the various supply rails. Power management is slowly incorporating the systems they are being designed for, and for this reason they should never be designed last. More detail on some of these techniques can be found in section 1.1.

CHAPTER THREE: HARDWARE – PRELIMINARY IMPLEMENTATION

3.1 SmartWatch – existing data-logger

The existing data-logger, named SmartWatch by Gallagher, was designed as a means to log the fence voltage at a periodic interval, which it could report back to base when it was requested; so it could be used as a means to find out when the fence stopped working properly, and possible why. The hardware in the SmartWatch, when broken down into sub-circuits seems quite simple, although some of the subsystems are in fact a lot more complicated than they would seem. A block diagram is provided in Figure 3.1, below.

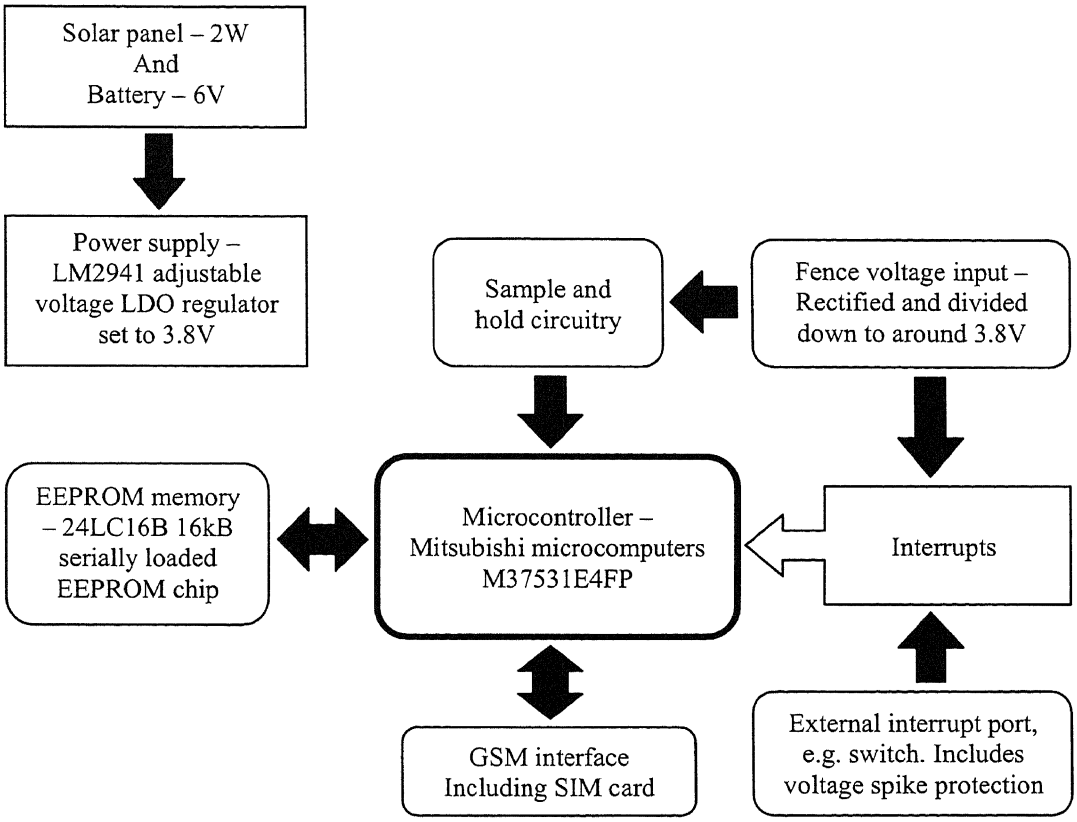

Figure 3.1: Block Diagram of the SmartWatch System

The main power source is a solar panel, which charges a six volt battery for providing power during the night, when the solar panel is effectively rendered useless without any sunlight. The Power supply is a National Semiconductor LM2941 adjustable output voltage LDO Regulator, with the output voltage set to 3.8 volts.

The fence voltage sampling circuit is one of the more complex circuits in the system. Due to the nature of the fence pulses, specifically their high voltage and the very short time the peak voltage is seen, typically ten kilo-volts in a spike

lasting for less than 150 micro-seconds, this part of the circuit has to not only lower the voltage spike to less than 3.8 volts, but also make the spike long enough for the microcontroller to read the voltage accurately. This is done using a resistive voltage divider, a rectifier, a sample-and-hold circuit connected to an Analog to Digital Converter (ADC) pin on the microcontroller, and an interrupt generator connected to one of the microcontroller's external interrupt pins, and will be explained in further detail in a later section.

The external interrupt circuitry is simply a connector with a voltage spike protection circuit around it to prevent the microcontroller getting damaged by being hit by a transient spike. It is connected to the microcontroller on one of the external interrupt pins, so it can generate and interrupt in the control routine when it needs to.

The unit was controlled by a Mitsubishi Microcomputers M37531E4FP Microcontroller, running on a four mega-hertz clock signal, with a Seiko S-805 series voltage detector for brown-out protection. The memory in the SmartWatch was an external, 16 kilo-byte Microchip 24LC16B Electrically Erasable Programmable Read Only Memory (EEPROM) chip, which was controlled by the microcontroller using an Inter-Integrated circuit (I^2C) Bus interface. This memory was enough to store over six months worth of data logs, so it could be left for an extended period time without needing to be attended to or downloaded from.

The GSM module that is used to report back to and receive control signals from the base, was an UbiNetics GM400, dual band, GPRS enabled, low power GSM module with data, voice, SMS and fax support. The module is controlled directly by the microcontroller, and was the only link to the Subscriber Identity Module (SIM) Card.

This circuitry was effective for what it was designed for, however, because it did not have the capability to monitor any environmental parameters such as temperature or humidity, it was often unable to provide the Research and Development team at Gallagher Group Ltd with enough information to formulate a definite reason for any failures, which is why they needed a new one.

3.2 New Data-Logger – First Revision

This was the first revision of the Data-logger designed for the project. This revision was designed as a starting point in the project, to give a new data logger that could be used to monitor the fence voltage, the energizers internal battery voltage, and the temperature both inside and outside the energizer enclosure.

Many of the systems have remained the same in this revision of the data-logger (as shown in the block diagram in Figure 3.2), as the systems were known to work, and the parts were available in the Gallagher inventory.

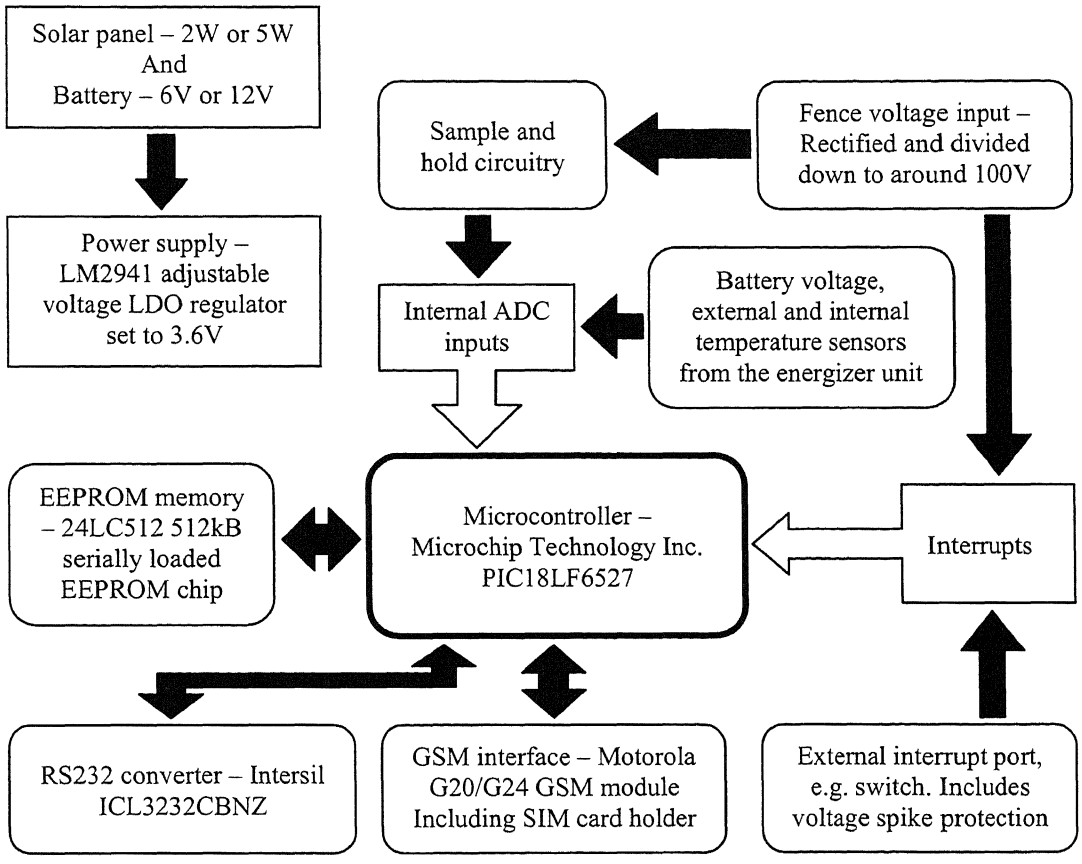

Figure 3.2: Block Diagram of the first revision of the Data-logger System

3.2.1 Power source

The solar panel and the battery were separated by power conditioning circuitry to help protect both from any damaging power surges or reverse connections that could cause damage to either. To protect the solar panel a rectifier diode was put in to prevent any reverse current during the night when the solar panel no longer supplies power, and to help protect both the battery and the solar panel from over-

voltages caused by over charging, a 6.8 volt zener diode and a rectifier diode were used to dissipate the power when the battery was full.

This revision could be powered off either a two watt solar panel with a six volt battery for night time power, like the existing SmartWatch using the parts specified on the power supply schematic (Appendix 1-a), or by changing three parts, the zener diode (D4), and two resistors (R2 and R3), a five watt solar panel and a 12 volt battery similar to the power source used by the PowerPlus S50 solar powered energizer could be used.

The reason for making the data-logger compatible with both power sources was to make sure it could be used in a climate where there are less hours of sunlight during the day, or inadequate sunlight on a regular basis, and using a larger solar panel helped it to harvest more energy as it is needed. The other option, as stated previously, is to harvest wind energy, however because Gallagher Group Limited do not currently have any wind generators, that was a lot harder to achieve.

3.2.2 Power Supply

The power supply used was the same one used in the SmartWatch, the National Semiconductor LM2941 adjustable output voltage Low Drop-Out Regulator because the design was already tested and the power supply worked. This power supply has of a drop-out voltage of as low as 0.2 volts for an output current of 0.1 amperes, and is capable of outputting one ampere of current continuously, with a dropout voltage of 1.0 volts over the full operating temperature range.

The input side of the LM2941 came directly from the battery, with a 220 nano-farad capacitor attached to ground for smoothing. The output of the power supply used two 330 micro-farad capacitors, to help keep the voltage up when the GSM module was connecting to the network and sending messages back to base, as it used a lot of power during the transmission process.

The only thing done differently to the SmartWatch in the data-logger was that the output voltage was set to 3.6 volts rather than 3.8 volts, because the new hardware in the data-logger only ran on a minimum of 3.3 volts, and a 3.6 volt rail was

enough to give a 0.3 volt drop before any of the circuit malfunctions would occur because of low voltage.

3.2.3 Microcontroller

The microcontroller used in the data-logger was the Microchip Technology Inc. PIC18LF6527 8-bit architecture, Enhanced Flash Microcontroller with 10 bit analog to digital converter and nanoWatt Technology. This microcontroller was chosen mainly because of the nanoWatt Technology and because it has two EUSART modules for communications and I^2C capability for the external EEPROM memory interface. A block diagram of the PIC18F6527 is provided in Figure 3.3.

The features of this microcontroller include:

- 40 mega-hertz maximum operating frequency
- Eight mega-hertz and 32 kilo-hertz internal oscillators
- 2.0 volts to 5.5 volts operating voltage
- 48 kilo-bytes flash program memory
- 1024 bytes data EEPROM
- 3986 bytes Static Random Access Memory (SRAM)
- 54 Input/Output (I/O) pins, 64 pins total
- 10-bit Analog-to-Digital Converter (ADC) supporting up to 12 channels
- Two Enhanced Universal Synchronous Asynchronous Receiver Transmitter (EUSART) modules
- Two Master Synchronous Serial Ports (MSSPs) capable of both Inter-Integrated Circuit (I^2C) and Serial Peripheral Interface (SPI) protocols
- Two 8-bit timers
- Three 16-bit timers
- Two Capture/Compare/Pulse Width Modulation (PWM) (CCP) modules
- Three Enhanced Capture/Compare/PWM (MCCP) modules
- In-Circuit Programming and Debugging capability using the Microchip MPLAB Integrated Development Environment (IDE) and appropriate debugging hardware.

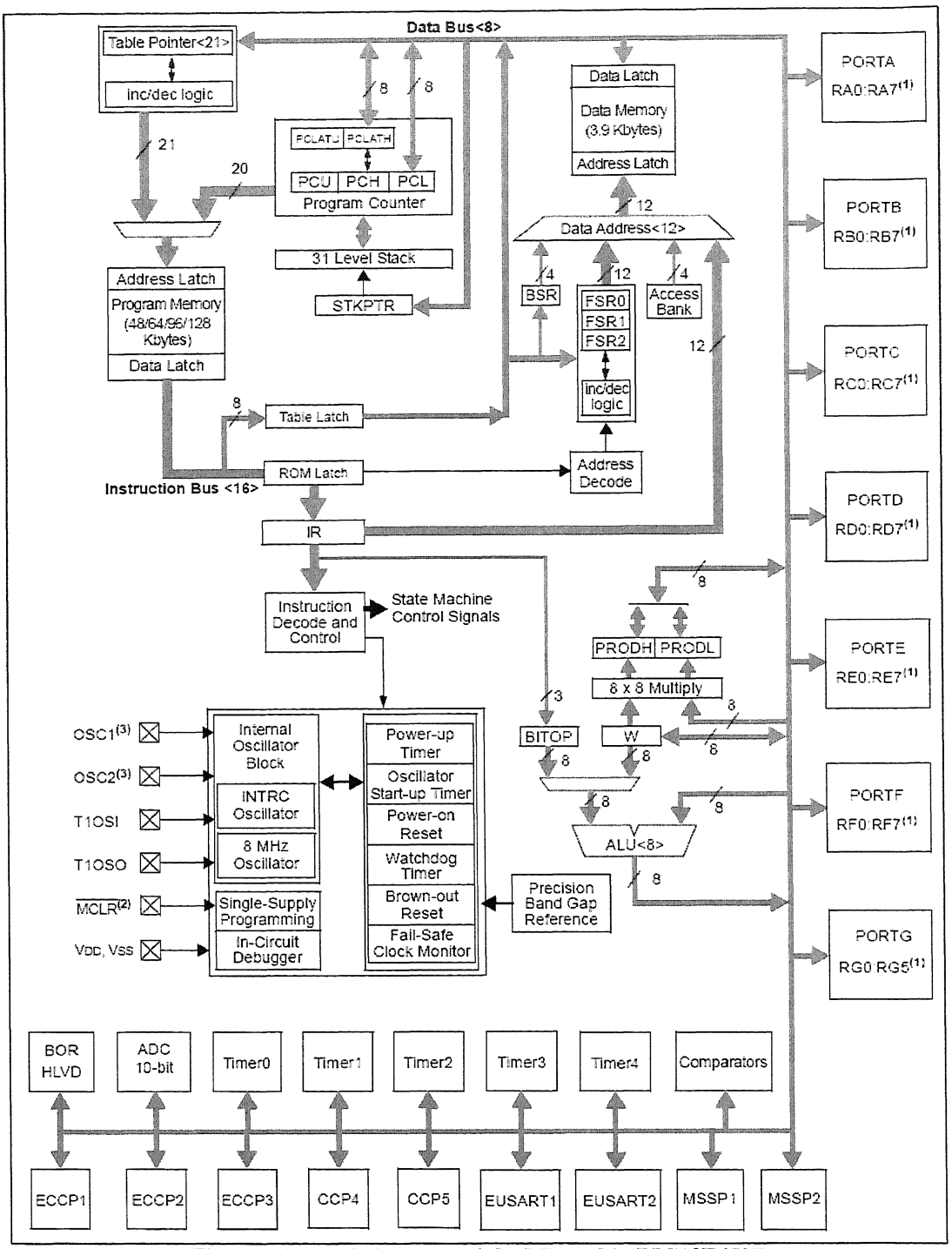

Figure 3.3: Block diagram of the Microchip PIC18F6527 (Microchip Technology Inc, 2004b)

The nanoWatt Technology allows the microcontroller to be put into one of its low power modes, either sleep mode, where the Central Processing Unit (CPU) and all the peripherals are turned off, or idle mode, where the peripherals are left running and the CPU is turned off. This gives the overall system a slightly longer battery life because it is using much less power in its low power modes, and can be as low

as 0.2 micro-amperes in sleep mode, according to the product datasheet (Microchip Technology Inc, 2004b).

3.2.4 External Memory

The external memory used in the data-logger was a Microchip Technology Inc. 24LC512 512 kilo-byte Complimentary Metal-Oxide Semiconductor (CMOS) serial EEPROM. It was connected to the microcontroller by an I^2C protocol serial communications port.

The chip could be hardware addressable by connecting pins one, two and three of the chip to either ground or the supply rail, which was useful with multiple modules because it allows the microcontroller to use a single I^2C port to control up to eight different EEPROM chips by addressing a given chip using the chip select bits of the control code (bits four, five and six), and even more I^2C devices that use a different control code (bits zero to three of the control byte). In the case of the data-logger one 512 kilo-byte EEPROM was enough, so the control code was 1010 (as set by the manufacturer) and the address was set to logic 000 by connecting all three address pins to ground.

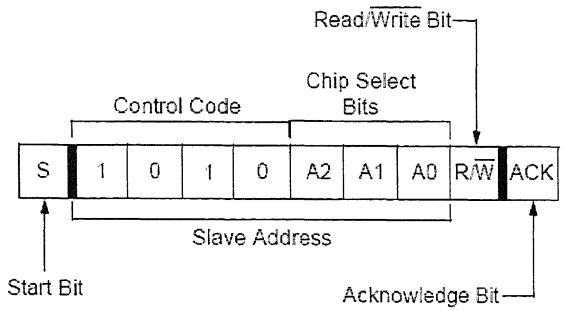

Figure 3.4: Diagram of the control byte used to address the EEPROM module (Microchip Technology Inc, 2004a)

The I^2C port required two connections to the microcontroller, one for the data signal, which was pulled high with a connection to the supply rail, and one for the clock signal. One other optional connection was the write protect line, which could be controlled by the microcontroller, given its own circuit to make sure the environment was within the optimal operation conditions, or connected to ground or the supply rail through a resistor to keep it in either read/write mode or read only mode respectively.

For the purposes of the data-logger the write protection pin was connected to an I/O pin on the microcontroller and through a 100 kilo-ohm resistor to the supply

rail to ensure the EEPROM could not be overwritten without permission from the microcontroller.

3.2.5 Sensing Circuitry

The high voltage sensing circuitry was the same as that in the SmartWatch, using a two stage resistive voltage divider, a rectifier, a sample and hold circuit, and an interrupt pulse generator. But looking at the schematic may make it seem a lot more complicated, because the resistive voltage divider is separated by the rectifier, as in Figure 3.5.

The ten kilo-volt pulse comes in via the two connectors, J5 and J6, and is divided down to approximately 110 volts by the resistors R10 and R11. The pulse is then rectified by the diodes to account for the leads being connected up the wrong way. At this point the pulse breaks into two signals, one way goes to an interrupt pulse generator, the other way is divided down again to approximately 3.8 volts, at which point it enters a sample and hold circuit.

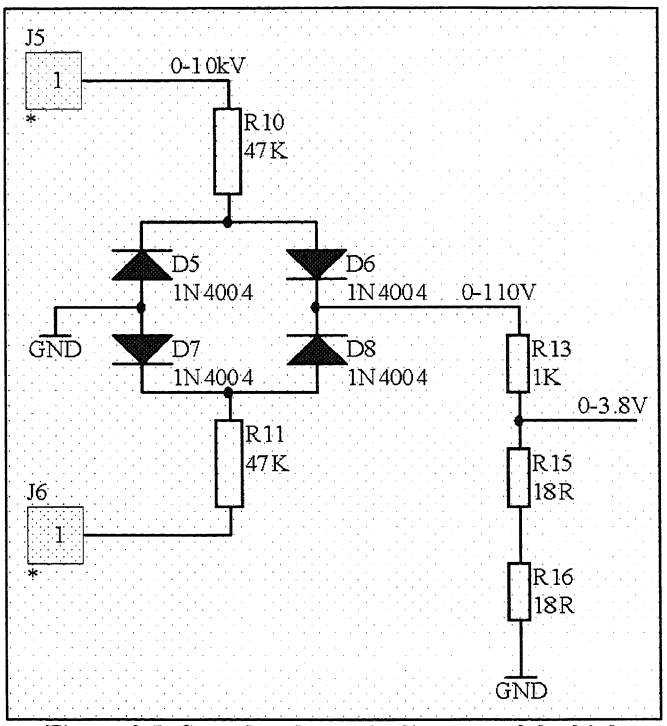

Figure 3.5: Sample schematic diagram of the high voltage sensing circuitry in the Data-logger

The interrupt pulse generator consists of a 47 kilo-ohm resistor leading from the 110 volt node to the base of a Bipolar Junction Transistor (BJT). The collector of the BJT connected directly to ground, and the collector connected to the supply voltage rail (3.6 volts)

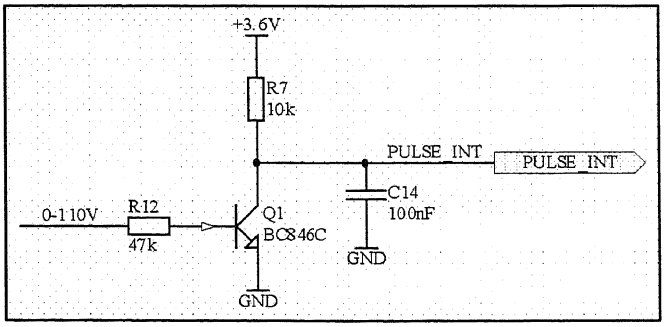

Figure 3.6: Sample shematic diagram of the intrrupt pulse generator circuit

through a ten kilo-ohm resistor. The collector is also directly connected to an interrupt pin on the microcontroller with a 100 nano-farad capacitor for smoothing, to generate the interrupt on a negative edge.

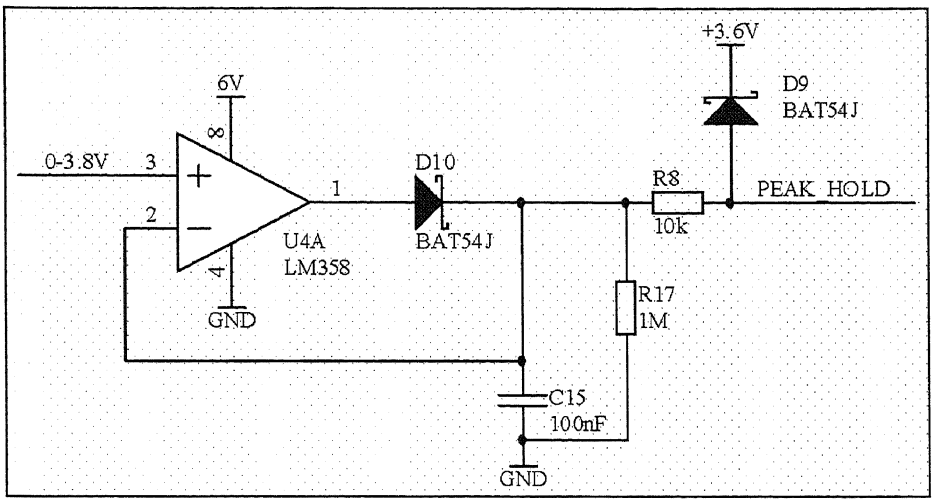

Figure 3.7: Sample schematic diagram of the sample and hold circuitry in the first revision of the data-logger

The sample and hold circuitry consisted of the 3.8 volt signal going directly into the positive input of an LM358D Operational Amplifier, with the output of the amplifier connected through a diode (D10) to a capacitor (C15) and the negative input of the amplifier. This enabled the signal to charge the capacitor through the operational amplifier up to the pulse voltage level, but not discharge it when the pulse had finished. This gave the micro controller more time to read the output voltage, before the resistor (R17) slowly discharged the capacitor to get ready for the next pulse.

The other sensing elements in the data-logger included two resistive temperature sensors, a battery voltage input capable of 24 volts for the energizer battery voltage and an external interrupt. These sensing lines all came off the board, so electro-static discharge and voltage transient protection had to be included, which consisted of a 15 volt Transient Voltage Suppression (TVS) diode, followed by a current limiting resistor (on all lines except the resistive temperature sensors). The lines from there go directly to the microcontroller, but they also have a 100 nano-farad capacitor to ground for smoothing, and two schottky diodes, one going to ground to prevent negative voltages, the other connected to the positive rail to prevent the line from high voltages. For more detail please refer the full circuit diagram of all sensing elements in Appendix 1-c).

3.2.6 Communications

The communications systems consisted of an RS232 port for a direct, physical connection to the computer and a GSM module for remote interrogation and control from anywhere in the world.

RS232 Communications

The Recommended Standard 232 (RS232) communications was implemented by using an Intersil Americas Inc. ICL3232CBNZ chip, which converts the EUSART Transistor-Transistor Logic (TTL) or CMOS logic into nominally positive (logic 0) and negative (logic 1) 5.5 volt logic for transmission to the computer; see Figure 3.8 for details.

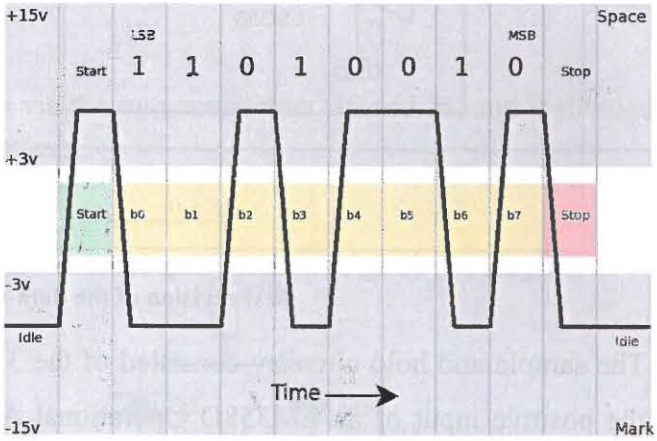

Figure 3.8: Diagram of the RS232 Protocol voltage vs. time graph (Wikipedia, 2001)

The ICL3232CBNZ chip operates on a voltage supply of between 3.0 volts and 5.5 volts, and has ESD protection on all transmitter outputs and receiver inputs to avoid damaging the chip when the transmission cable gets a transient voltage spike. It operates on less than one milli-ampere, and provides its own positive and negative voltage rails for the transmitter outputs using its integrated charge pumps.

The data-logger makes full use of the two transmitting outputs and two receiving inputs for full duplex RS232 communications with flow control, using the transmit and receive pins of the EUSART and two I/O pins on the microcontroller; using one I/O pin for the Request To Send (RTS) line, and the other for the Clear To Send (CTS) line. This way both options are covered, as the option for not using the flow control can be achieved by only connecting the transmit and receive lines on the cable, leaving the RTS and CTS lines floating.

GSM Module

The GSM module used for the data-logger was the Motorola, Inc. G24 GSM module, and was chosen because it was a current module, i.e. still in production, and the Gallagher team had used its Predecessor the G20, in one of their products in the past, and would be likely to upgrade to the G24 in the near future. Also, because the data-logger only needed to use the GSM component of the module, it would also be backwards compatible with the G20 module.

Figure 3.9: Photo of the Motorola G24 GSM module (Motorola, 2005)

Both the G20 and G24 modules ran off a supply rail of between 3.3 volts and 4.2 volts (3.6 volts was recommended), with a maximum input current of 2.0 amperes, which it needed for transmitting to the GSM network; and a minimum supply current of less than 2.5 milli-amperes in idle mode or 85 micro-amperes in power off mode. They also used the same connector plug on the Printed Circuit Board (PCB), a Molex 70-way, 0.5 milli-metre pitch SlimStack board-to-board plug (Molex Part number: 52991-0708).

Both modules also had a 3.0 volt power supply for the SIM card to ensure it had the correct supply voltage, so the SIM card was connected directly to the 5 pins on the GSM module necessary for reading and writing to the SIM card.

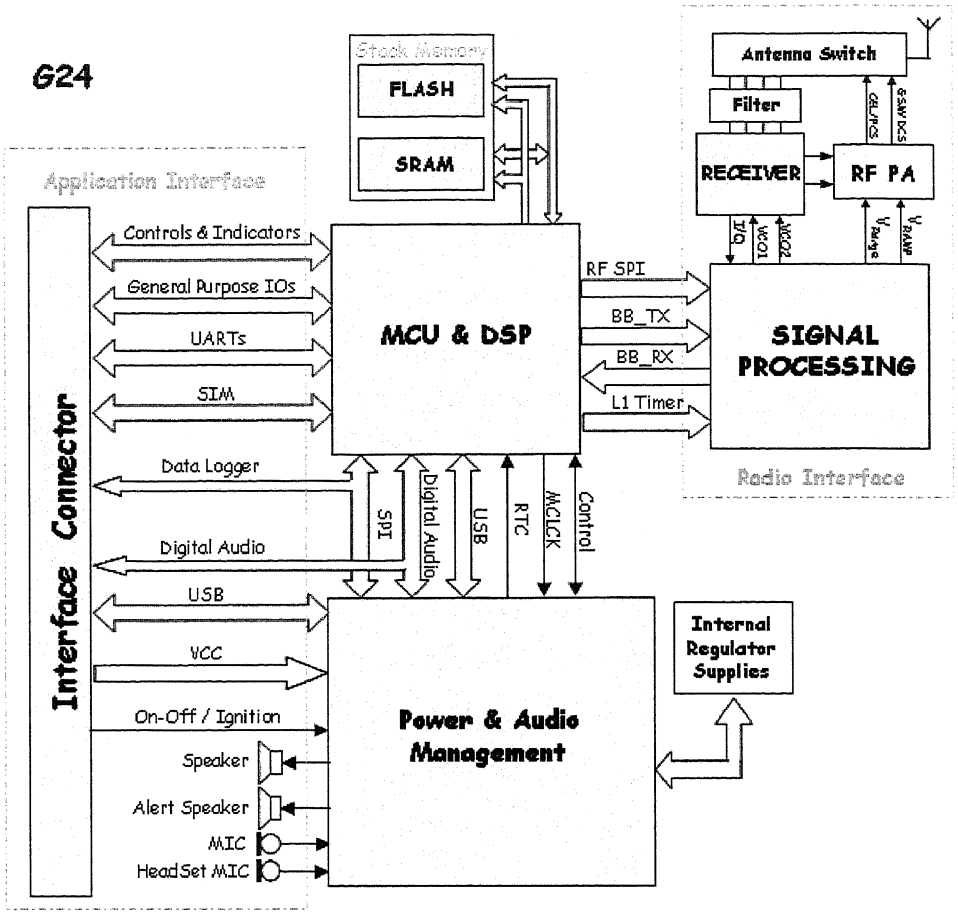

Figure 3.10: Block diagram of the primary functional components of the G24 (Motorola, 2006)

The notation for all the communications pins on the G24 GSM module (and the G20 module) appeared to be backwards, for example, the TXD_N pin was actually the receiver in the serial communications interface. This notation was devised because the GSM module could otherwise be known as the Data Communications Equipment (DCE), and the microcontroller as the Data Terminal Equipment (DTE), and because it could become confusing to circuit designers it became more practical to name it as what the DTE, or the transmit pin of the EUSART in the data-loggers case, has labelled the connection (as shown in Figure 3.11). Likewise, the other pins used for the serial communications interface were also named based on what the DTE would have named the connection.

The main power on the GSM module could be controlled using either of two pins, the IGN (ignition) pin, or the ON _N pin, both of which are connected directly to I/O pins on the microcontroller. When the power was turned on, the module

would begin powering up, but in the first 0.9 seconds, if either IGN or ON_N signals were not asserted (IGN was asserted high or ON_N was asserted low), the module would shut down until either signal was asserted. It was also required that the IGN and ON_N signals be left unasserted for at least 100 micro-seconds after turning on the power, so that the supply rail had enough time to settle, as the module would wait until then before starting the power up routine.

The module could be powered up from the off state by either asserting the ON_N signal for more than 0.5 seconds, but less than 1.5 seconds, or by asserting the IGN signal for the duration of the time the module needed to be on, provided that it was longer than 30 seconds. Once powered up the module could be put back into low power mode by either asserting the ON_N signal for more than two seconds, disserting the IGN signal (pulling it low), or by AT command, the command set used to control the GSM module. The module also had a low power automatic shut down feature for when the supply rail dropped below the minimum supply voltage of 3.3 volts.

The module also had sleep mode, where it turned off most of its peripherals and powered down into a low power state, but still keeps in contact with the network. The module could be put onto this sleep mode by issuing an AT command through the serial communications interface. To keep the GSM module connected to the network in sleep mode it periodically wakes up and polls the network for incoming data, at which point the module can also receive commands via the serial communications interface.

There were two ways to wake the GSM module up manually, one was by asserting the WKUPI_N pin low, which wakes the GSM module up for as long as it stays asserted and returns the module back to sleep mode by disserting it. The other way was to issue an AT command telling it to turn off sleep mode while it was awake for polling the network.

The GSM module indicated its power state using the RESET_N output, and the CTS_N output, although it was meant to indicate the status of the serial communications interface, it could also be used as an indication of when the module was in sleep mode or not. So when both outputs were disserted the

module was powered off, when RESET_N was asserted and CTS_N was disserted the module was in sleep mode, and when both outputs were asserted the module was in idle mode.

When the module starts transmitting, the TX_EN_N pin was asserted (pulled low), so by connecting it to an interrupt pin on the microcontroller, it can wake the microcontroller up from sleep. By doing the same thing with the WKUPO_N (wake up out) output the module was able to wake the microcontroller when it receives a transmission from the network.

There is also a General Packet Radio Service (GPRS) detection pin, called GPRS, which told the microcontroller when the GPRS network was available. Because some G24 GSM modules had Multimedia Messaging Service (MMS), this would allow more data to be sent back to base in a single message. For more information on the Motorola G24 GSM Module please refer to (Motorola, 2005) and(Motorola, 2006).

Table 3.1: Summary of the pins connected between the microcontroller and the G24 GSM module in the first revision of the data-logger

G24 Pin-out Number	Pin Name	Description
1,2,3,4	GND	Ground
5,6,7,8	VCC	Positive supply rail
9	RTS_N	DTE Request To send pin
11	RXD_N	DTE Receive Data – G24 module serial communications interface transmitter
15	CTS_N	DTE Clear To Send pin
16	WKUPI_N	Wake up In – wake module up from sleep mode
21	TXD_N	DTE Transmit Data – G24 module serial communications interface receiver
25	RESET_N	GSM module power status indicator
26	WKUPO_N	Wake up Out – wake microcontroller up from sleep mode when receiving data from network
39	TXEN_N	Transmit enable – GSM transmission in progress
44	SIM RST	SIM card reset

46	SIM_CLK	SIM card clock
48	SIM_VCC	SIM card supply rail, internally generated
49	GPRS	GPRS detection indicator
50	SIM_PD_N	SIM card ground rail
G24 Pin-out Number	Pin Name	Description
51	IGN	Ignition –turn the G24 module on for as long as this pin is high
52	SIM_DIO	SIM card data in/out
53	ON_N	ON – assert for 0.5 to 1.5 seconds to turn module on. Assert for two seconds to turn module off

3.2.7 Additional Functions

The first revision of the data-logger included Light Emitting Diodes (LEDs) to indicate what was happening in the circuit. These could be used for anything from power and status indicators, to transmit and receive indicators for the GSM module. They were connected through current limiting resistors to the microcontroller, which supplied all the power they needed to turn on.

There was also a voltage divider from the main battery voltage, already mentioned in the power source sub-section, which allowed the microcontroller to monitor the battery voltage of the data-logger. This meant that if the voltage got too low the power would be running out and the microcontroller could switch various high power draining circuit components off to preserve power, or if the voltage got too high, meaning the solar panel is generating too much energy, it could attempt to use some of the excess power by switching more components onto full power mode.

3.2.8 Printed Circuit Board Design

When it came to designing the Printed Circuit Board (PCB), it was decided early that because the data-logger could work off both the two Watt, six volt power source and the five Watt, twelve volt power source, it should be able to fit into either of the two enclosures. So using the measurements of both the SmartWatch monitoring system PCB and the PowerPlus S50 Energizer PCB, the data-logger

PCB was designed so that it could easily fit into both enclosures and with room to spare; the final measurements of the PCB were 153.67 milli-metres long by 60 milli-metres wide.

One of the challenges in designing the PCB was to make sure the high voltage tracks would be far enough away from the low voltage tracks, and each other, that there would be no arcing, or voltage jumping across the PCB where there is no copper. Ten milli-meters of clear PCB was recommended between the high voltage tracks and the low voltage tracks, and by using a slot cut into the PCB, the clearance between the high and low voltage tracks were cut down slightly more. Fortunately the SmartWatch had been previously designed and the circuit being used in the data-logger was the same. While custom terminals had to stay in the same position, a lot of the components could be moved in closer to each other without harming the immunity to arcing by an unmanageable amount.

It was also quite difficult to find an efficient placement for the other components, especially the GSM module, SIM card holder and microcontroller, however moving the components around and trying various positions; everything eventually fell nicely into place. Appendix 2: contains pictures of what the PCB of the first revision looked like from the top and bottom, and an indication of how the components were laid out in the top silk screen layer, also a photo of the PCB is provided in Figure 3.12.

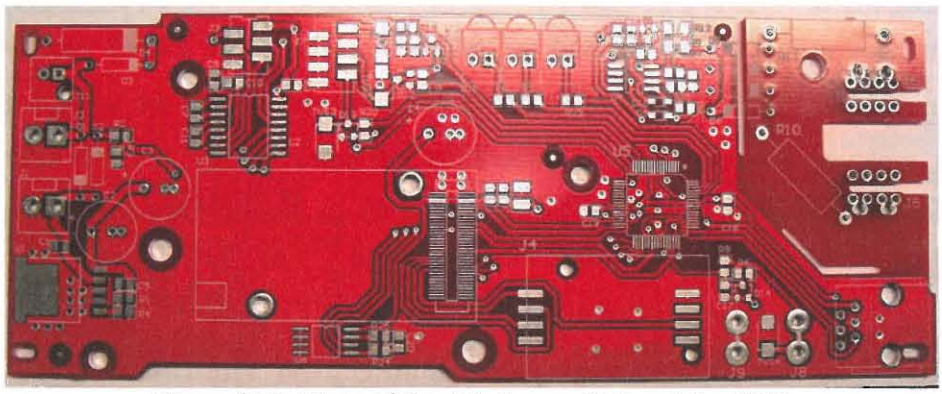

Figure 3.12: Photo of the data-logger first revision PCB

3.2.9 Program Code

The programming done for the PIC1F6527 microcontroller was written in the Microchip MPLAB IDE suite, using the Microchip C18 compiler for C code. The

programming of the first revision, due to all the faults in the hardware, was done to test the systems onboard the data-logger and make sure they all worked before designing the second revision, rather than programming a working unit that could be put in the field for testing. For this reason the programs were just small parts of what the overall program would be.

Clock and I/O pins

The first thing to get the microcontroller to do was simply turn on the LEDs, and while this seems like an easy task, the internal oscillator was not the default source for the system clock, so none of the program operations were being computed, therefore the commands weren't working. It turned out that a single line of code could change this, `#pragma config OSC=INTIO7`, which set up the configurations bits responsible for selecting the oscillator to use the internal eight mega-hertz oscillator. Once the system clock was running it took almost no effort at all to get the LEDs to light up, so the next task could be started; using an interrupt from the external interrupt pin to toggle the LEDs on and off.

Interrupts

Using the INT2 interrupt was not a simple task, as there were so many different control registers to set up, including the Port-B data direction register TRISB, the interrupt control registers INTCON, INTCON2 and INTCON3, and the Reset control register RCON. Using these registers the INT2 interrupt pin was set up as a negative edge triggered interrupt input, and then the interrupt was enabled. Once the other registers were set up the global interrupt enable (GIE) bit in the INTCON register needed to be set to enable all unmasked (enabled) interrupts.

With all the interrupt enable and data direction bits set up, all that needed to be done was to program the interrupt service routine to alternate the LEDs when the INT2 interrupt flag was set, but first the program had to enter the interrupt service routine. To do that the program which was written mainly in C++ code, it needed some assembler code to move the program counter from the limited code space of the interrupt vectors to the nearly unlimited space of the program memory, as shown in Figure 3.13. Because there are both high priority and low priority interrupts, the interrupt service routine has to be referenced to both the high and low priority vectors to make sure the interrupt is handled.

With the interrupt priority vectors referenced to the interrupt handler routine all that needed to be done was to separate out the INT2 interrupts from the other types of interrupts. The easiest way to do this was to poll the INT2IF flag and if it was set, then an INT2 interrupt had occurred, and toggle the LEDs on or off.

```
void InterruptHandler(void);
//------------------------------------------------------
// High priority interrupt vector
#pragma code InterruptVectorHigh = 0x08
void
InterruptVectorHigh (void)
{
  _asm
    goto InterruptHandler //jump to interrupt routine
  _endasm
}

//------------------------------------------------------
// Low Priority interrupt vector
#pragma code InterruptVectorLow = 0x18
void
InterruptVectorLow (void)
{
  _asm
    goto InterruptHandler //jump to interrupt routine
  _endasm
}

//------------------------------------------------------
// Interrupt routine
#pragma code
#pragma interrupt InterruptHandler

void InterruptHandler(void)
{
      // Interrupt code
}
```

Figure 3.13: Sample code for the interrupt vectors being redirected to the interrupt handler in the program code

Timers

With the interrupts working it was then possible to start using the timer interrupts, more specifically the TMR0 overflow interrupt. To check that the timer was actually working the TMR0 interrupt routine was used to increment Port-E, the port with the LEDs on it. Because TMR0 counted through so fast, once every 32.768 milli-seconds on a two mega-hertz instruction clock with no pre-scaling, the interrupt routine was still too fast to see.

By using the whole Port-E as a counter, with the LEDs in Port-E pins four, five and six, it acted as a post-scaler to the interrupt routine, slowing it down by

another 16 times to make the LEDs count at a rate of just under two counts per second; easily visible to the human eye.

Analog to Digital Converter

The analog to digital converter took a lot of time to make work, because on top of getting the control registers right, there was also a hardware fault to debug; namely, the analog to digital converter reference voltage pins, AVDD and AVSS were not connected.

With the reference voltage connected the analog to digital converter control registers and the respective port data direction registers set as inputs before the system could work. To test the analog to digital converter readings a variable resistor was used to adjust the voltage between ground and the supply rail, and each LED would light up when the analog to digital converter reading was greater than one of three values value specified in the program code; i.e. when the reading was greater than 100 one LED would light up, when it was greater than 150 another LED would light up, and so on.

To set up the analog to digital converter for the test input, the TRISF register was set to make pins zero to four inputs, and the analog to digital converter control registers, ADCON0, ADCON1 and ADCON2, were set up to use AVDD and AVSS as the reference, the A/D conversion clock derived from the A/D RC oscillator and the conversion time for 20 clock cycles, and turn the analog to digital converter on.

```
unsigned int sample_adc(char channel)
{
unsigned int level_input = 0;

ADCON0 = (channel << 2) + 3;  // Start the ADC on 'channel'
while(ADCON0 & 0x02);         // wait for conversion to finish
level_input = ADRES;          // copy result to level_input
return level_input;           // return result to subroutine
}
```

Figure 3.14: Sample code for how to use the ADC

To read the analog to digital converter using the sample_adc function (as in Figure 3.14) a four bit channel number is passed into the function, which uses this number to start the ADC on the selected channel. The function then goes into a loop, which stalls the program until the reading is complete. At this point the

twelve bit reading is taken from the 16 bit ADRES register and returned as a value to where the function was called.

Although this is an inefficient way to read the analog to digital converter because it stalls the microcontroller in a loop while it works, this code was written only to test the microcontroller and its associated circuitry; not for the final firmware for the data-logger product. The ADC could be set up to interrupt the program when the reading is complete, so the program could continue while the ADC was running.

EUSART Communications

Each of the two EUSART peripherals was controlled by three registers, for EUSART1 these were the Transmit Status and Contol register one, TXSTA1, the Receive Status and Contol register one, RCSTA1, and the Baud rate Control register one, BAUDCON1, and for EUSART2 they were TXSTA2, RCSTA2 and BAUDCON2.

The TXSTA1 and TXSTA2 registers controlled the transmit functions of the EUSARTs, including transmit enable. The RCSTA1 and RCSTA2 registers control the receiving functions of the EUSARTs, including the Serial Port Enable bit, SPEN, which turns on the serial port. The BAUDCON registers controlled most the baud rate options. The baud rate itself was controlled by the Serial Port Baud Rate Generator registers SPBRG1 and SPBRGH1 for serial port one (SPBRG2 and SPBRGH2 for serial port 2). If the baud rate generator was set to eight bit resolution it only used the SPBRG resister, but used both registers for 16 bit resolution, which enabled finer tuning of the baud rate.

For communicating with the computer the EUSART was set up in asynchronous mode with a baud rate of 9615 bits per second using 16 bit resolution (the closest baud rate to 9600 bits per second using the eight mega-hertz oscillator), eight data bits for both transmit and receive, and continuous receive enabled.

The serial communications were tested by writing a program that could receive a character from the serial port, through the RS232 converter, and send it back to the serial port, all done without flow control, i.e. the CTS and RTS pins were not used. To check that it was working hyperterminal was used to send a character

over the serial port, and when the character came back from the microcontroller, the serial communications were working.

Communications to the GSM module

The communications to the G24 GSM Module was a lot more complex, because not only did it need flow control, but the microcontroller also had to use timers and other inputs and outputs to turn the GSM module on, wait for the serial communications interface to start, and monitor the other pins to make sure the module was operating properly.

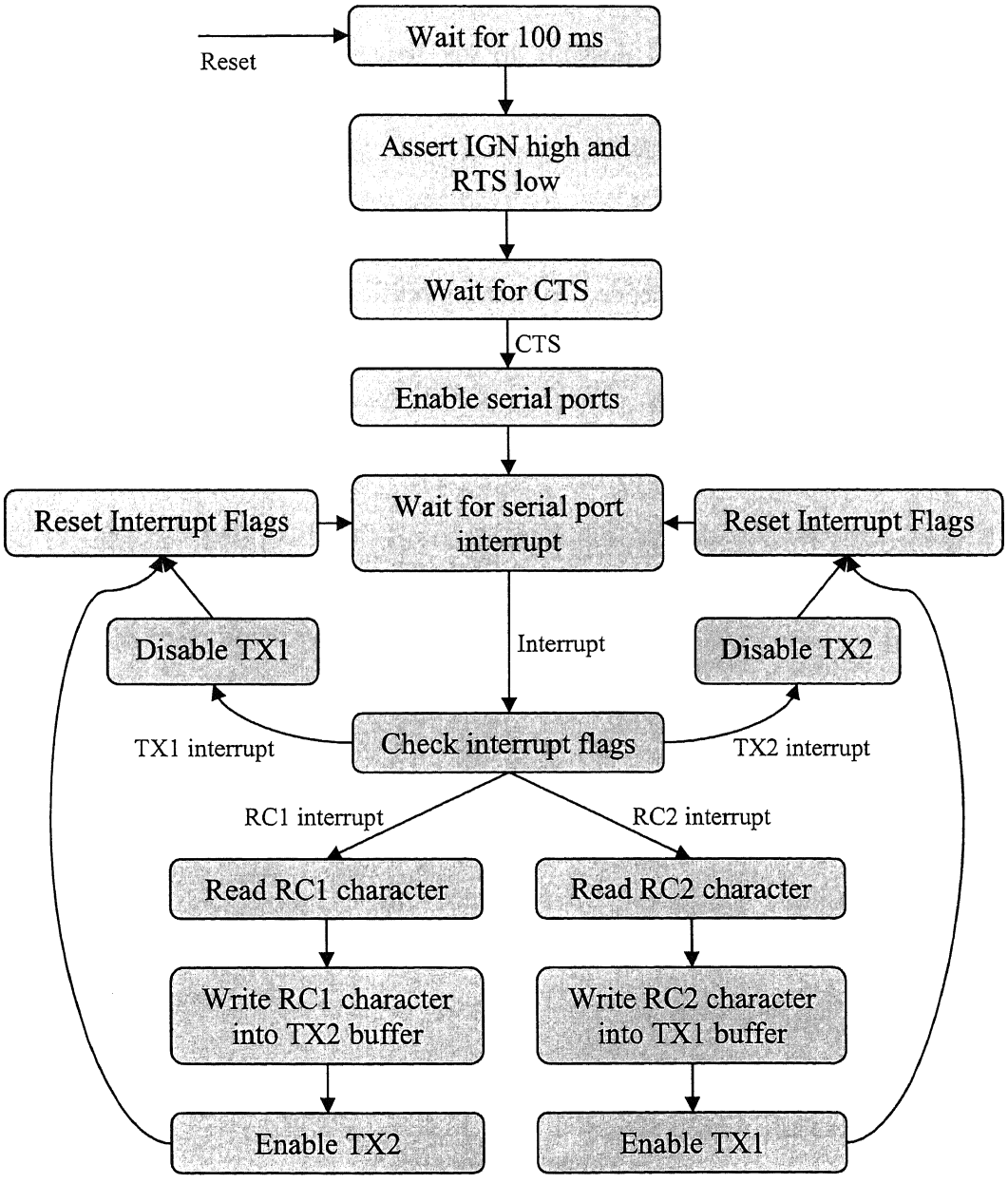

Figure 3.15: Flow Diagram of the program used to test the microcontrollers ability to communicate with the GSM module

To turn the GSM module on the IGN pin was asserted, as it did not require any timers to dissert it after a certain period of time, and the RTS pin was asserted at all times so there was no trouble with communicating back to the microcontroller.

For the sake of testing the communications to the GSM module it was a lot more efficient to use the microcontroller merely as a buffer, and essentially connecting the GSM module to the computer serial port. The program in the microcontroller used the interrupts to monitor the receivers on both the serial ports, and when on the receiver on one serial port received a character, it loaded that character straight into the transmit buffer of the other serial port, as shown in Figure 3.15.

Using this program it was possible to get hyperterminal to send commands directly to the GSM module and receive the responses that the GSM module returned.

Pin assignments

Because the first revision needed so many modifications, and a second revision was always part of the plan anyway, it was inevitable that the pin assignments would have to change, and many pins on the microcontroller would be changed to do something completely different.

To make it easier to convert the program from the first board revision to the second board revision, pin references were created in program header files for many the pins that were used; i.e. the IGN pin on RA5 could be called by the C code as GSM_IGN instead of RA5. This made it easier to convert the program because rather than going through the program line by line, changing RA5 to the new pin assignment, it could be changed once in the header file, and the compiler would know which pin the name GSM_IGN belongs to. An example of the code in one of the header files is supplied in Figure 3.16.

```
// defining the pins used to connect to the GSM module
#ifndef __GSM_BITS
#define __GSM_BITS

#define GSM_RTS          RC0
#define GSM_CTS          RC1
#define GSM_WAKEUP_OUT   RB0
#define GSM_WAKEUP_IN    RB4
#define GSM_ON_OFF       RA4
#define GSM_IGN          RA5
#define GSM_GPRS_DET     RC5
#define GSM_TX_EN        RB3
#define GSM_RESET        RA7

#endif __GSM_BITS
```

Figure 3.16: Sample Code of a header file used to convert the names of pins to the pin designations to make it easy to change the pins throughout the code

3.2.10 Problems with the PCB

As any new design almost definitely does the first revision ran into problems while programming and testing the hardware. Most of the mistakes were errors made from reading data sheets incorrectly and building the PCB under false impressions.

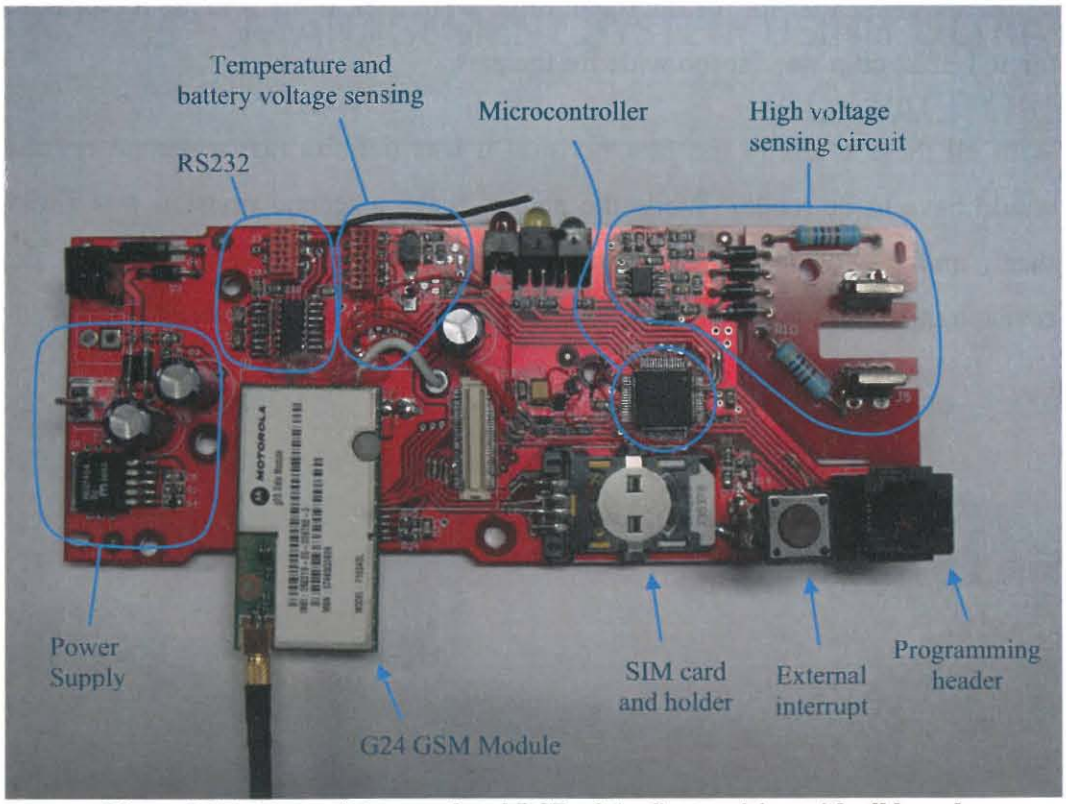

Figure 3.17: Photo of the populated PCB of the first revision with all board modifications made

One of these mistakes was to design the footprint for the GSM module in a mirror image to what it was supposed to be. Because of this mistake the whole first revision had to be scrapped and a new PCB needed to be made. However testing was done on the system by using jumper wires to another connector, so it was proven that the GSM module interface worked in the circuit and the microcontroller didn't have to be changed.

The power supply that was chosen was not up to the task; even the three 330 micro-farad capacitors in tandem with the one ampere power supply was not enough to keep the supply rail permanently above the 3.3 volt threshold. During testing the power supply would often dip below the working threshold of the GSM module when it connected to the network, which completely froze the module until the power was reset.

Other mistakes included not connecting the microcontrollers analog supply rails, AVSS and AVDD, to ground and positive 3.6 volts respectively, which prevented analog to digital converter from working, the SIM card connector and the programming header for the microcontroller were backwards, and the footprint for the ICL3232 chip was far too wide for the part.

With all these faults in the first revision it was definite that a second revision would have to be made. While the plan to make a second revision was always there, and it would include a lot more environmental sensors than the first revision, it would have been good to know that the first revision had worked.

CHAPTER FOUR: ENERGY/POWER MANAGEMENT SYSTEM USING ULTRA-CAPACITORS

4.1 Ultra Capacitors

Ultra-capacitors are very similar to standard capacitors in terms of their electrical characteristics. Both have similar charge and discharge curves and similar equivalent circuit characteristics, and they use the same formulas for both series and parallel connections to each other; only ultra-capacitors are much larger.

For example, a standard capacitor can have a capacitance value from anywhere between one pico-farad and ten milli-farads with an equivalent series resistance values as low as 35 milli-ohms and as high as 2000 ohms. An ultra-capacitor could have a capacitance value of between about 0.1 farads and 3000 farads in a single cell, with equivalent series resistance values of between 0.29 milli-ohms and 0.5 ohms.

The cost for the high capacitance rating comes from the breakdown voltage rating, where a standard capacitor could have a voltage rating of up to 1000 volts, an ultra-capacitor cell can have a voltage rating of between two volts and three volts, because the activated carbon takes the place of other improved insulators that can be used in standard capacitors.

The specific energy, or gravimetric energy density, measured in watt hours per kilo-gram, and the volumetric energy density, measured in watt hours per litre, is also much larger in ultra-capacitors. For example, the energy in a capacitor (E) is equal to half the capacitance (C) multiplied by voltage (V) squared, i.e.

$$E = \frac{1}{2} C V^2 \tag{1}$$

This equation can be used to calculate the energy of a capacitor and an ultra-capacitor of similar size and mass, i.e. a 220 micro-farad, 50 volt aluminium electrolytic capacitor and a 90 farad, 2.7 volt ultra-capacitor. The results of the calculations are 0.275 joules for the capacitor, and 328 joules for the ultra-capacitor; a multiple of over 100 times. Given that the two were of similar size and mass, the ultra-capacitor had over 100 times the energy density as what the capacitor had, in both gravimetric and volumetric measurements.

While the voltage has a major effect on the energy of the capacitor, to achieve a higher voltage in a capacitor you have to either increase the physical size of the capacitor, or drastically reduce the capacitance. So having 1000 volts is not really an advantage in terms of energy density, because the energy per volume or mass has not increased by that much.

Capacitors store charge on two parallel plates with a dielectric in between, creating an electric field where the energy is stored. The capacitance (C), or stored charge, is proportional to the permittivity of the dielectric (ε), the area of the plates (A), and inversely proportional to the distance between the plates (d).

$$C = \varepsilon \frac{A}{d} \tag{2}$$

The reason an ultra-capacitor has a much higher capacitance, is because rather than using plates, they use porous activated carbon as the electrodes, which has significantly more surface area because the electric field could permeate through the carbon's pores, which allows charge to build up on the surface area inside the activated carbon; not just on the front face like in a standard capacitor.

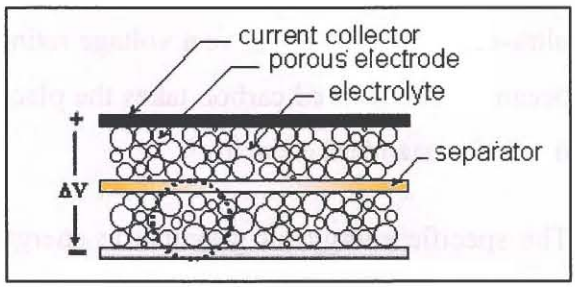

Figure 4.1: Diagram of the layers of an ultra-capacitor (Nesscap Co. Ltd., 2005)

4.1.1 Charging

Charging through a resistor

For an ultra-capacitor charging through a fixed resistor as shown in Figure 4.2, just like a capacitor, the charge curve follows an inversely exponential growth, which is dictated by the capacitance (C), resistance (R) and source voltage (V_S) of the circuit. We can work out the capacitor time constant (τ), or the time it takes to charge the capacitor from zero volts to 63 percent of the source voltage using the formula:

$$\tau = R \times C \tag{3}$$

The capacitor time constant is also used to work out the total charge time, the time that it takes to charge up to nearly the source voltage (V_S), as the charge time is defined to be approximately five times the capacitor time constant, as shown graphically in Figure 4.3.

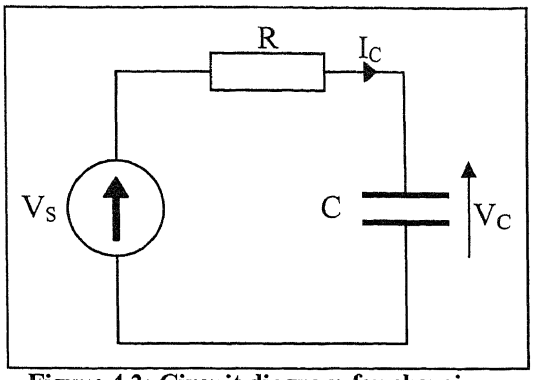

Figure 4.2: Circuit diagram for charging a capacitor

For a comparison between the charge times of a capacitor and an ultra-capacitor, a 1000 micro-farad capacitor with 0.1 ohms equivalent series resistance being charged up to 2.5 volts using only its internal resistance to limit the current, the time constant for the charge curve would be 0.1 milli-second, and the time to full charge would be 0.5 milli-seconds. Doing the same thing with a 100 farad ultra-capacitor with 0.01 ohms of equivalent series resistance gives a time constant of one second, or a total charge time of five seconds.

For the circuit shown in Figure 4.2, the charging would occur as an exponential curve . Because $\Delta Q = I \times \Delta t$, and $\Delta V = \Delta Q/C$, the momentary increase in voltage ($\Delta V/\Delta t$) is equal to the current divided by the capacitance, i.e.

$$\frac{\Delta V}{\Delta t} = \frac{I}{C} \tag{4}$$

So because the current decreases with a lower voltage drop across the resistor, the rate of increase in voltage decreases as the capacitor charges. Using the same equations the following equation for the capacitor voltage is derived:

$$V_C = V_S\left(1 - \exp^{\frac{-t}{RC}}\right) \tag{5}$$

From this formula the charge time (t_r), i.e. the time it takes to charge the capacitor to 0.99 V_S, is calculated as $t_r = 5RC$, as stated above. A graphical representation of this exponential charge curve along with the exponential discharge curve is shown in Figure 4.3.

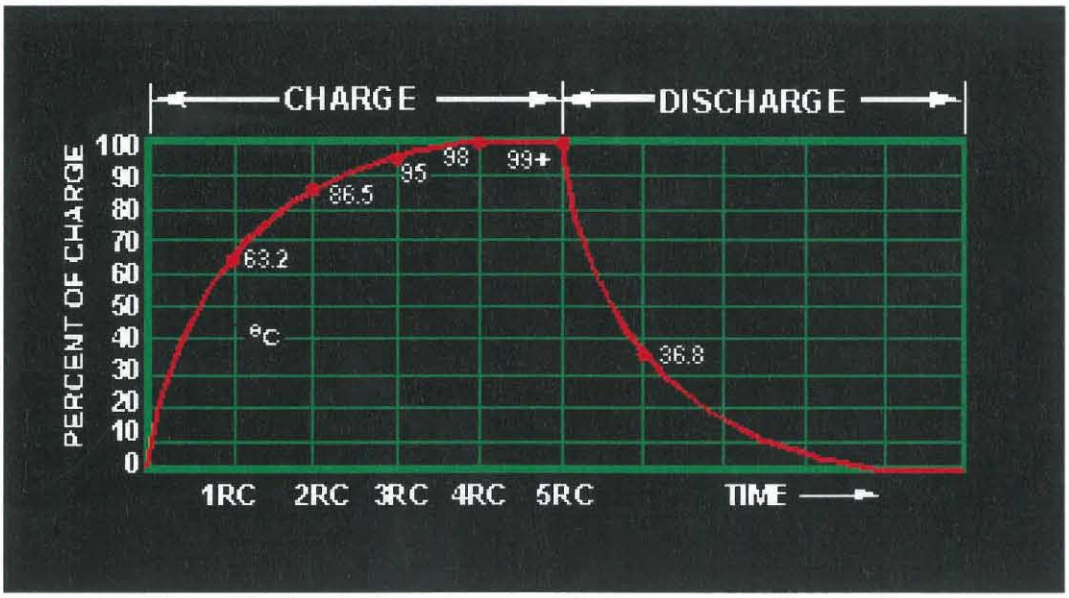

Figure 4.3: Graph of the charge and discharge curves of a capacitor

By connecting an ultra-capacitor to a power supply with unlimited current output the capacitor would charge much more quickly, but because of the equivalent series resistance of the ultra-capacitor (shown in detail in sub-section 0) it would still follow the same trend, but with a much shorter time constant.

Charging with Constant Current

When charging an ultra-capacitor with a constant current, as equation (4) suggests, the momentary increase in voltage is constant, so the voltage increases in a straight line, i.e.

$$\frac{\Delta V}{\Delta t} = Const. \tag{6}$$

To demonstrate this effect a bench top power supply was set to an output of five volts and given a current limit of two amperes. There was only one type of ultra-capacitor available at the time of testing, a few Nesscap 90 farad, 2.7 volt ultra-capacitors. Because the system they were being designed for was the data-logger, the voltage had to be at least five volts, so of the ultra-capacitors were connected in series to create an effective 45 farad, 5.4 volt ultra-capacitor.

The monitoring equipment used for this experiment consisted of a Tektronix MSO4042 oscilloscope taking 10000 samples every 200 seconds, and two Fluke multimeters. One of the multimeters was measuring the voltage across the ultra-

capacitor, the other measuring the current going into the ultra-capacitor, to verify periodically that the readings on the oscilloscope were accurate.

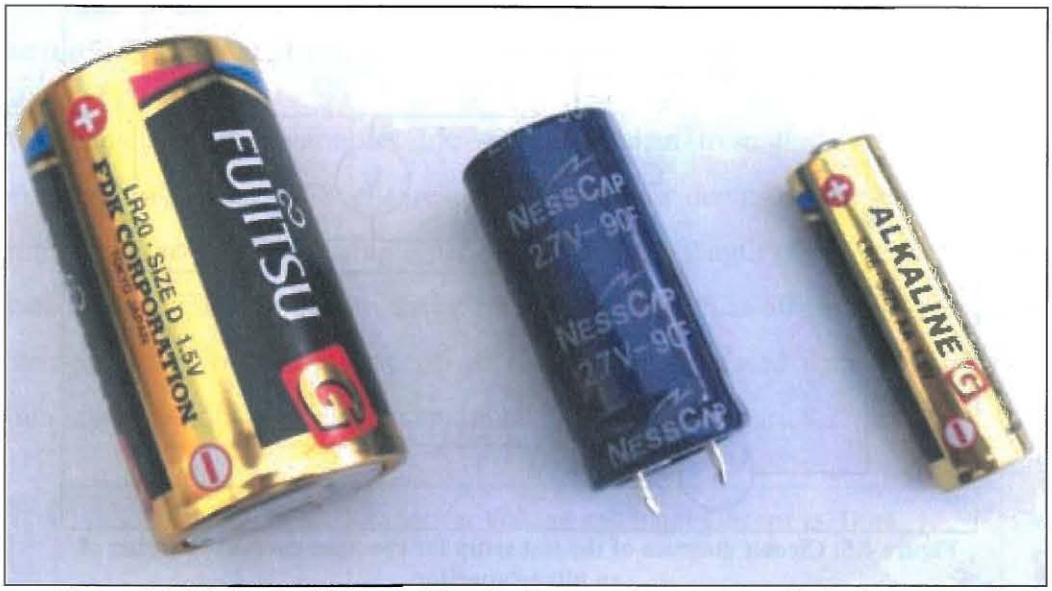

Figure 4.4: Photo of a 90 farad, 2.7 volt ultracapacitor next to a D-size battery and an AA-size battery

Two channels of the oscilloscope were used, one to monitor the voltage across the ultra-capacitor, the other to monitor the input current. The channel monitoring the voltage (channel one) was connected with the ground on the negative lead from the pair of ultra-capacitors and the probe connected to the positive lead. The channel monitoring the current (channel two) was connected across a ten watt, 0.1 ohm shunt resistor that was placed in series with the ultra-capacitor.

Because the oscilloscope was not isolated the grounds of both channels had to be connected up to the same node, which meant for this test the channel two probe was technically connected the wrong way round, as the direction of current flowing in would give the shunt resistor a voltage drop in the direction opposite what the oscilloscope was measuring; and therefore the oscilloscope would measure a negative voltage across the shunt resistor. To work around this the oscilloscope channel was set up to invert the channel two input.

With all the monitoring equipment connected up to the ultra-capacitors as shown in Figure 4.5, the power supply was switched on. The ultra-capacitors charged up from 0.1 volts to 4.5 volts in a straight line, with two amperes of current flowing into them for 89 seconds. Using these values in formula (4) gives the result of C

= 40.9 farads which, falls within the tolerance rating of the ultra-capacitors, which was negative ten percent to positive 20 percent.

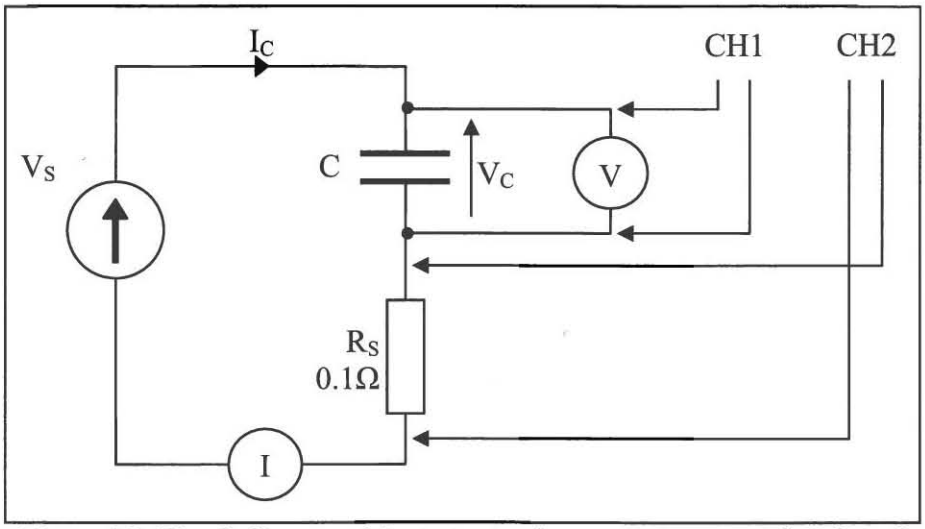

Figure 4.5: Circuit diagram of the test setup for constant current charging of an ultra-capacitor

After the 4.5 volt mark the current began to decay exponentially, which caused the voltage to begin dropping off and gradually curving over until it reached five volts. This was because the resistances of the circuit, including the shunt resistor, the resistance of the multimeter, the internal resistance of the power supply, and the equivalent series resistance of the ultra-capacitors all combined were enough to affect the input current at such a low voltage difference.

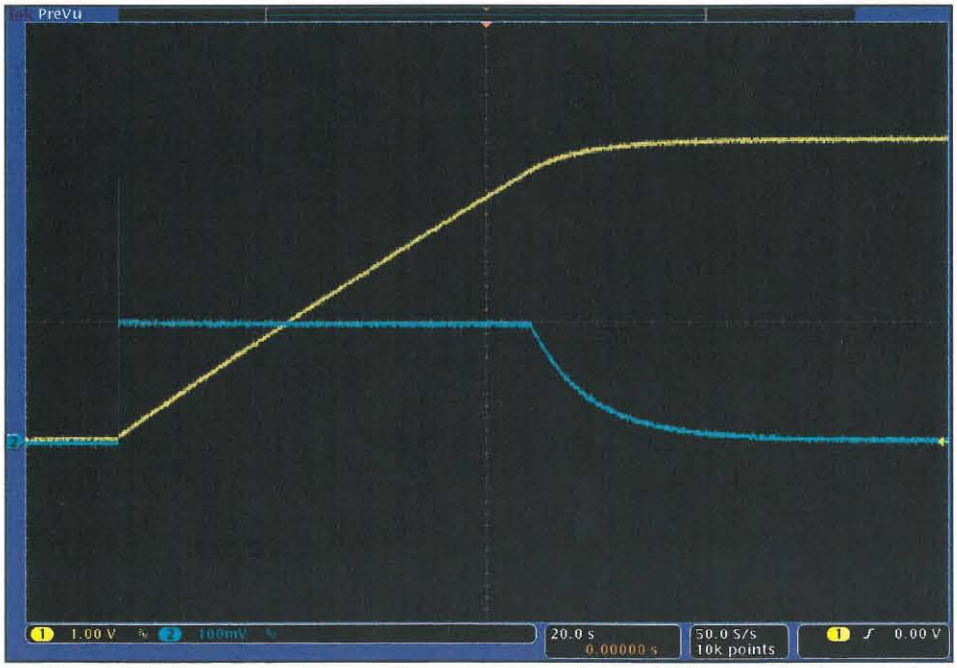

Figure 4.6: Snapshot of the oscilloscope screen image of the constant current charging of an ultra-capacitor

The screen image of the oscilloscope in Figure 4.6 shows the whole simulation in graphical form, with channel one (yellow) showing the voltage across the ultra-capacitor at one volt per division, and channel two, showing the input current of the ultra-capacitor at effectively one ampere per division.

A comma separated variables file was also taken from the oscilloscope, and processed in Microsoft Excel spreadsheet, to narrow down the number of samples from 10000 to 200, one sample per second for the length of the test. This was done by doing an average on every 50 samples, which at 50 samples per second averaged every one second worth of data. The processed data, which can be found in Appendix 4-a) was then graphed, as shown in Figure 4.7.

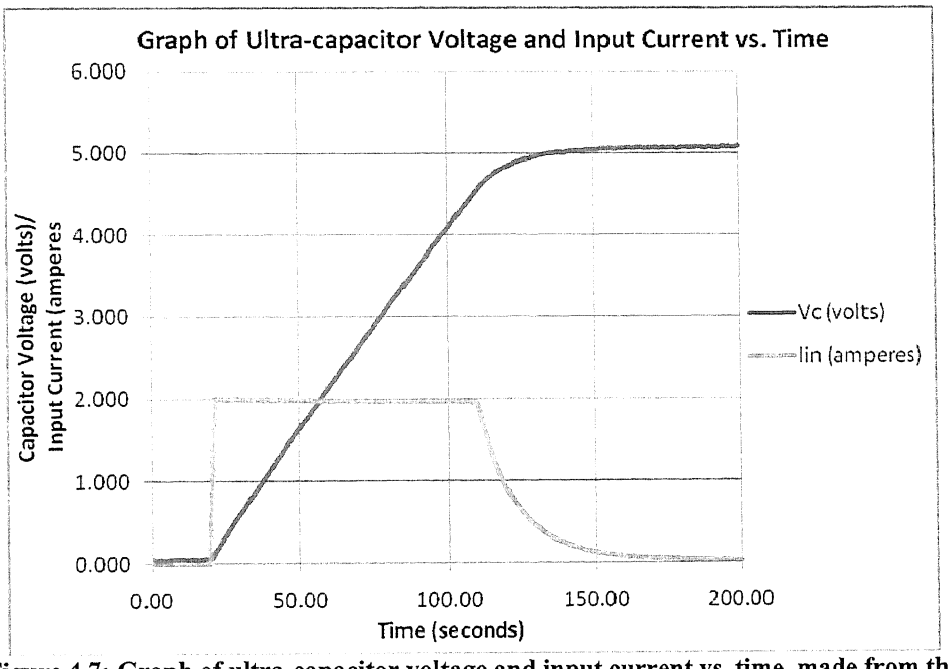

Figure 4.7: Graph of ultra-capacitor voltage and input current vs. time, made from the processed data for charging an ultra-capacitor at a constant two amperes

4.1.2 Discharging curves

The discharging curves of both standard capacitors and ultra-capacitors are also the same, and are very similar to charge curves. The difference between the charge and discharge curves are that the discharge curves are inverted, but the constant current discharge is a straight line, and the discharge through a resistor shows an exponential decay in both voltage and current. The voltage of a capacitor discharging through a resistor from a starting voltage V_0, follows the curve set by the an equation derived in the same way as equation (5):

$$V_C = V_0\left(\exp^{\frac{-t}{RC}}\right) \tag{7}$$

An experiment to test the discharge through a resistor was undertaken, using the same capacitor pair as used in the constant current charging test along with the same monitoring setup. The discharge resistor was made up of five 50 watt five ohm resistors, wired up in parallel to make an effective one ohm resistance, but the extra resistance of the shunt resistor and the multimeter in current mode increased the resistance to approximately 1.5 ohms. The circuit diagram for the test is shown in Figure 4.8.

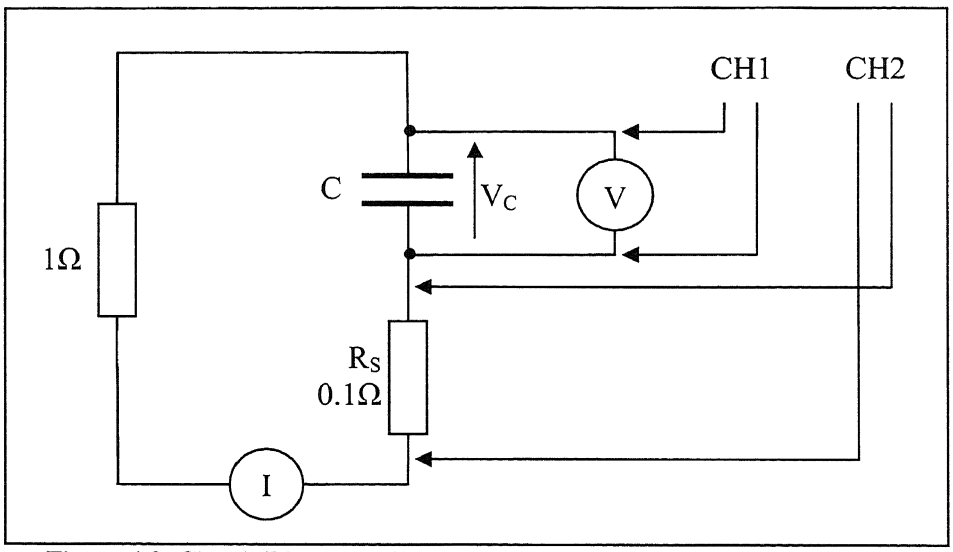

Figure 4.8: Circuit Diagram of the of the resistor ultra-capacitor test setup

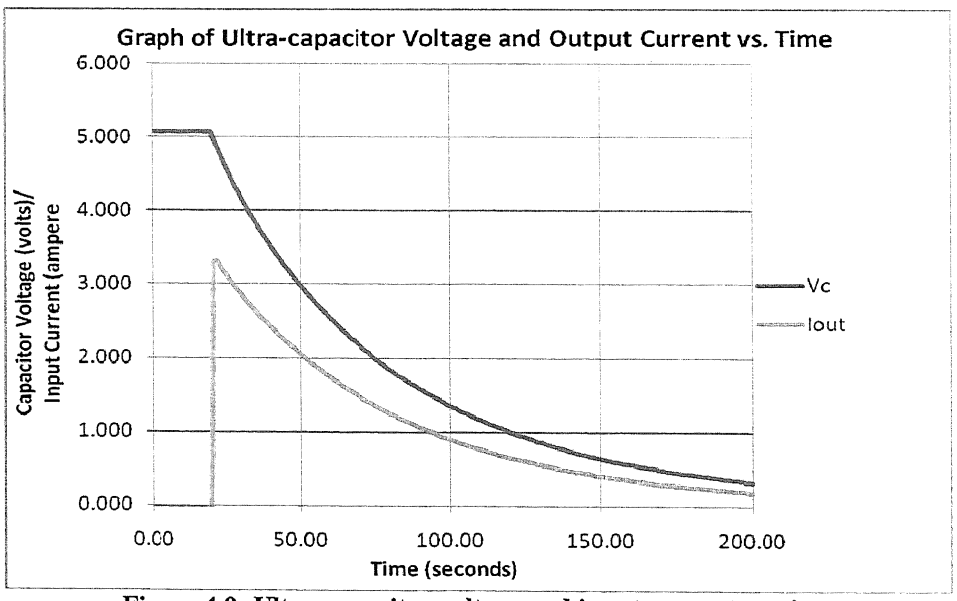

Figure 4.9: Ultra-capacitor voltage and input current vs. time

When the circuit was connected the output current started 3.3 amperes, and then both the voltage and the current immediately began decaying as dictated by equation (7). The ultra-capacitor did not fully discharge in this test, it discharged down to 0.33 volts over the 180 seconds the test was run for, at which point the current was 0.19 amperes. The data was extracted from the oscilloscope and processed, the resulting graph displayed in Figure 4.9, and the data itself in Appendix 4-b).

4.1.3 ESR

Capacitors and ultra-capacitors have similar circuit properties, including their equivalent circuit, with capacitance (C), leakage resistance ($R_{LEAKAGE}$), Equivalent Series Resistance (ESR), and Equivalent Series Inductance (ESL), as shown in Figure 4.10. The ESL, which comes mainly from the inductance of the leads, gives the capacitor characteristics of an inductor at higher frequencies where the impedance from inductance is much greater. However because the ESL only has an effect on the ultra-capacitor at high frequency, it is a very minor problem for the purposes of energy storage. The leakage resistance is usually extremely high, and is caused by current leaking through the dielectric inside the capacitor; this is the part of the capacitor that is responsible for self discharging.

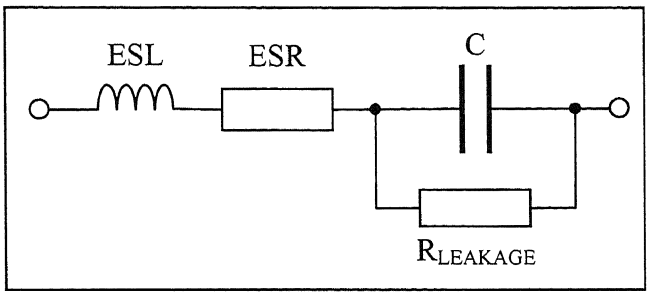

Figure 4.10: Equivalent circuit of a capacitor or an ultra-capacitor

The ESR is a more prominent effect. It causes a near instantaneous voltage drop inside the capacitor when the capacitor starts discharging, and when the capacitor stops discharging the voltage rises again by the same amount as its initial drop. This effect is not so much a problem at low output current, because the voltage drop caused by ESR is proportional to the current. At high current the voltage drop at the terminals can be hundreds of milli-volts, which is a major cause of power loss in an ultra-capacitor.

For example, a Cap-XX HS206 ultra-capacitor has a capacitance of 560 milli-farads and an ESR of 80 milli-ohms. When a step current of 1.4 amperes is drawn

from the capacitor the output voltage drops from 4.97 volts to 4.89 volts almost instantly, then starts evening out into the normal discharge curve. The voltage drops along the normal discharge until it the output current steps back down to zero amperes, where the voltage rises back up by the same amount as it stepped down in the first place.

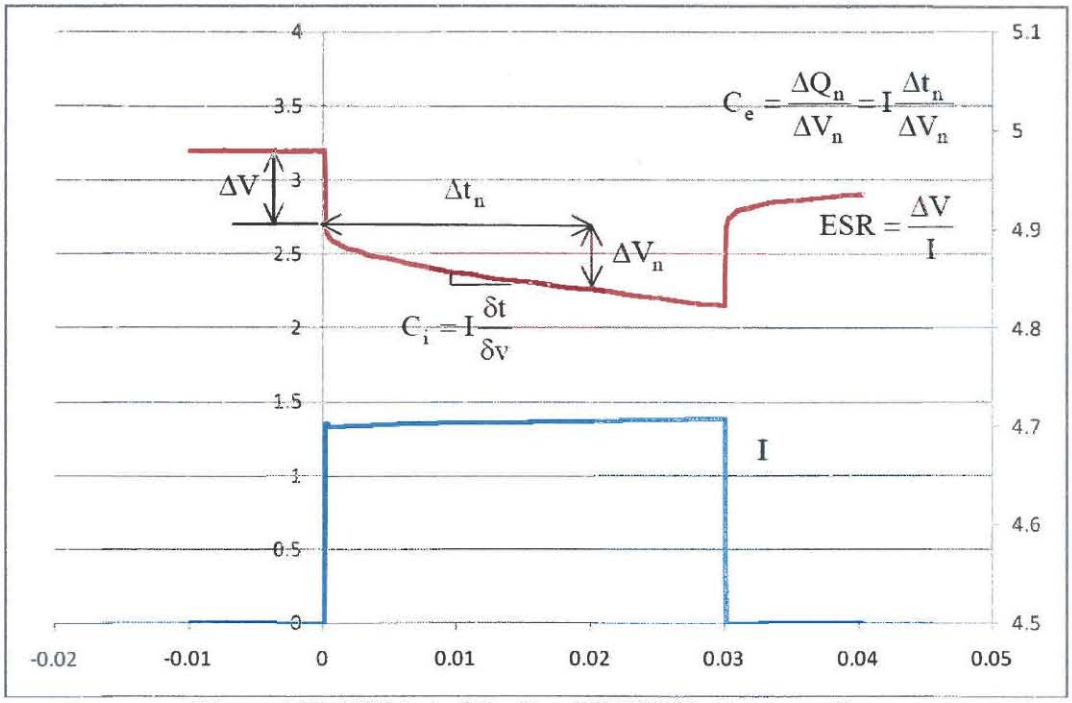

Figure 4.11: ESR test of the Cap-XX HS206 ultra-capacitor (Cap-XX Pty limited, 2007)

Figure 4.11 shows the effect in graphical form, where the axes are voltage (volts) on the right side, current (amperes) on the left side, and time (seconds) on the bottom. The blue line represents the output current and the red line is capacitor terminal voltage.

The ESR can be calculated from the graph by first taking a reading for the initial change in voltage when the load was connected and again for when the load was disconnected. The ESR is calculated from the voltage drop (ΔV), i.e.

$$ESR = \frac{\Delta V}{I} \tag{8}$$

A test was performed to test the ESR response of the Nesscap ultra-capacitor pair from the previous experiments. The test was set up in the same way the discharge test was set up, with the ultra-capacitor pair discharging through a resistor,

however because in this test the effect would be more visible if the current was greater, the resistance of the load was 0.4 ohms; which made the total resistance 0.86 ohms, including the shunt resistor and multimeter.

The initial current drawn from the capacitor by this resistance when it was connected up was 5.8 amperes, and because the test was run for only five seconds the effect of the discharge of the ultra-capacitor was negligible; so it is safe to say that the current remained at 5.8 amperes during the whole test.

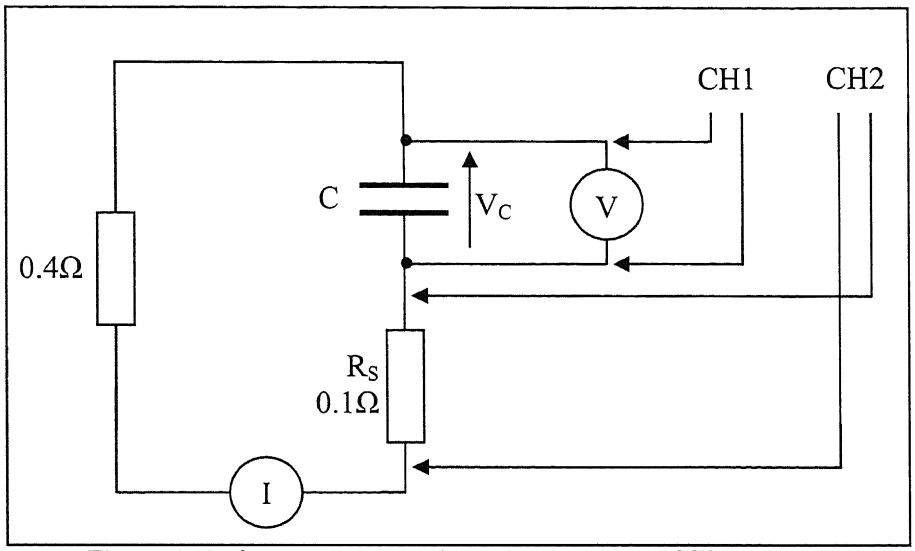

Figure 4.12: Circuit diagram of the ultra-capacitor ESR test setup

The other difference for this test was that a different oscilloscope was used, a Tektronix TPS2024, four channel, isolated inputs, two giga-samples per second oscilloscope, because the MSO4054 oscilloscope was unavailable at the time. The channels were connected in the same way as in the previous tests, with channel one monitoring the capacitor voltage, and channel two monitoring the shunt resistor to measure the current as shown in Figure 4.12.

As expected the voltage dropped as soon as the load was applied, then discharged slowly as the current was drawn from it, and jumped back up when the load was disconnected, as shown in Figure 4.13.

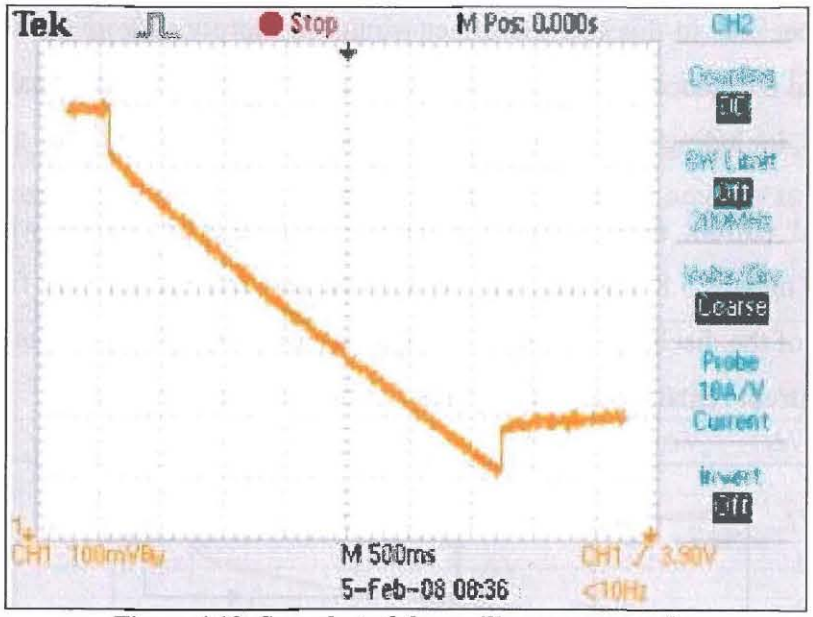

Figure 4.13: Snapshot of the oscilloscope screen for the ultra-capacitor ESR test

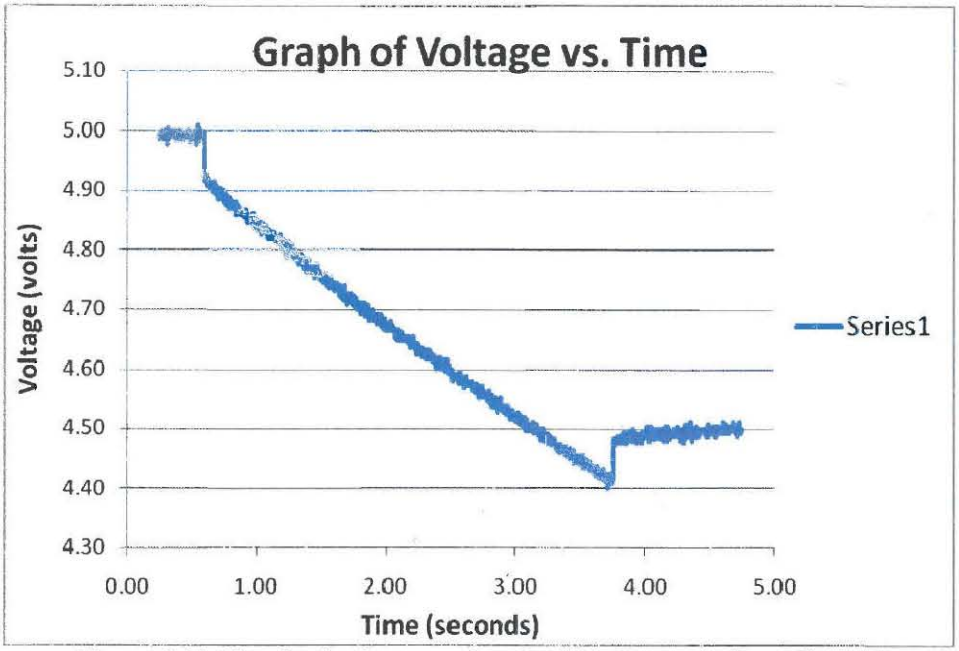

Figure 4.14: Graph of voltage vs. time for the ultra-capacitor ESR test

The results that were taken from the experiment were graphed, and because in this experiment the transients in the data needed to be recorded, the graph for the experiment was made from the raw data, as shown in Figure 4.14. As the graph shows, and the data backs up, the immediate voltage drop when the load was connected was 0.07 volts, and when the load was disconnected the immediate voltage rise was also 0.07 volts. Using these values in formula (8) gave an ESR value of 12 milli-ohms for both ultra capacitors, or 6 milli-ohms for each ultra-

capacitor, which is comparable to the value given by the datasheet (Nesscap Co. Ltd., 2005) which specifies that it will have an ESR of less than 8 milli-ohms.

4.1.4 Voltage Balancing

Because the breakdown voltage of an ultra-capacitor is so low, around 2.5 volts, and often five volts or more is required for a power supply; ultra-capacitors often need to be connected in series to make up the voltage required. However, when connecting ultra-capacitors in series and charging them up to their maximum voltage, care must be taken. This is because the capacitance of a given ultra-capacitor product could vary a lot, depending on the tolerance the manufacturer has set, i.e. for a tolerance of negative ten percent to positive 20 percent, the capacitance of each ultra-capacitor could vary up to 30 percent.

When two ultra-capacitors of varying capacitance are connected in series and charged like in Figure 4.15, the voltage across C_1 depends on the ratio C_1 divided by C_1 plus C_2, and the input voltage, as shown in the equation below:

$$V_{C1} = V_S \times \frac{C_2}{C_1 + C_2} \qquad (9)$$

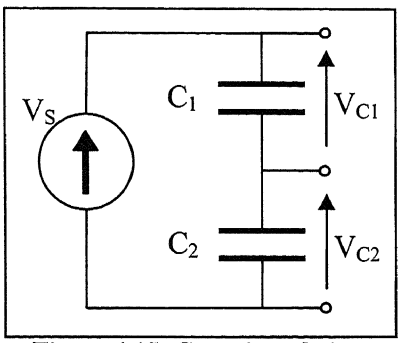

Figure 4.15: Capacitors being charged in series

Using this equation it can easily be shown that charging ultra-capacitors of different values in series results in different voltages across each ultra-capacitor, so if the rated voltages of both ultra-capacitors are equal, then one ultra-capacitor would reach its breakdown voltage before the other. At this point if voltage across both ultra-capacitors is less that the source voltage then the ultra-capacitors will keep charging, therefore overcharging the already fully charged capacitor. This could cause permanent damage to an ultra-capacitor and needs to be accounted for with a voltage balancing circuit.

For example, take two 90 farad 2.7 volt ultra-capacitors from opposite ends of the tolerance range, negative 10 percent and positive 20 percent, their values are 81 farads and 108 farads, respectively. If these two ultra-capacitors are connected in series with no voltage balancing circuitry as shown in Figure 4.15 with C_1 is 81

farads and C_2 is 108 farads, and charged up to five volts total, the voltages across each capacitor can be calculated using equation (9), i.e.

$$V_{C1} = 5 \times \frac{108}{81+108} = 2.86 \text{ volts}$$

$$V_{C2} = 5 \times \frac{81}{81+108} = 2.14 \text{ volts}$$

As seen in calculations the voltage across the 81 farad ultra-capacitor gets up to 2.86 volts, 0.16 volts above its rated voltage, which is likely to cause damage to the ultra-capacitor, which could mean a dead ultra-capacitor in the worst case, or an ultra-capacitor with degraded performance and/or lifetime in the best case. The percentage different in this case is

Voltage balancing circuits are designed to prevent overcharging without cutting down on the capacity of the other ultra-capacitors in the circuit. They effectively bypass any fully charged ultra-capacitors or batteries so that the other components in series with them can get fully charged as well can get charged. The circuits could be passive, using a high current resistive voltage divider to help maintain an even voltage, or even using zener diodes to bypass each ultra-capacitor when the voltage exceeds the zener voltage. These passive circuits however are not very power efficient, and in the case of the resistor balancing circuit the energy would constantly be drained through the resistors.

Active balancing circuits are much more common due to their higher efficiency, and the ability to balance capacitors at higher currents. These circuits normally use an operational amplifier, a voltage reference and a very low current resistive voltage divider for comparison with the reference. For smaller ultra-capacitors it is possible to connect the output of the operational amplifier through a resistor to the ultra-capacitor for balancing, as in Figure 4.16. This circuit is the layout for two ultra-capacitors in series, but can easily be modified for as many in series as are needed to achieve the required voltage.

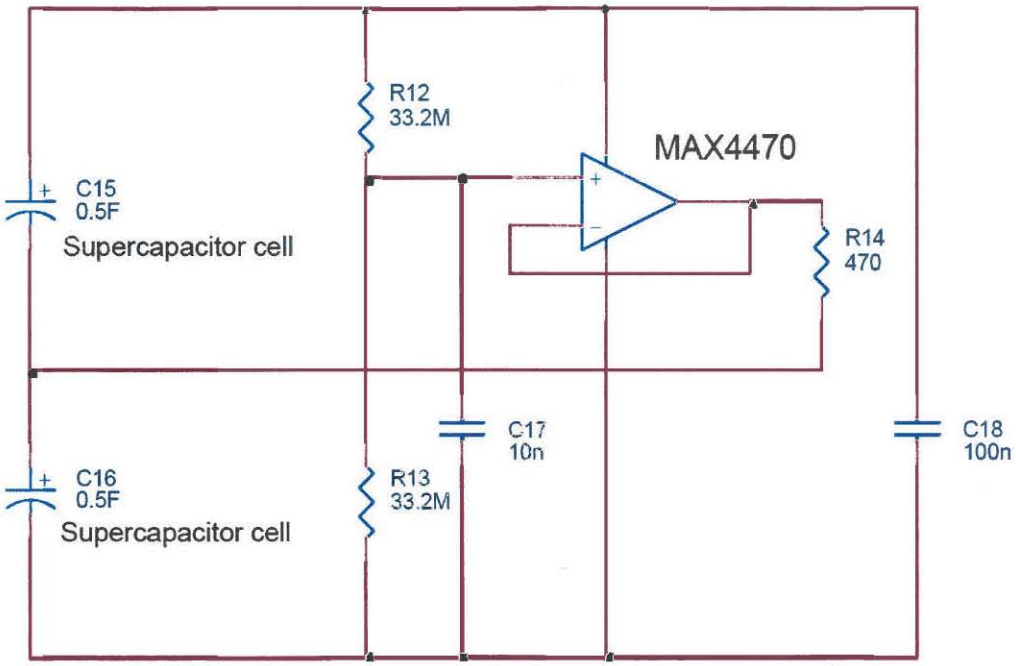

Figure 4.16: Active voltage balancing for ultra-capacitors (Cap-XX Pty limited, 2006)

For higher capacitance ratings however, a much higher current option must be used, where the output of the operational amplifier, or comparator in this case, controls a switch for a bypass resistor, as shown in Figure 4.17. In this case the bypass circuitry operates for a single ultra-capacitor, rather than a whole lot tied together. This gives better reliability because it doesn't rely on the voltages across other ultra-capacitors, only on its own voltage to work, so the bypass, and consequently the balancing circuit is more effective.

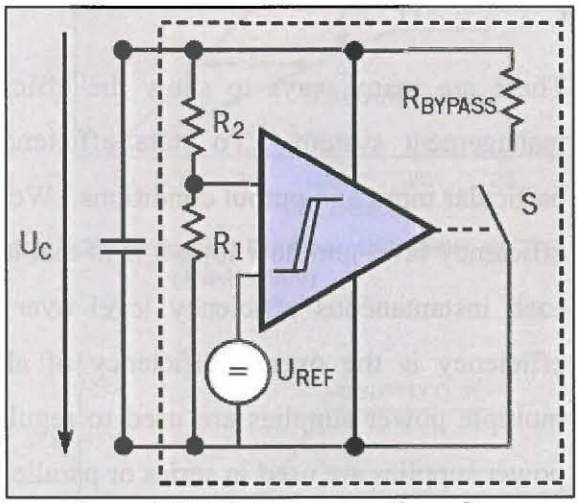

Figure 4.17: High current active voltage balancing for an ultra-capacitor cell (Prophet, 2003)

A major disadvantage to this circuit is that it requires a reference voltage and a comparator that operate at low input voltages which presents a problem in the design stage; but once the design is working for a given ultra-capacitor it can be copied for any other ultra-capacitor with the same rated voltage.

4.2 Modern Power Management Systems

Most modern embedded electronic systems run on low voltage, normally five volts or 3.3 volts, but recently coming down to as low as 2.5 volts or even 1.8 volts. They often draw a wide range of currents, from milli-amperes or sometimes even lower in sleep mode up to many amperes or even tens of amperes is common in full running mode. One thing all these embedded systems have in common is that they work better with a clean, smooth voltage on the supply rail.

Often a single power supply works fine for an embedded system, especially for those that are powered off the utility mains, so they have near unlimited power and efficiency is not as much of an issue. However when the system is powered off a battery a higher efficiency would make it run for a much longer period of time, and even running off the utility power it would cost less to use a more efficient power supply. Because of this the goal for many designers of most embedded systems is to design the most efficient power management system for a particular application.

There are many ways to show the efficiency of a power supply or a power management system. To state efficiency normally means the efficiency at particular input and output conditions. Weighted efficiency takes into account the efficiency level and how long it is at that level, so it is effectively the averages of each instantaneous efficiency level over the full operating period. The line efficiency is the overall efficiency of all the power conversion stages when multiple power supplies are used to regulate multiple voltage rails, whether the power supplies are used in series or parallel or both.

Among the simplest of ways to make a system more efficient is to, quote, "Turn it off if you're not using it, lower the voltage, and reduce clock frequency" (Vrana, 2001). A good power management system will turn parts of the circuit off that are not being used, or at least put them into low power or sleep mode, and will have the main processor running on the minimum frequency the application needs to run properly thus conserving energy, as power used by an integrated circuit is proportional to the square of the frequency.

Because some individual power rails in a power management system with multiple supply rails could be switched off some of the time, there may need to be a power supply start up sequence. Some devices require one voltage rail be powered up fully before another rail begins power up, which is called sequential power up (Figure 4.20). Other devices need the voltage rails need to start power and reach their regulation voltages at the same time, which is called radiometric power up (Figure 4.20), or that the voltage of each rail must not deviate from each other until the lower voltage reaches its operating level which is called simultaneous power up (Figure 4.20).

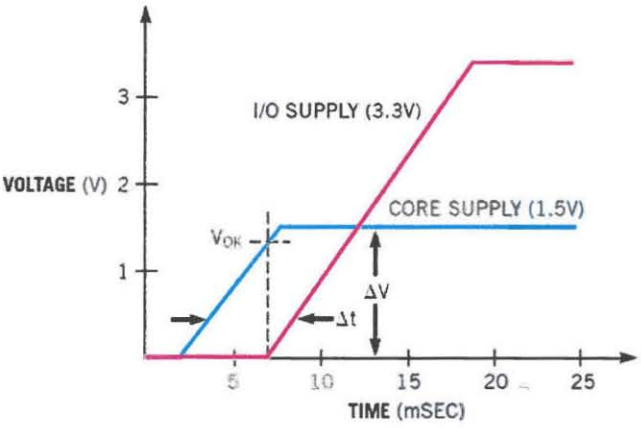

Figure 4.20: Example of sequential start up (Rush, 2000)

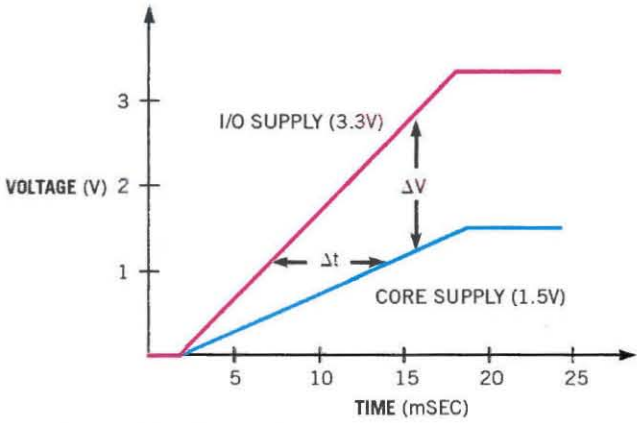

Figure 4.20: Example of radiometric power up (Rush, 2000)

A lot of modern integrated power supplies and power management circuits come with extra pins and features such as soft start and shutdown that can be used to ramp the voltage up at any rate chosen, which can be used for radiometric or simultaneous start up, or prevent a start up until another power rail is ready, which can be used for sequential start up.

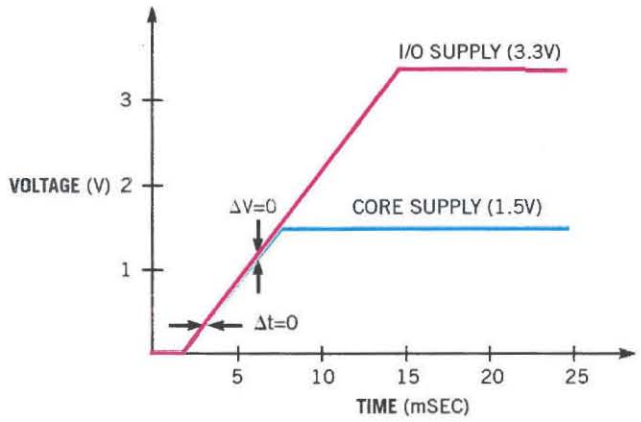

Figure 4.20: example of simultaneous power up (Rush, 2000)

Power management systems are commonly used for embedded systems, especially where multiple supply rails are needed. For example, in a system controlled by a Field Programmable Gate Array (FPGA), Digital Signal Processor (DSP), or Microprocessor which can operate at between 1.2 volts and 1.8 volts on the internal integrated circuit, but has buffers that output 3.3 volts to the external circuit. There may even be a need for positive and negative five volts rails for an operational amplifier and a twelve volt rail for motor outputs, and still the overall efficiency of the power system is often the main priority.

To get the best line efficiency for a multiple rail power management system, sometimes the efficiencies of individual power supplies must be sacrificed. In many cases the efficiencies of individual power supplies can be increased by a first converting the input voltage down to a lower bus voltage, which is converted down to the required rail voltages by separate power supplies, as shown in Figure 4.21, which often leads to greater overall efficiency. This also leaves the option of putting a low noise power supply on the final regulation stages of the power management system.

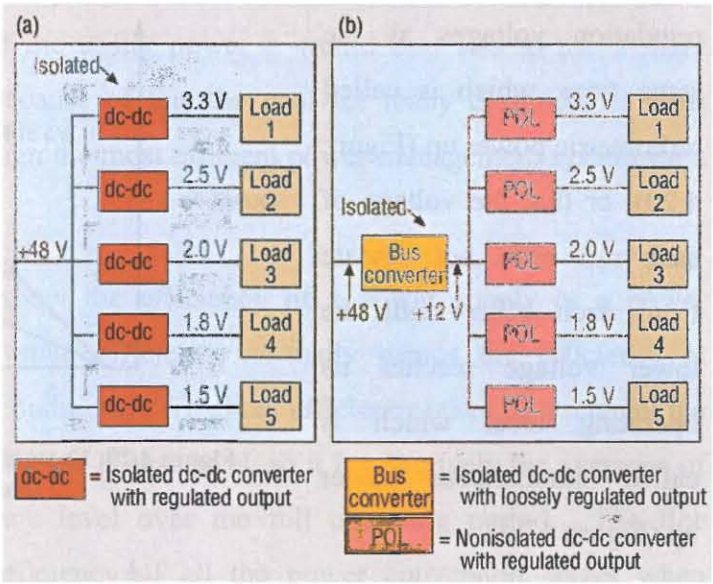

Figure 4.21: Example of how a bus converter can be used in a power management system (Morrison, 2004)

To help design a power management system it can be easier to break a circuit down into sub-circuits, and design a separate power supply for each sub-circuit, especially when there are multiple power rails or parts of the subsystem are likely to be switched off during normal circuit operation. A diagram of this is shown in Figure 4.21, where there are multiple power supplies each providing a different voltage rail.

In either case, it is possible to use a different power storage device for the input to each power supply, which gives near independence to each of the sub-circuit and allows the to be able to run even while other sub-circuit are shutting down due to lack of power. Doing this gives an opportunity to keep the main circuit going even after all the peripheral sub-systems have been forced to shut down, which means the control process can remain active for longer and possibly help get the whole system active again. An example of this is in Figure 4.22, where the energy storage component for each sub-circuit is an ultra-capacitor bank. The ultra-capacitor banks can be any size the sub-circuit needs it to be, and can be charged from a power source or battery when it runs low on energy by switching on the switch to the power source.

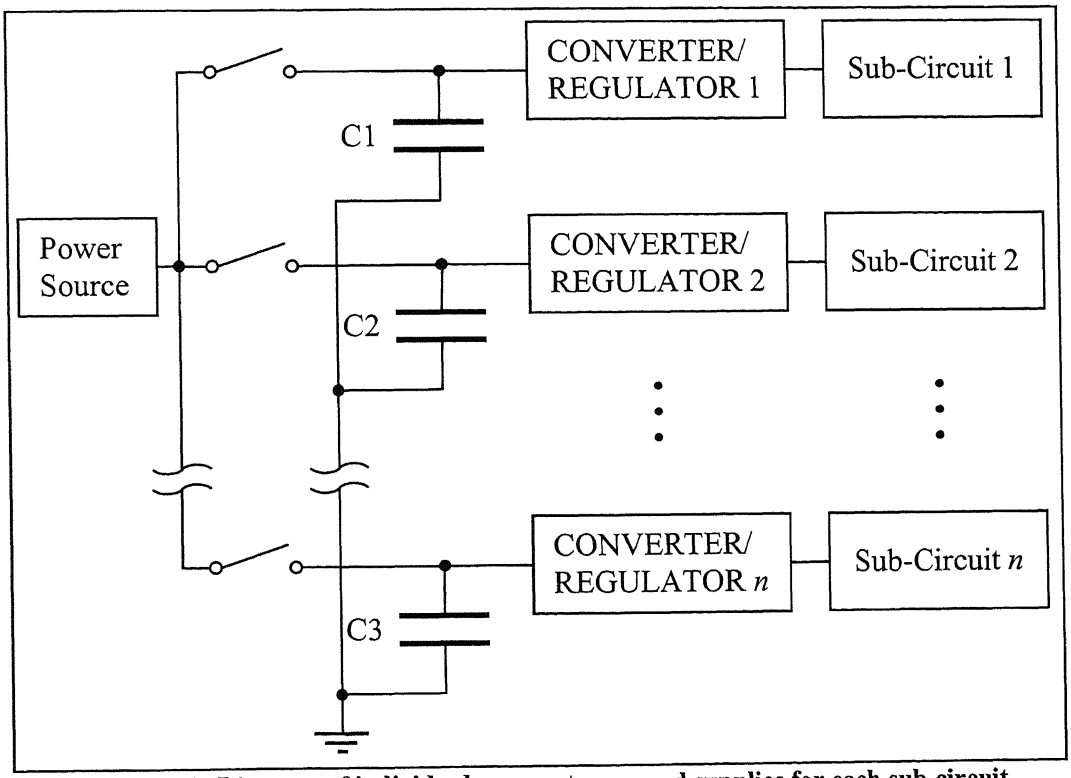

Figure 4.22: Diagram of individual power storage and supplies for each sub-circuit

Other factors apart from the efficiency that must also be considered include the Electro-Magnetic Compatibility (EMC) of the power supply, load current transient response, voltage ripple on the output and temperature response. When designing a power management system these factors must be taken into account to ensure the proper operation of the embedded system. Even when the power supply is simply for a motor or actuator other factors need to be designed for, like spikes and surges from the motors. If a motor is powered off the mains power

supply it needs a line filter to stop these spikes or surges propagating back through onto the mains line, where it could easily affect other devices in the area.

4.2.1 Power Supplies – Input Voltage Characteristics

It is common knowledge that step-down regulators and converters require the input voltage (V_{IN}) to be higher than the output voltage (V_{OUT}) to work properly; and the minimum difference between the output and input voltages that the converter works is called the minimum drop-out voltage ($V_{DROPOUT}$), where $V_{DROPOUT} = V_{IN} - V_{OUT}$.

When using batteries for power storage the dropout voltage is relatively easy to overcome by using a higher voltage battery or using a lower output voltage, because the discharge curve of a battery is relatively flat most of the time, until almost all the charge is gone when it drops rapidly. However, when using ultra-capacitors as a storage device the dropout voltage can be a major problem, as the voltage drops linearly with constant current. Because of this effect the capacitor voltage reduces to the drop-out voltage a lot faster than with a battery, which is a potential problem for anyone designing a system using an ultra-capacitor as storage.

Two experiments were performed to test how two different types of converters, a Low Drop-Out regulator (LDO), and a step down Switch Mode Power Supply (SMPS), worked with an ultra-capacitor as the storage device, what each system does when the dropout voltage of the converter is not achieved and how they react to a change in input voltage when they are regulating. The tests were performed using the capacitors as used in the tests above, only this for these tests three 90 farad, 2.7 volt capacitors were wired up in series making an 8.1 volt, 30 farad capacitance. The capacitors were charged to 6.8 volts in each case, and the load for these tests was a variable resistor which was adjusted to draw one ampere of current from the output.

The monitoring equipment was theTPS2024 oscilloscope, this time using all four channels, one for the input voltage or capacitor voltage, one for the input current, one for the output voltage and the last one for the output current. For each channel being measured a multimeter was also used to confirm that the

oscilloscope was displaying the correct voltage. The test configuration is shown in circuit diagram form in Figure 4.23.

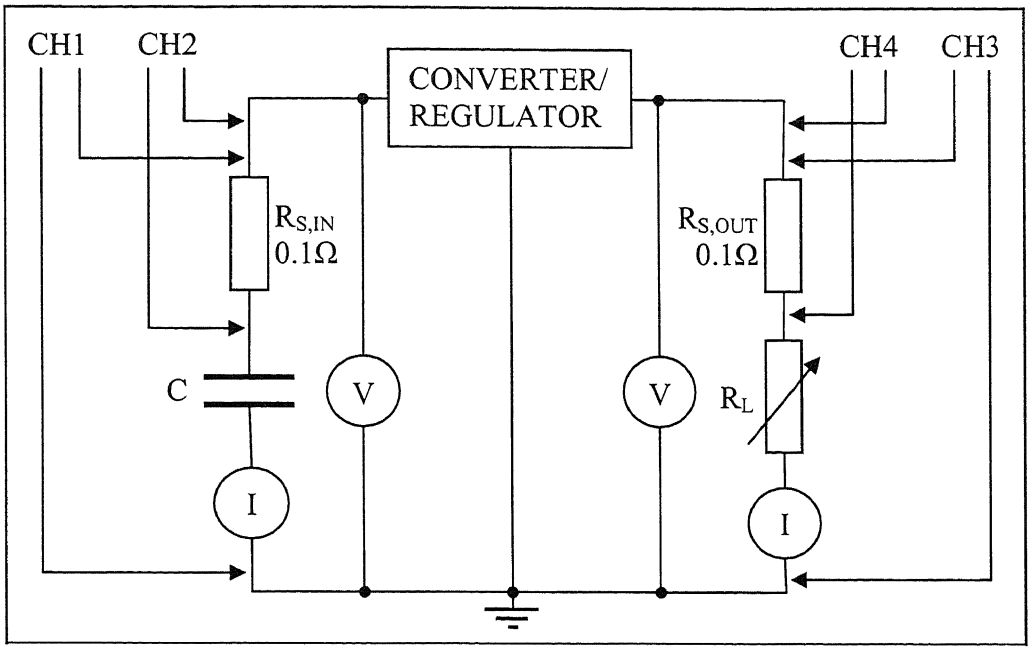

Figure 4.23: Circuit diagram for testing the dropout voltage of a step down converter or regulator

Low Drop-Out Regulator

The low drop-out regulator used for this test was a National Semiconductor LM2941, the same chip that was used in the first revision of the data-logger. When put into the test circuit and connected to the power source (the ultra-capacitor) the LDO regulator started up and pulled the output voltage up to 3.6 volts, as set by the feedback circuit. During the regulating stage of the test the output current and input current were doth one ampere, and they were equal all throughout the test.

71 seconds after the discharge started the voltage began to drop because the regulator had come to its minimum drop-out voltage, and could no longer properly regulate. This point related to an input voltage of 4.44 volts, which meant that the LDO had a minimum drop-out voltage of 0.84 volts at one ampere of output current. After the 71 second point the output voltage started to drop, and consequently, because the load was largely resistive, so did the load current.

The data from this test was averaged out in a similar way to the previous tests, only taking the averages of every 10 samples in this case and cutting off the data

that was acquired before the regulator was switched on, then the results were graphed, as shown in Figure 4.25.

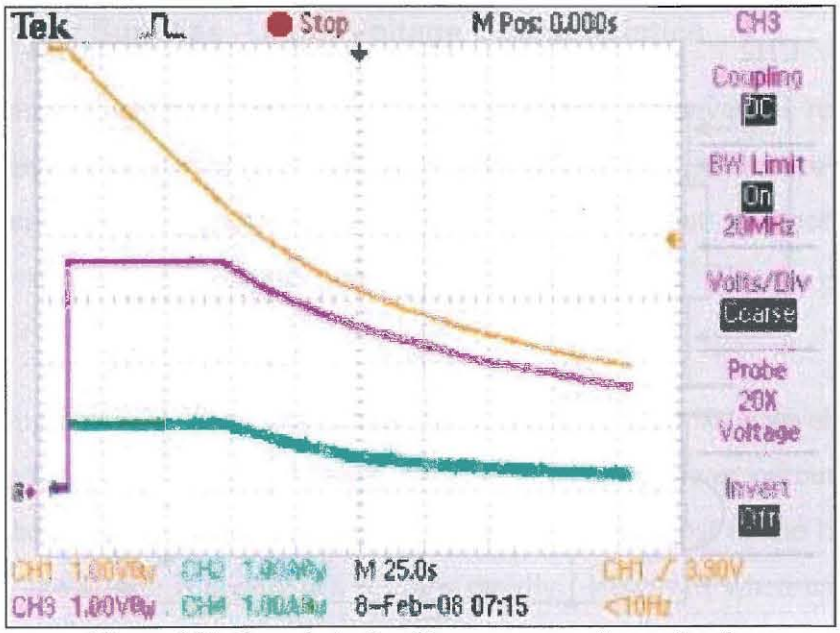

Figure 4.24: Snapshot of oscilloscope screen image for the ultra-capacitor discharging through an LDO regulator with a one ampere load.

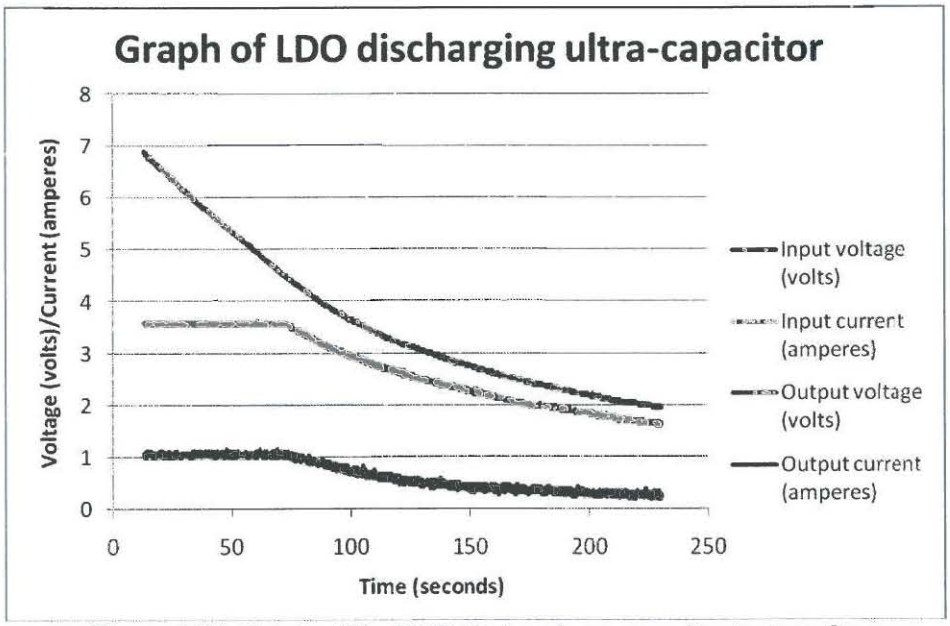

Figure 4.25: Graph of the LDO discharging a capacitor test results

Switch Mode Power Supply

The switch mode power supply used for this test was a Linear Technology LT3434 high voltage, three ampere, 200 kilo-hertz step-down switching regulator. The output of the regulator was set to 3.4 volts by a voltage divider from the output to the feedback line.

When the power supply and load were attached to the ultra-capacitor the output voltage immediately jumped up to 3.4 volts, where it stayed while the switch mode power supply was regulating. 99 seconds after the load was connected the drop-out voltage was reached, the voltage dropped immediately to 3.1 volts. The input voltage at this point was 4.3 volts, so the minimum dropout voltage of the LT3434 power supply was 0.9 volts when the output current was one ampere.

The regulator at this point dropped out of its regulation phase, so the output voltage and current began to drop as though through a resistor. The regulator stayed in this mode a further 91 seconds, until the input voltage dropped to 2.6 volts, at which point it switched off, as the internal circuitry is designed to do.

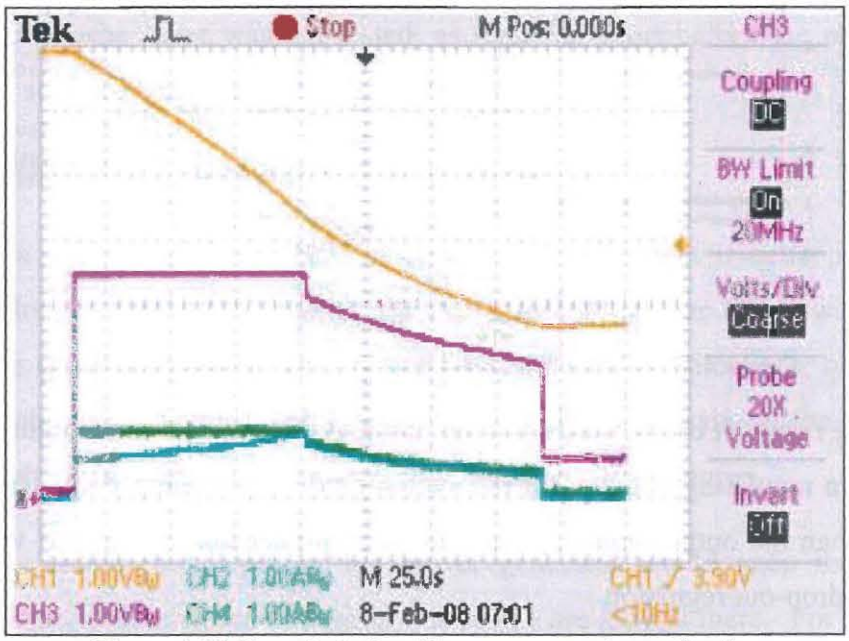

Figure 4.26: Snapshot of oscilloscope screen image for the ultra-capacitor discharging through a SMPS with a one ampere load.

As the snapshot in Figure 4.26 shows, the input current is much lower than the output current at the start of the test run. This is because while the switch mode power supply is regulating the input current (I_{IN}) needed for a particular output current (I_{OUT}) is roughly proportional to the ratio between the output voltage (V_{OUT}) and the input voltage (V_{IN}), i.e.

$$\frac{I_{IN}}{I_{OUT}} \propto \frac{V_{OUT}}{V_{IN}} \tag{10}$$

Also seen on the screen shot is that the output voltage only dropped to 0.6 volts. This is because an active load was used, and when the power supply switched off the base emitter voltage on the transistor in the active load stopped any current passing once the voltage dropped below the threshold voltage, effectively holding the output voltage at 0.6 volts. The results for the test were processed and graphed, as shown in Figure 4.27.

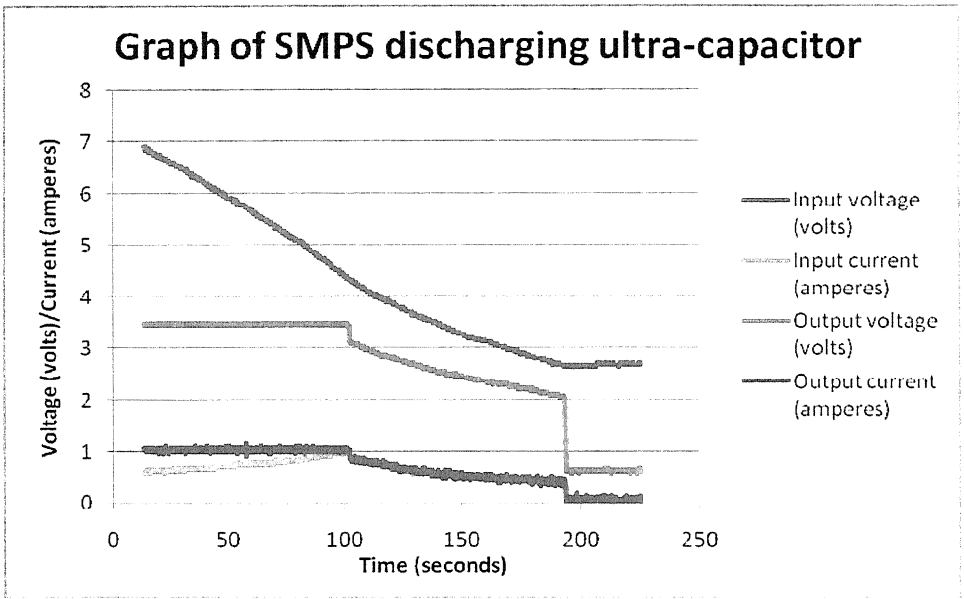

Figure 4.27: Graph of the LDO discharging a capacitor test results

From the results it can be stated that the input voltage must remain higher than the minimum regulating voltage, for the switch mode power supply this is 0.9 volts[4] higher than the output voltage, and 0.84 volts higher than the output voltage for the low drop-out regulator.

So using an ultra-capacitor as the power storage could require some management in itself. This could be done using either a very large ultra-capacitor bank for storage so the system can run for extended periods of time, or multiple ultra-capacitor banks so that the input bank can remain at the correct voltage by being charged through a step up converter, such as a charge pump, from the other ultra-capacitor banks, which utilises more of the stored energy in the other banks, as shown in Figure 4.8.

[4] Note that these dropout voltages are for one ampere, to maintain a higher output current the drop-out voltages will increase on both cases

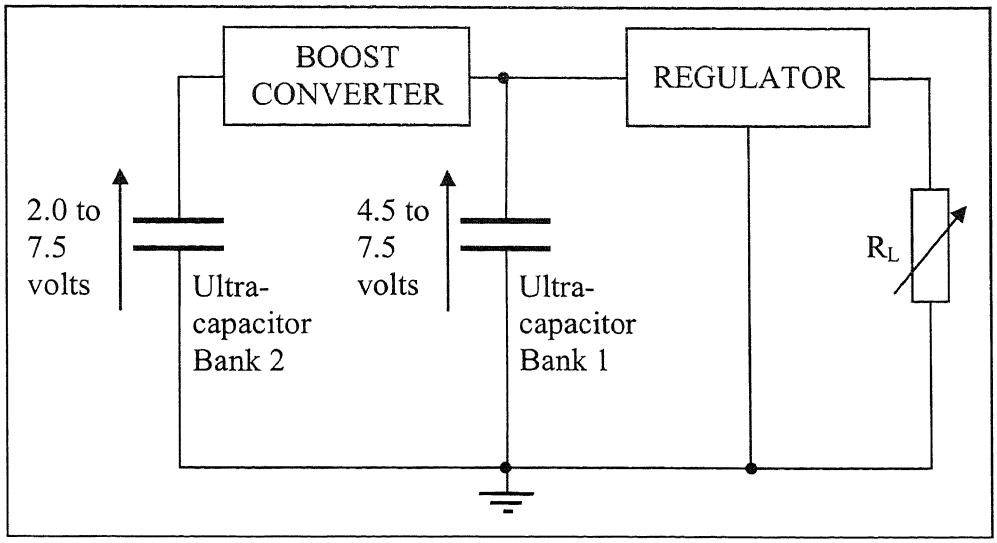

Figure 4.28: Diagram of the setup for using multiple ultra-capacitor banks to keep a constant input voltage for the power supply

Unfortunately the latter was not tested, as time ran short before the parts were obtained, so there was nothing to test the idea with.

4.2.2 Efficiency of Individual Power Supplies

Because a self powered integrated system like a data logger is better if it stays running longer, one of the major design considerations for the power supply should be efficiency; which should be considered in all applications, regardless. This is because with greater efficiency the overall power drain on the source is less, which means that the system overall will stay powered longer.

While increasing the output of the power generator would keep the system running longer, the chances of a generator failure are always there. For example, a solar panel works well during the day and a battery backup keeps the system running at night, but during winter time when the days are much shorter and the nights are much longer, the solar panel output might not be enough to power the system properly. With a more efficient power supply or management system the time it takes for the system to fully run out of power would last longer.

Because of this it is necessary to test the efficiency of a power supply and work out the most efficient power supply for the application. This can be done by measuring the input voltage (V_{IN}) and input current (I_{IN}), and using them to calculate the input power (P_{IN}) using the formula:

$$P_{IN} = V_{IN} \times I_{IN} \tag{11}$$

The output power (P_{OUT}) can be found in the same way, using the output voltage (V_{OUT}) and output current (I_{OUT}). Once the input and output power has been calculated the efficiency can be calculated using the following equation:

$$Efficiency = \frac{P_{OUT}}{P_{IN}} \tag{12}$$

or, combining equations (11) and (12):

$$Efficiency = \frac{V_{OUT} \times I_{OUT}}{V_{IN} \times I_{IN}} \tag{13}$$

Depending on how the efficiency is displayed, either a decimal or a percentage, the result of equations (12) and (13) may be multiplied by 100 to display a percentage.

Using equations (11) and (12) it was possible to use the results from the discharging tests to find out the effect of input voltage on efficiency of each of the power supplies[5] with one ampere of output current. This is because the input and output voltage and current were all measured, and the voltage dropped as the power was drained from the ultra-capacitor, which gave an input voltage curve that could be used for calculating the voltage response.

To find out the output current effect on efficiency a test was performed where the input and output voltage remained reasonably constant, input voltage about 6.9 volts and output voltage at 3.6 volts for the low drop-out regulator and 3.4 volts for the switch mode power supply. The output current was ramped up as slowly as possible so the oscilloscope could get enough readings of each current measurement.

The oscilloscope used for this experiment was the TPS2024 oscilloscope, which was connected up in the same way as in the test for discharging the ultra-capacitor through the regulators. The only difference to the test setup was that the power

[5] Note: Efficiency was only calculated for values in the regulation phase of each power supply

source in this case was a bench top power supply rather than an ultra-capacitor, as shown in Figure 4.29.

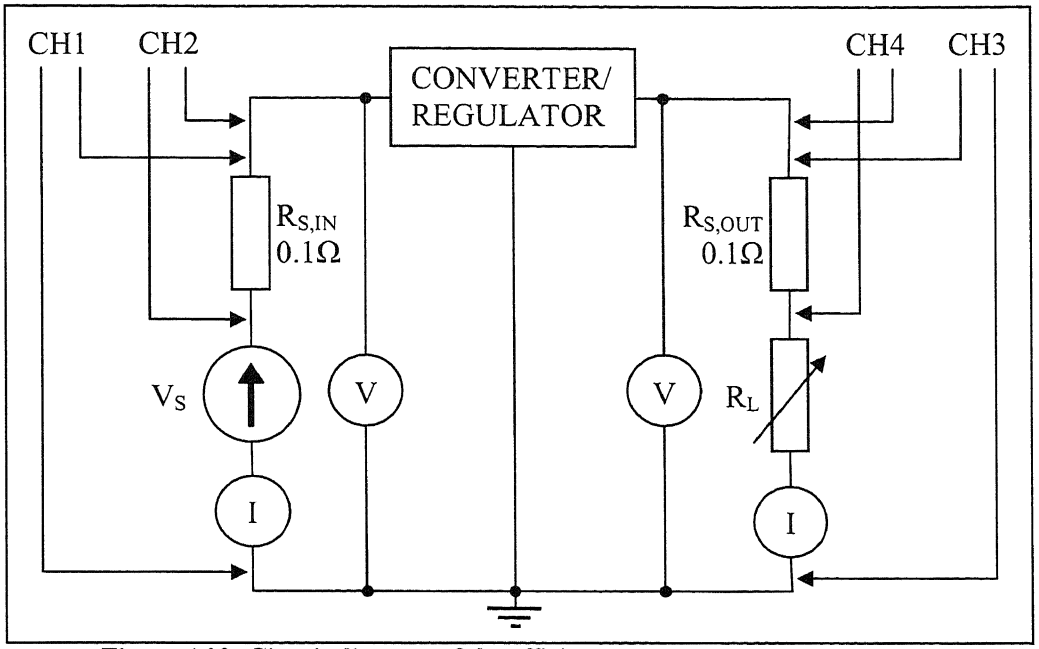

Figure 4.29: Circuit diagram of the efficiency vs. output current test setup

Low Drop-Out Regulator

The effect of input voltage on efficiency is effectively linear, as output voltage remains constant while in the regulation state, and the input and output currents are reasonably equal, i.e.

$$I_{IN} \approx I_{OUT} \tag{14}$$

or:

$$\frac{I_{OUT}}{I_{IN}} \approx 1 \tag{15}$$

and because Vin is the only variable in equation (15), inputting the information into the equation results in:

$$Efficiency \approx \frac{Const}{V_{IN}} \times 1 \tag{16}$$

which simplified shows that the efficiency is inversely proportional to the input voltage, i.e.

$$Efficiency \propto \frac{1}{V_{IN}} \tag{17}$$

Because of this relationship the efficiency will decrease as input voltage increases, which the results from the experiment back up.

The voltage response for the low drop-out regulator, as calculated using the results from the previous tests, started off at 55.5 percent for 6.9 volts, and as the voltage decreased, the efficiency of the low drop-out regulator increased, as expected with the input and output currents remaining the same the whole time. The efficiency peaked at 82 percent in the regulating phase, which happened right before the drop-out voltage was reached, which goes to show that a low drop-out regulator should only be used with a battery that is not far above the regulated voltage, where the efficiency is high. The results (shown in Appendix 4-c) were graphed, and are shown in

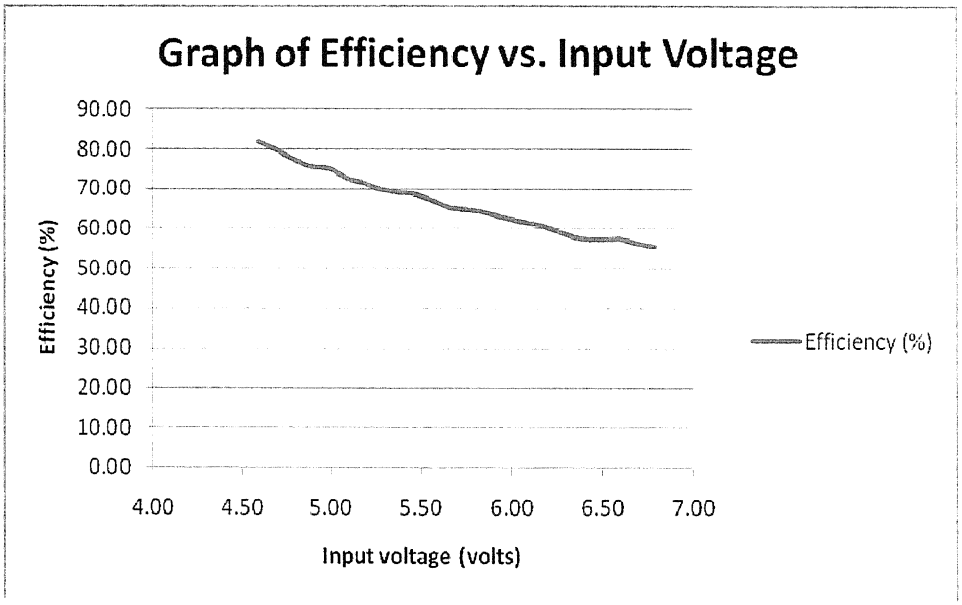

Figure 4.30.

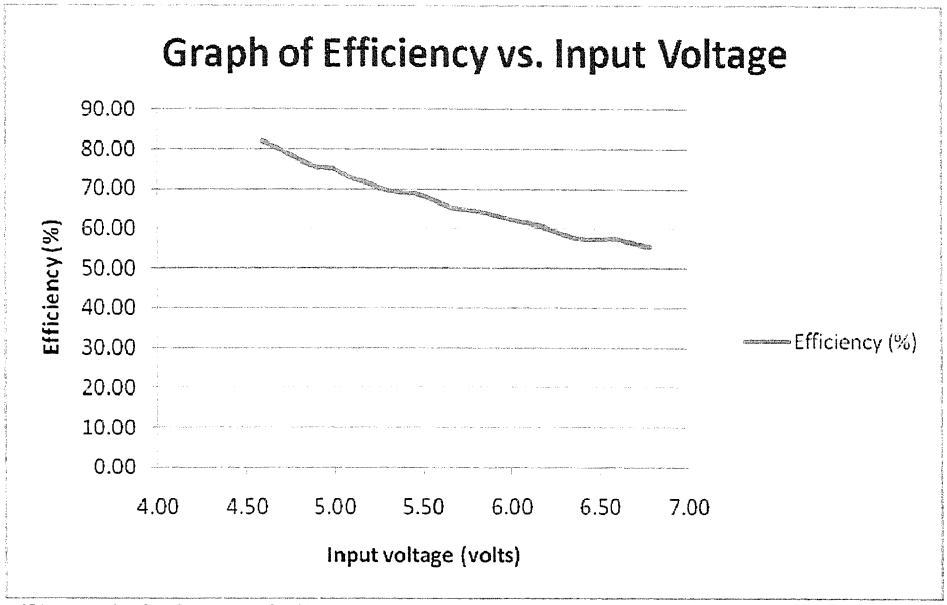

Figure 4.30: Graph of efficiency vs. input voltage for the low drop-out regulator

The results also show that a low drop-out regulator has a very low efficiency when the drop-out voltage is high, such as in an ultra-capacitor system where the capacitor voltage may have to be higher to maintain a constant supply to the system for longer periods of time.

To find the effect of efficiency versus the output current is a lot harder, because for a low drop-out regulator the input and output currents are so close to each other as in equation (16).

Because the input and output voltages can be assumed constant, equation (15) would only rely on the input and output current, i.e.

$$Efficiency \propto Const \times \frac{I_{OUT}}{I_{IN}} \tag{18}$$

In the case of an LDO, because the input current tracks the output current, the effect on efficiency depends on the relative difference in the two variables, rather than simply the change in variables themselves. Therefore, the effect on efficiency is minimal at higher output currents, but at lower currents the current required by the LDO control circuitry has a much larger relative effect, which pulls the efficiency down.

Switch Mode Power Supply

The efficiency of a switch mode power supply is much harder to calculate using formulas, because the ratio of the output current and input current is in proportion to that of the input voltage and output voltage, i.e.

$$\frac{I_{IN}}{I_{OUT}} \propto \frac{V_{OUT}}{V_{IN}} \tag{19}$$

Therefore, any increase or decrease in the input voltage will be matched by a decrease or increase, respectively, in the input current, which keeps efficiency at a reasonably constant value, as backed up by the results of the experiment.

When the test started with approximately one ampere at 3.47 volts output, the efficiency of the LT3434 power supply was about 87 percent, and as the voltage dropped there was a trend of efficiency dropping slightly, finishing at about 82 percent when the voltage was about 4.4 volts, just before the regulating region stopped. The graph of efficiency vs. input voltage which was calculated from the results of the discharge test, is provided in Figure 4.31, and the data is shown in Appendix 4-d).

These results show that the input voltage had very little effect on the efficiency of the converter, not even close to the effect it had on the low drop-out regulator. For this reason a switch mode power supply is one of the more ideal types of converters for a widely varying input voltage range.

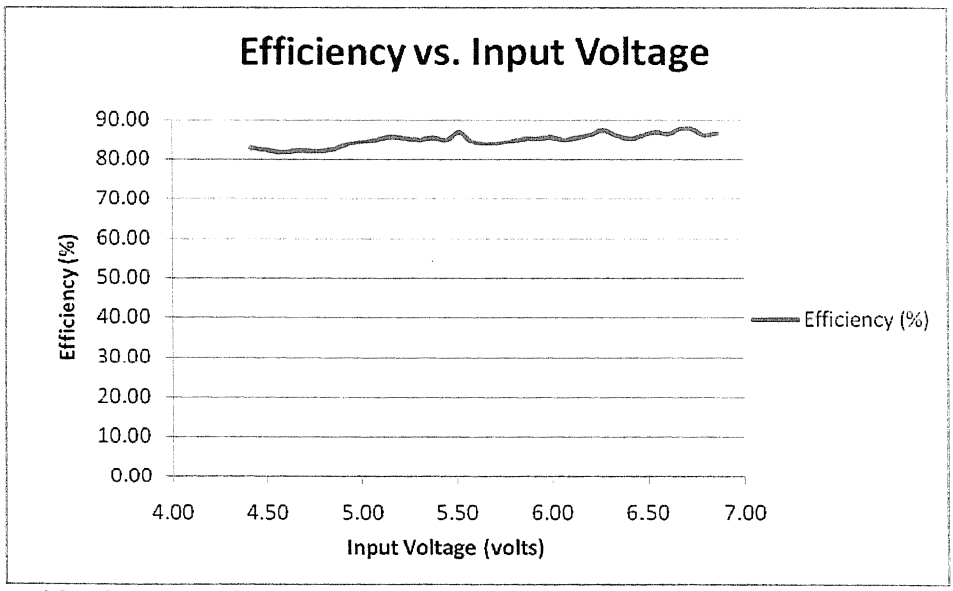

Figure 4.31: Graph of efficiency vs. input voltage for the LT3434 switch mode power supply

A varying output current has more of an effect. For example, with a switch mode power supply that has been designed for 1.5 amperes output current, the efficiency would normally be greatest at that output current, but will drop off when the output current is higher or lower than 1.5 amperes. This is because in a switch mode power supply design the output current depends largely on the inductor size and the duty cycle of the switch. So the target output current is set by selecting an appropriately sized inductor and the duty cycle changes to suit a range of currents around the target. However as the output current gets too far away from the target the duty cycle has to stay on or off for much longer periods of time, which strains the inductor and other components, therefore affecting the efficiency.

Many switch mode power supply chips have various techniques built into them, including burst mode for low currents or using two different switches with different inductors connected to each of them. Although these techniques do improve the range of output currents that provide reasonable efficiency, they still can not improve the efficiency at extremely low currents where the power supply control current and the losses over the inductor are much more significant, so it is often better to use an LDO in this case.

CHAPTER FIVE: FINAL IMPLEMENTATION INCLUDING POWER MANAGEMENT SYSTEM

5.1 Block Diagram of the Second Revision

The hardware of the second revision, although it was largely based on the first revision, had many differences, ranging from pins on the microcontroller being reorganised, to the board dimensions being changed. Many of these changes were made to correct mistakes made on the board, while many others were made to add new features, efficiency, expandability and reliability. A block diagram of the new hardware can be found in Figure 5.1, below.

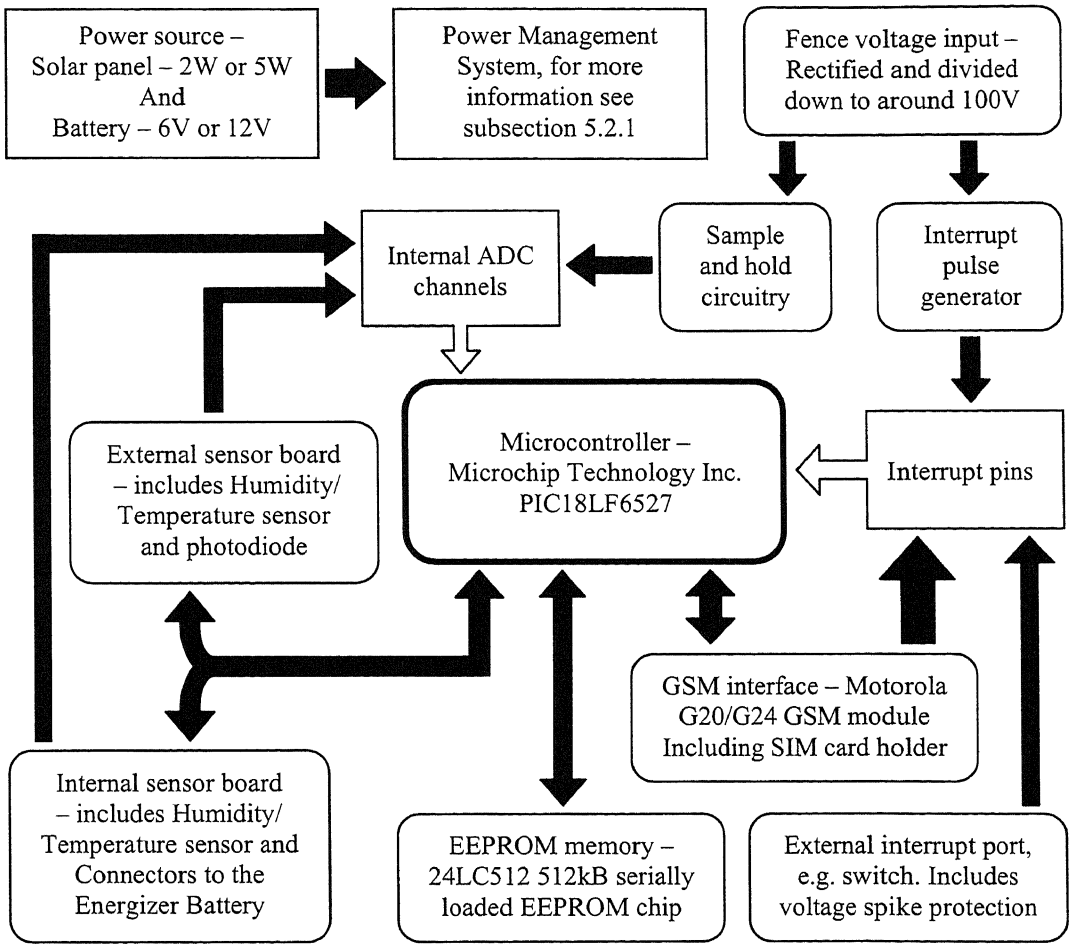

Figure 5.1: Block diagram of the second revision of the data-logger

Among the changes in the second revision were a new Power Management System, updated sample and hold circuitry, new temperature and humidity sensors with serial outputs, and a photo diode for sensing the light level. There was also a ten pin connector (not shown in the block diagram) for possible future upgrades to the system that could use a digital I/O port or PWM outputs, connected to the supply rail, ground, and all eight bits of Port-E.

Because the second revision had to be both researched for and designed in a limited time frame, some compromises had to be made regarding various parts of the design. Two of the main compromises were the efficiency of the power supply, because it would take too long to find a new one and get a working design to add on to the PCB, and leaving some environmental factors out, like lightning detection, pressure and rain fall.

The full schematics of the second revision, including the Main schematic, Power Supply schematic, Sensing schematic, and Communications schematic, can be found in Appendix 5:, and some sample circuits are shown throughout the next subsection.

5.2 Circuit Description of the Second Revision

5.2.1 Power Management System

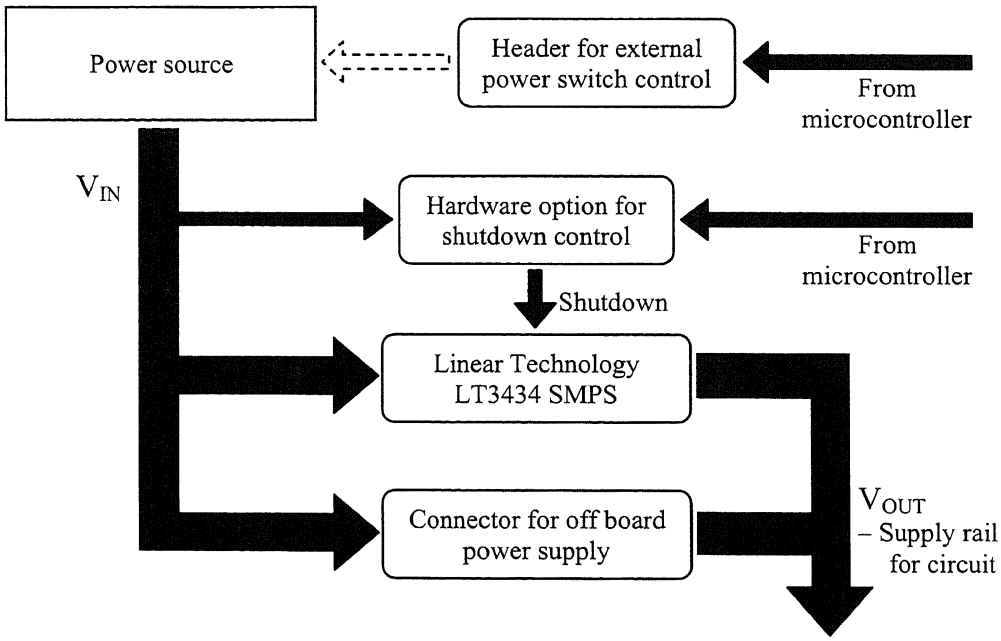

Figure 5.2: Block Diagram of the power management system hardware on the data-logger board

The power management system for the second revision of the data-logger was designed to work with different options for the power source, power storage devices, and different input voltages. The system was built around a Linear Technologies LT3434 three ampere, adjustable output voltage, Step-down (Buck) Switch Mode Power Supply (SMPS) with a Bipolar Junction Transistor (BJT)

output, because it was used in other Gallagher products and was already in the Gallagher inventory listing.

The LT3434 power supply had an efficiency of approximately 85 percent at an output current of two amperes with an input voltage of twelve volts and an output voltage of 3.3 volts, as shown in Figure 5.3, which was the current draw when the GSM module was transmitting to the network. However, at an output of one milli-ampere, for the same input and output voltages, the efficiency was approximately 60 percent, so it was not a good power supply to use when the output current was low; like during sleep mode when the output current could easily be less than 2.5 milli-amperes.

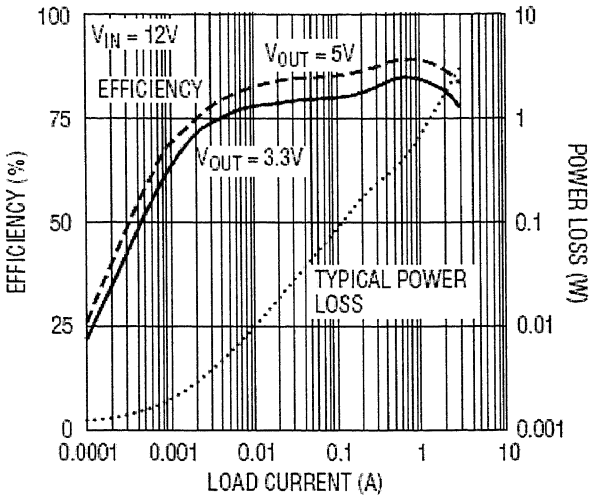

Figure 5.3: Graph of Efficiency and Power loss vs. load current for the LT3434 power supply (Linear Technology Corporation, 2006)

The power supply had an optional shut down pin, which could be used to turn the power supply off when it was not needed. The power management system used this by connecting the pin up to the microcontroller, which could turn the power supply on when the extra current was needed and turn it off to save power at all other times. Because this would require another power supply to power up the microcontroller to start with, and the other power supply would be off-board and working through a connector, and the using the controlled shutdown pin needed to be optional. This was done by placing a zero ohm link on the PCB, to connect the shut down pin to either the input voltage or the microcontroller pin, in the place of either R39 or R40, but not both, so as to avoid connecting the microcontroller pin to the input voltage, as shown in the circuit diagram in Figure 5.4.

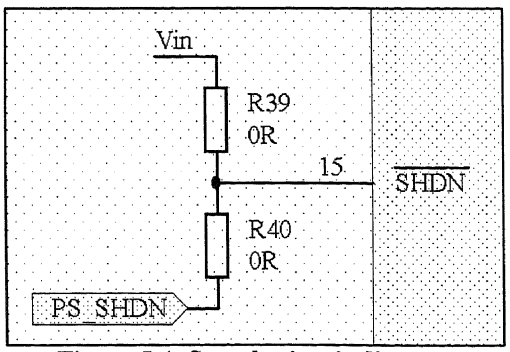

Figure 5.4: Sample circuit diagram showing the select method for the shut down pin.

The output voltage of the Power management system was set to 3.6 volts, so each of the power supplies in the system had to be set to the same voltage. On the LT3434 this was done using a resistive voltage divider to divide the required output voltage (3.6 volts) down to the 1.25 volt (plus or minus 0.025 volts) reference voltage on the feedback pin of the power supply control chip. This provided the control chip a reference for the power supply to maintain, which was how it provided regulation of the output voltage.

The output of the power supply chip was connected straight into a 27 micro-henry inductor, with a fly back diode (a Fairchild semiconductor SS24, two ampere average, schottky rectifier) from ground on the same connection, and on the other side of the inductor was a 100 micro-farad tantalum capacitor, and the voltage divider to the feedback pin, as seen in Figure 5.5. These parts formed what is known as the step down switch mode power supply topology, which is the simplest form of a switch mode power supply.

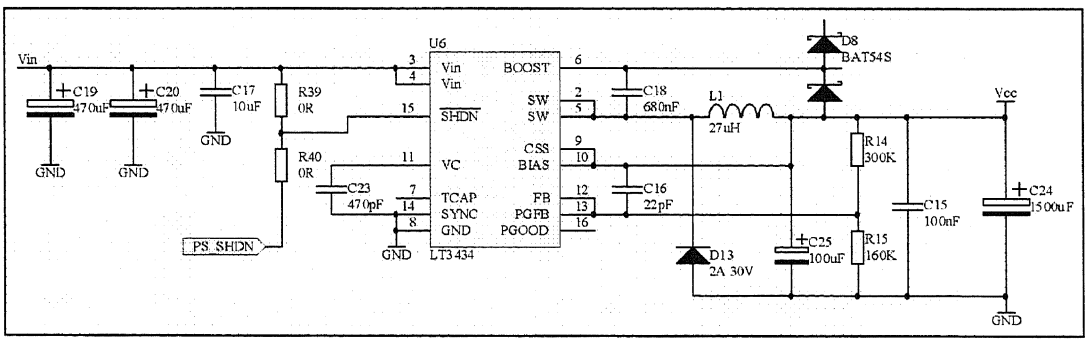

Figure 5.5: Sample schematic diagram of the LT3434 power supply and all associated circuitry

Because there was not enough room on the PCB for another power supply, and the power management system needed a small power supply for when the data-logger was in sleep mode, the smaller power supply had to be put on a separate PCB and provide power through a connector. Because the power supply was so small, however, it was possible to fit on a daughter board directly above the LT3434 power supply, using a Tyco-amp MicroMatch six way surface mount header on the main PCB and a matching through-hole plug on the daughter board.

The power supply selected in this case, was a Linear Technology Corporation LTC1433, 450 milli-ampere, adjustable output voltage, Step-down (Buck) Switch Mode Power Supply. This power supply, like the LT3434, used the step down

converter topology, but the LTC1433 power supply had two outputs, one for lower output currents (up to 100 milli-amperes constant switch current) and the other for higher output currents (up to 600 milliamperes constant switch current); which effectively made it a single integrated circuit power management system.

The peak efficiency of the LTC1433 power supply using the circuit shown on the first page of the data sheet (Linear Technology Corporation, 1998), was approximately 93 percent for an input voltage of five volts, an output voltage of 3.3 volts, and an output current of 120 milli-amperes, as shown in Figure 5.6. By using another configuration shown in the data sheet, it was possible to get more than 95 percent efficiency from this power supply, but the output current range was much narrower, so that particular configuration was not ideal for this application.

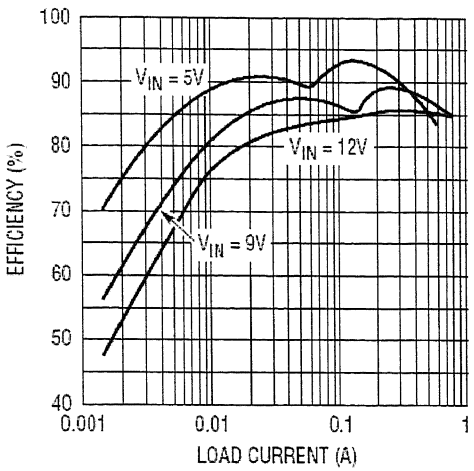

Figure 5.6: Graph of Efficiency vs. load current for the LTC1433 power supply (Linear Technology Corporation, 1998)

The final design of the power supply daughter board, as shown in , was connected to the system using the six pin header and plug pair, using pins one and two for the input voltage, pins three and four for the output voltage, and pins five and six for ground. The input power was smoothed by a 100 micro-farad tantalum capacitor and a 100 nano-farad capacitor high frequency noise suppression. The output, coming from both the small switch (SSW) and the big switch (BSW) outputs connected to a fly back diode (an On Semiconductor MBRS130, one ampere average, schottky rectifier) from ground, and a 22 micro-henry inductor which lead to the 3.6V supply rail, and a 100 micro-farad tantalum capacitor. The feedback pin, called the output voltage sense (V_{OSENCE}) pin on the LTC1433, was connected through a resistive voltage divider to the 3.6V rail, and the Program voltage pin was left floating to make the reference voltage on the V_{OSENSE} pin 1.19 volts.

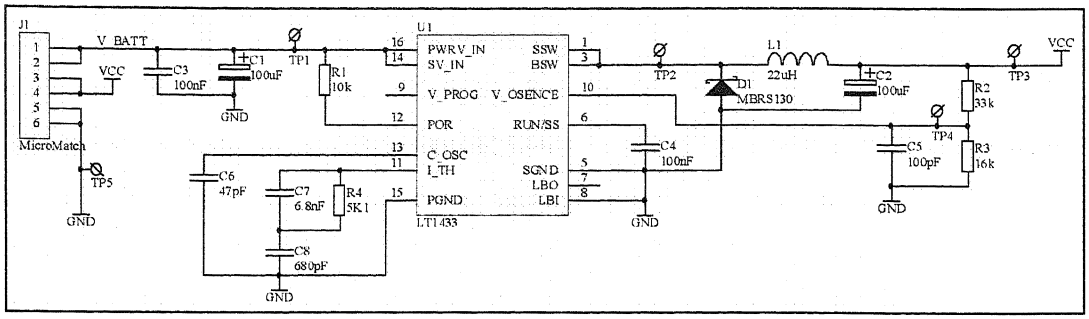

Figure 5.7: Sample schematic diagram of the daughter board power supply

Although the design of the power management system was based around using a six or twelve volt battery as the power storage, because that was the most likely storage method, the design was also built to work using ultra-capacitors as the storage device. Because the main difference between the ultra-capacitor and the battery is the discharge curve, ultra-capacitors would support the input voltage to the power supply for a shorter period of time to the battery, even if they had the same energy storage capacity.

This problem could be remedied by using multiple capacitor banks, as mentioned in the last section, one powering the device, and the others for keeping the voltage at a safe level on the first bank through step up converters. To help with this an extra external going output was added that could be used as a switch for turning on the charge pumps when the voltage of the power source gets too low.

The external going output was protected using a 15 volt transient voltage suppressor to absorb most of the transient, a series resistor to limit the current, a schottky diode going to ground and another going to the positive voltage rail to absorb the last of the transient.

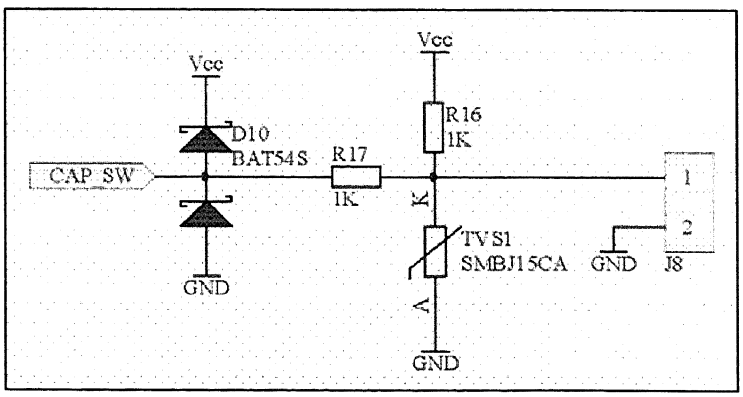

Figure 5.8: Sample schematic diagram of the external going switch output

5.2.2 Microcontroller

The Microcontroller used in the second revision of the data-logger was the same as that used in the first revision, the Microchip PIC18F6527. The microcontroller

worked well in the first revision so there was no reason to change it, but if there was a need for larger program memory space, the other three 64 pin microcontrollers in the series were drop-in replaceable, so up to 128 kilo-bytes of program memory could be used without needing to change the hardware or the program code that had been written up until that point.

Most of the pins of the microcontroller were used in the second revision of the data-logger, leaving just 15 pins unused, four analog to digital converter pins, one eight pin port (Port-E), and the two pins associated with the internal oscillator, namely the buffered outputs of the internal oscillator.

The eight pin port was routed to a Tyco amp MicroMatch 10 way surface mount, which for convenience also had one way connected to ground, and another pin connected to the supply rail. The analog to digital converter pins and oscillator output pins were all routed to test pads, one milli-metre radius pads normally used for checking what is happening on a particular connection. The last of the 15 pins, pin 4 of Port-G (RG4), was left floating.

For the second revision the need for a real time clock was apparent, as the data logger would ideally be able to log down the time each data log was entered. This was done by connecting a 32.678 kilo-hertz crystal oscillator to the input pins of timer one. When using the crystal oscillator as the input for timer one and using the 16 bit timer function, timer one overflowed every two seconds.

Using the timer overflow interrupt and updating the clock at every interrupt provides an accurate time which could be used to tell what time of day it was. The timer could also be accessed on the fly, i.e. while it was still running, so it could also be used to get millisecond accurate timing between pulses.

The data EEPROM used in the second revision was the same at that used in the first revision, a Microchip 24LC512 serially loaded EEPROM chip. The difference to the previous version is that the write

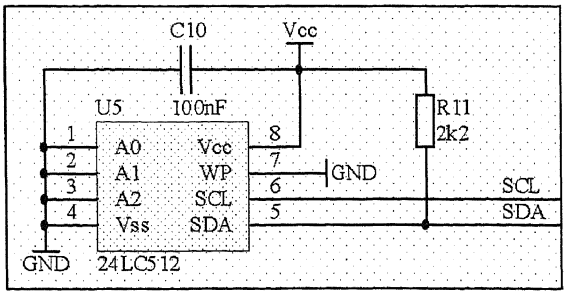

Figure 5.9: Sample circuit of the external data EEPROM chip connection

protect pin of the chip was connected to ground in the second revision, allowing it to be written to all the time.

In the second revision the LEDs were also changed, as the right angle through-hole LEDs were big and bulky, and took up too much physical space on the board. They were replaced with smaller surface mount LEDs, still right angled so the light went to the same place, but they took up less than half the space on the PCB. They were also connected to different pins on the microcontroller, so the pins they were on in the first revision could be used for the output port, Port-G.

For a schematic diagram of the main schematic, containing the microcontroller, external serial EEPROM memory, external 32.678 kilo-hertz external oscillator, programming header, LEDs and Port-G connector, refer to Appendix 5-b).

5.2.3 Sensing

High Voltage Sensing

The high voltage sensing in the second revision of the data-logger was almost exactly the same, with the fence pulse coming in through a three stage voltage divider, divided down to 110 volts, rectified, then divided again, but in this revision to 3.5 volts.

This was done by simply replacing one of the 18 ohm resistors with a 15 ohm resistor (R16), and ensured that the output voltage of the operational amplifier did not exceed the 3.6 volt power rail voltage on the microcontrollers analog to digital converter so that it could always read the voltage properly under the specified ten kilo-volts.

The sample and hold circuitry had also been changed to hold the sample for as long as the microcontroller needed it to be held, by using an N-type field effect transistor to discharge it. To keep options open the footprint for the discharge resistor was left on the board but marked as do not place (DNP), as shown in Figure 5.10.

The interrupt pulse generator was left exactly the same as it was in the first revision, with a 47 kilo-ohm resistor running from the 110 volt node to a bipolar junction transistor, which pulled down the interrupt pin on the microcontroller.

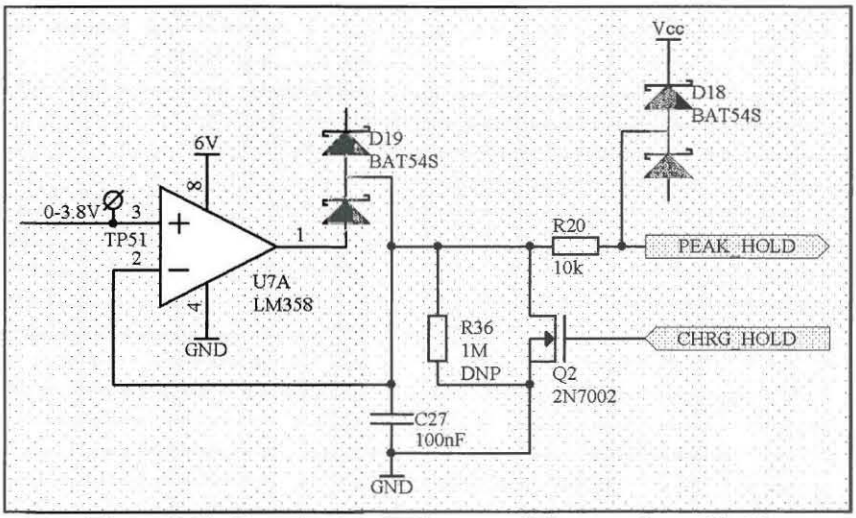

Figure 5.10: Sample circuit diagram of the sample and hold circuit on the second revision of the data-logger

Humidity, Temperature, Insolation and Battery Voltage Sensing

A new sensor was found that could be used to monitor the temperature and humidity with one sensor, the Sensirion SHT11 humidity and temperature sensor. This sensor would work on any voltage between 2.4 and 5.5 volts, had a current requirement of just 550 micro-amperes in measuring mode, and as low as 0.3 micro-amperes in sleep mode.

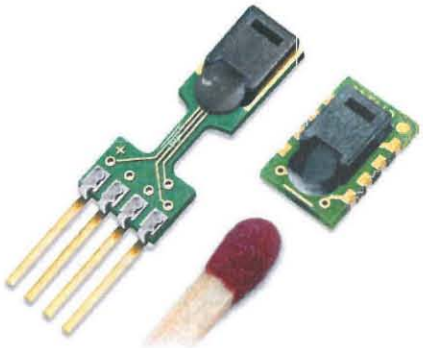

Figure 5.11: Photo of the Sensirion SHT71 (pinned version) and SHT11 (surface mount version) next to a large match head (Sensirion, 2007)

It used a serial interface similar to the Inter-Integrated Circuit protocol, only it was designed for low current consumption, and had a default measuring resolution of 14 bit for the temperature, and 12 bit for humidity. The dimensions of the SHT11 are 4.93 milli-metres by 7.47 milli-metres, comparable to the size of a large match head, as shown in Figure 5.11. This sensor was used for temperature and humidity sensing both inside and outside the energizer, each mounded on their own daughter board with other sensing elements or connectors.

The sensor used for sensing the insolation (or irradiance) of the environment was an Avago Technologies APDS-9003 miniature surface-mount ambient light photo-sensor. This photo-sensor is in a package just 1.5 milli-metres by 1.6 milli-metres by 0.55 millimetres, and has a light receiving area of 0.505 milli-metres by 0.36 milli-metres.

The APDS-9003 photo-sensor works on between 2.4 volts and five volts, just like the SHT11 humidity and temperature sensor. Rather than using an output voltage, the sensor outputs a constant current, so the output voltage can be tuneable by changing the load resistor, i.e. high resistance provides higher output voltage using ohms law.

For the first testing the value of the load resistor was set to one mega-ohm, to get the largest possible voltage output for testing and using the sensor, but should one mega-ohm be too much for the sensor the option of changing the load resistor to a more suitable value was there.

The SHT11 temperature and humidity sensor, and the APDS-9003 photo-sensor were incorporated into one daughter board, which was designed for monitoring the external environment. The schematic diagram and a drawing of the PCB of the external sensor daughter board are shown in Figure 5.12 and Figure 5.13, respectively.

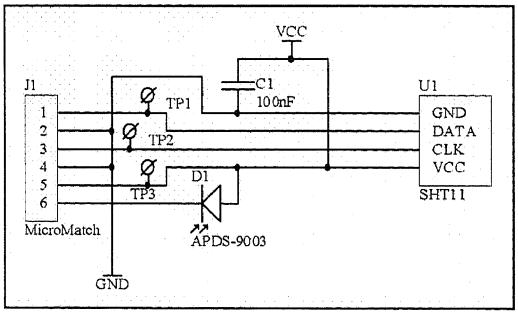

Figure 5.12: Schematic diagram of the external sensor daughter board

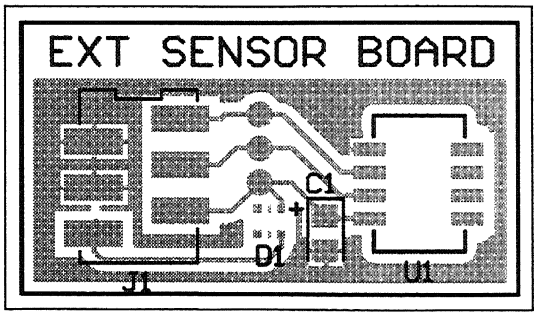

Figure 5.13: Drawing of the PCB of the external sensor daughter board

The battery voltage sensing was incorporated into the daughter board with the SHT11 sensor for monitoring the energizers internal environment, by adding two blade terminals for connecting the battery leads onto, and also adding a small rectifier made using two BAT54S dual series schottky diodes. While the schottky diodes were not capable of high current, they didn't need to be, because the current going through them for measuring the battery voltage would be limited by the voltage divider on the main PCB.

The schematic diagram and a drawing of the PCB of the internal sensor daughter board are shown in Figure 5.14 and Figure 5.15, respectively.

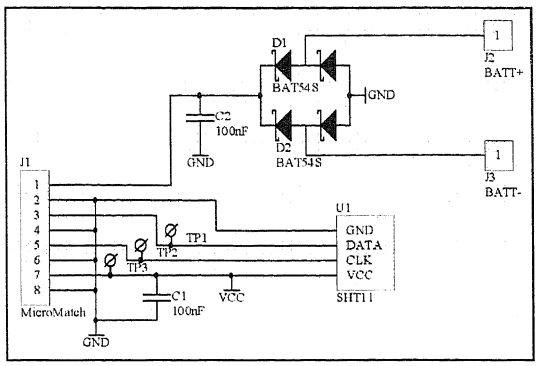

Figure 5.14: Schematic diagram of the external sensor daughter board

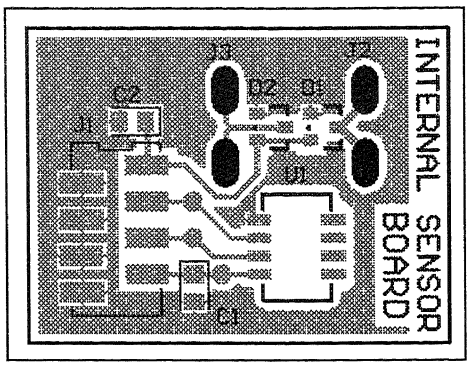

Figure 5.15: Drawing of the PCB of the external sensor daughter board

Each line to both the internal and external sensor daughter boards was also protected on the main PCB by a 15 volt transient voltage suppressor, a series resistor, and a schottky diode to both ground and the positive supply rail for transient protection, similar to the protection used for the external switch output. For example, the photo sensor input line is protected by the circuit mentioned above, before it gets to its current sense resistor (R38), as shown in Figure 5.16.

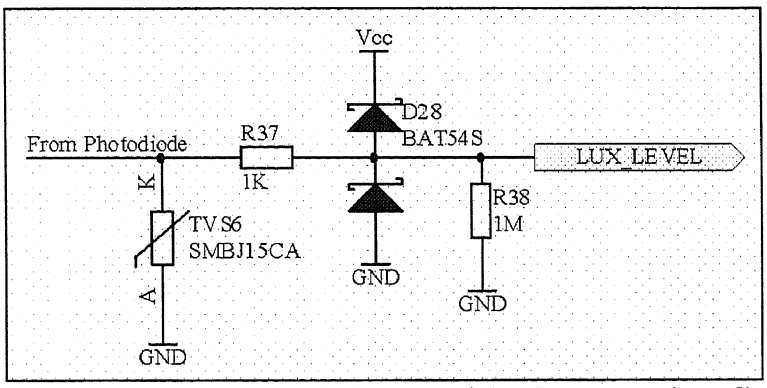

Figure 5.16: Sample schematic diagram of the photo sensor input line

The only differences to this were that the battery voltage line used the series resistor as part of its voltage divider, from up to 24 volts down to 3.6 volts, before the diodes to ground and the positive rail, as shown in Figure 5.17.

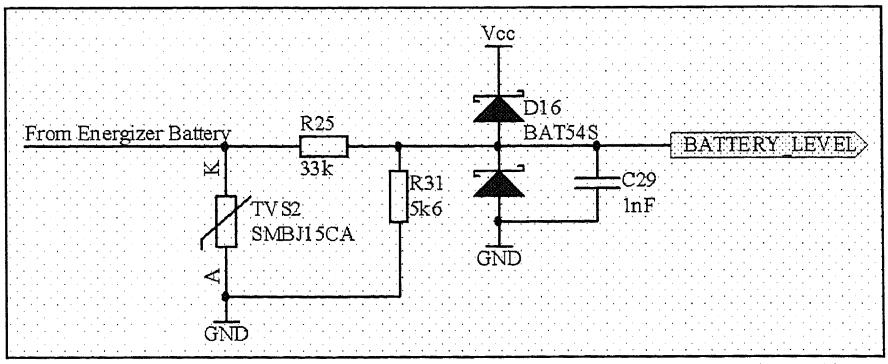

Figure 5.17: Sample schematic diagram of the energizer battery input line

External interrupt

The external interrupt line the was in the first revision was also kept exactly the same, with the two blade terminals one to ground and the other pulled high by a pull up resistor. The terminal that was pulled high was also put through the protection circuitry as mentioned above, the transient voltage suppressor, series resistor, and two schottky diodes.

5.2.4 Communications

RS232

The RS232 communications on the second revision were quite similar to those on the first revision, using the same family of Intersil RS232 converters, only using one with two extra pins, a shutdown pin and an enable pin, the ICL3222CBZ. Apart from the shutdown and enable pins the chip was essentially the same, with the pin-outs lining up almost identically, but with two extra pins on the top end, as shown by the sample schematic diagram in Figure 5.18.

The shutdown pin on the ICL3222CBZ allows the microcontroller to shut down the transmission functions and the on board power supply, placing the device in low power mode but leaving the receivers on. The enable line is an active-low receiver enable line, so the receivers can be turned off.

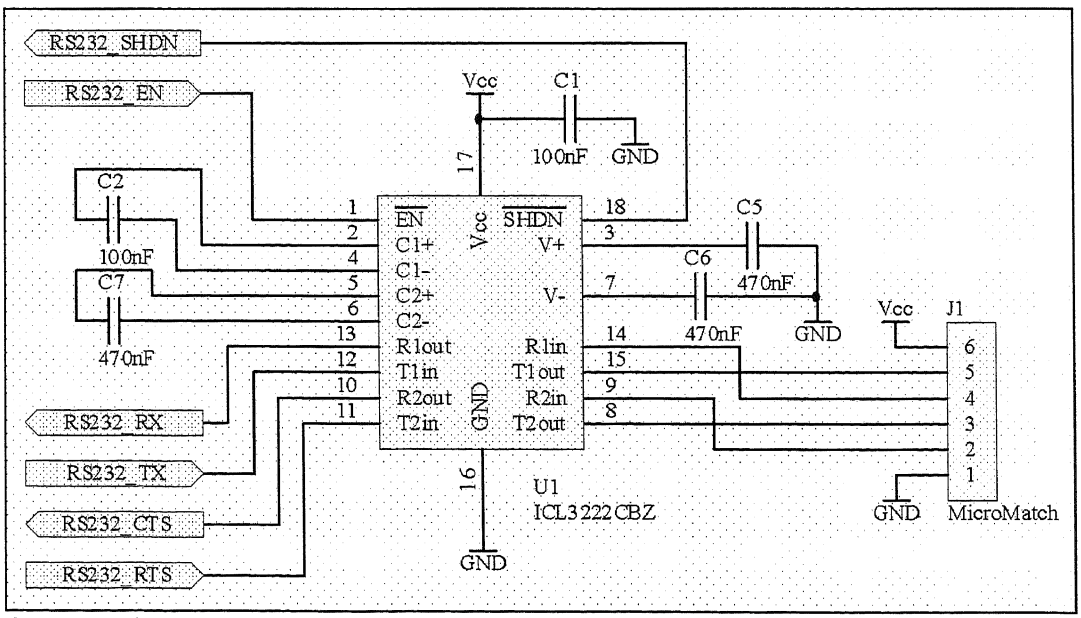

Figure 5.18: Sample schematic diagram of the RS232 communications it the second revision of the data-logger

These functions would be useful for when the data-logger was not physically connected to a computer, so it does not need the RS232 communications on, thus the system can conserve more power during these times. However, should a computer be connected to the data-logger at any time, it could send a sample packet to signal to the microcontroller that there was something connected and it should turn the RS232 communications on.

GSM communications

The GSM module used in the second revision was the same as in the first revision, the Motorola G24 GSM module. The main differences between the two revisions were that the footprint on the PCB was correct on the second revision, and the connections between the module and the microcontroller were buffered in the second revision.

The modules output lines were buffered using a Philips 74LVC07A hex buffer with open-drain outputs and Transistor-Transistor Logic (TTL) level inputs. Because there were only six outputs that needed to be buffered and the inputs could be as low as 2.575 volts, this buffer chip was ideal.

The chip was powered by connecting the respective pins to ground and the positive supply rail. Each line coming out of the module was connected directly to one buffer input, and the output of each buffer was connected to its respective microcontroller pin, and pulled up by a 100 kilo-ohm resistor.

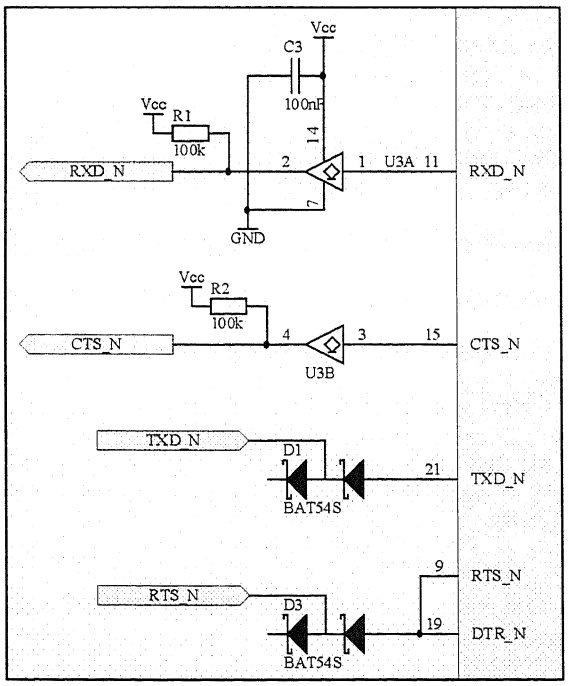

Figure 5.19: Sample schematic diagram of the buffer lines used for the inputs and outputs of the GSM module

For the inputs of the GSM module all but the IGN line were buffered using diodes coming from the module. Because the module had internal weak pull ups, they pulled the line high, and when the microcontroller had to change the

voltage on that line it could simply pull the voltage down, which would pull the whole line down, or release it, allowing the line to go up. An example of both the input and output buffers of the module is provided in Figure 5.19. In the sample schematic diagram the top two lines, RXD_N and CTS_N, are outputs from the GSM module, and the other lines, TXD_N, RTS_N and DTR_N, are inputs.

Other differences to the GSM module from the first revision to the second revision included connecting the SIM card holder correctly, and connecting the DTR_N pin to the RTS_N pin, to ensure the G24 GSM module's serial communications interface would transmit back to the microcontroller. Combined with the other changes to the GSM communications helped to ensure the GSM module on the second revision worked, and communicated without errors to the microcontroller.

5.3 Printed Circuit Board

5.3.1 Main Board

The main Printed Circuit Board on the second revision was very similar in shape to the first revision, but after checking how much room was in both enclosures the board was designed for, it was found that the power supply end of the PCB could be extended by up to 25 milli-metres. The board needed to be enlarged somehow because of all the extra components and larger power supply; and this extension was just what it needed.

The final dimensions of the PCB were 60 milli-metres by 173 milli-metres with an extension from the previous board of just under 20 milli-metres. The high voltage section was exactly the same as in the first revision, and the GSM module, LEDs and EEPROM circuitry were all in similar positions to the first revision; but all the other components were moved around to find the cleanest placement of parts.

The microcontroller was in a similar position to the previous revision, but had been moved down and to the right a bit to make room for the extra circuitry that was put above it, and rotated to find the best angle for routing. The sample and hold circuitry was rearranged to make room for the new field effect transistor that

was added, and the battery voltage line was brought over from the power supply side to near the sample and hold circuitry and the microcontroller.

The 32.678 kilo-hertz crystal oscillator was also put between the microcontroller and the sample and hold circuitry, as that was the best place to put it given the placement and orientation of the microcontroller. The programming header was placed between the LEDs and the sample and hold circuitry, making room in the bottom right corner of the PCB. The space it left was occupied by the RS232 converter and its associated header, and the ten pin connector with the eight pins of Port-G was sitting next to it, in the position the external interrupt line was in previously.

The external interrupts circuit was moved to the left, into the position previously occupied by the SIM card holder. Because the external interrupt circuitry only took up a small amount of the space that was left by the sim card holder, all the buffer circuitry for the GSM module was also put into that space. The sim card holder was moved up to above the GSM module, where the environmental and energizer battery voltage sensor circuitry was in the previous revision.

The sensing circuitry was moved to the left into the space that the RS232 circuit and solar power conditioning circuit previously occupied. The solar power conditioning circuit, including the input smoothing capacitors, and the battery and solar panel connectors were placed around the edge of the new board extension. The LT3434 power supply was placed in between the power conditioning circuit and the GSM module, with the short components in line with the aerial out of the GSM module, and the taller components scattered around it.

A diagram of the top layer and silkscreen of the PCB is provided in Figure 5.20. It shows in more detail where components are placed and where the top layer tracks are routed. A view of the bottom layer is also provided in Figure 5.21, which shows the routing of the bottom layer tracks.

Unfortunately time ran out and the PCB for the second revision did not have time to be populated or programmed, so no tests on could be done on the board to see how it performed. However, because there was still three months of funding left after the due date for this thesis that work could be completed in that time.

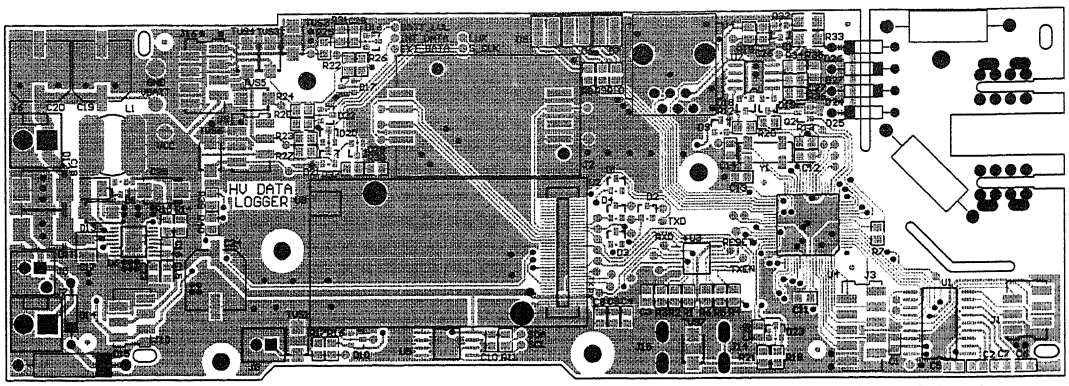

Figure 5.20: Diagram of the lop layer and silk screen of the second revision of the data-logger PCB

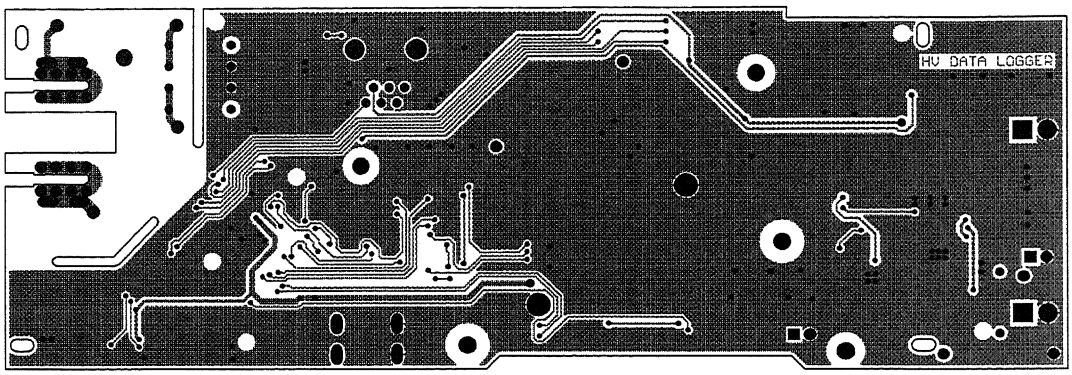

Figure 5.21: Diagram of the bottom layer of the second revision of the data-logger PCB

5.3.2 Power Supply Daughter Board

The daughter board for the external power supply was not a simple task because it needed to fit in a small space, limited by the 3.6 volt storage capacitor, power connectors and the antenna lead for the GSM module. Because of these restrictions the power supply on the daughter board had to be moulded around the connector onto a board measuring just 19 milli-metres by 22 milli-metres. The final layout of the PCB for the daughter board needed to have components both the top and bottom layers, as shown in Figure 5.22 and Figure 5.23 respectively.

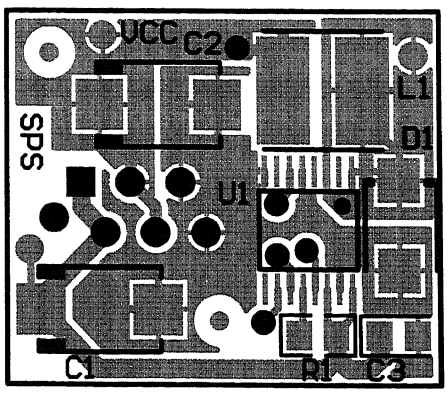

Figure 5.22: Top layer of the power supply daughter board PCB

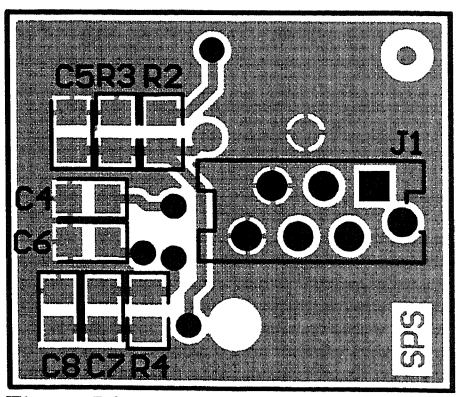

Figure 5.23: Bottom layer of the power supply daughter board PCB

CHAPTER SIX: CONCLUSION

6.1 Review

The project to design the data-logger arose from Gallagher Animal Management Systems' need to be able to test and monitor new and existing electric fences and energizers to critically find out how well a particular energizer is performing. The unit could not run off the energizers battery or power system, so it would affect energizer it was monitoring in the smallest way possible, so it had to be self powered.

A review of the existing data-logger product and what was required by Gallagher Group Limited was done. It did not have any facility for monitoring any environmental parameter, it could only monitor up to 10 kilo-volts and could not monitor the battery voltage in the energizer, so a redesign was needed.

The research part of the project was to design a power management system that could use ultra-capacitors to help make it more effective. One of the main goals for power management in the data-logger system was to make the system as efficient as possible, so that the data-logger could last for a longer time without sufficient charging from the solar panel. Most of the components in the design of the data-logger system were also considered, to make sure the whole system drew the smallest amount of current possible during the time it was not being used.

Given the data on ultra-capacitors they appear as a possible solution for energy storage in this application. The use of ultra-capacitor technology as an energy storage method was more efficient than electrochemical batteries, because the internal resistance is so much smaller, and energy is not lost in the chemical conversion process. The only disadvantage to using ultra-capacitors is the cost, and the size of the ultra-capacitors needed to store the same amount of energy. However given that ultra-capacitors are more environmentally friendly and have a much longer life time, the advantages of the two technologies weigh out evenly.

6.2 Analysis of Results

6.2.1 Ultra-capacitors

The experiments on the ultra-capacitors show that it is possible to use ultra-capacitors for energy storage provided there is sufficient capacitance. For

example, the 30 farad capacitance being discharged at one ampere through the low drop-out regulator took 71 seconds going from 6.9 volts to 4.4 volts which relates to a discharge in energy from approximately 714 joules to 290 joules, almost 60 percent of the initial energy.

Because this current will only be drawn on occasion in the data-logger when the GSM module needs to connect or transmit to the network, this will not happen very often. However given that the capacitor could go for weeks without getting charged at all, the energy stored needs to be enough to power the device during that time, and multiple GSM transmissions during that time as well.

One way to help get around this is to use the method shown in Figure 4.28, with the small ultra-capacitor bank powering the data-logger unit itself, and that ultra-capacitor bank trickle charged from another much larger ultra-capacitor bank through a charge pump or step up converter or even a combination of both. This would allow use of a larger voltage range in the larger ultra-capacitor bank, and therefore much more energy to be used from them.

The ESR of an ultra capacitor can also be a problem at higher currents, because the voltage of the capacitor drops at high output currents, which means that it gets to the regulators/converters drop-out voltage faster under high current loading. It is also one of the ways a capacitor loses energy, because the resistance converts the energy to heat, which is another loss of energy that has to be planned for.

6.2.2 Power Management System – Power Supply Selection

From the results of the tests, it was deduced that the more efficient regulator/ converter type of the two tested to use in the data-logger was the switch mode power supply. The main reason for this was because the efficiency of the switch mode power supply remained reasonably constant at an average of about 85 percent over the whole input voltage range, where the efficiency of the low drop-out regulator varied greatly, getting down to 55 percent and up to just under 82 percent at its maximum, as shown in Figure 6.1.

For lower currents, i.e. less than 10 milli-amperes, it would be advisable to use a switch mode power supply that was configured for that small amount of current,

as the input voltage will be quite large under optimal operating conditions and a switch mode power supply could handle that with better efficiency than a low drop-out regulator as shown in Figure 6.1.

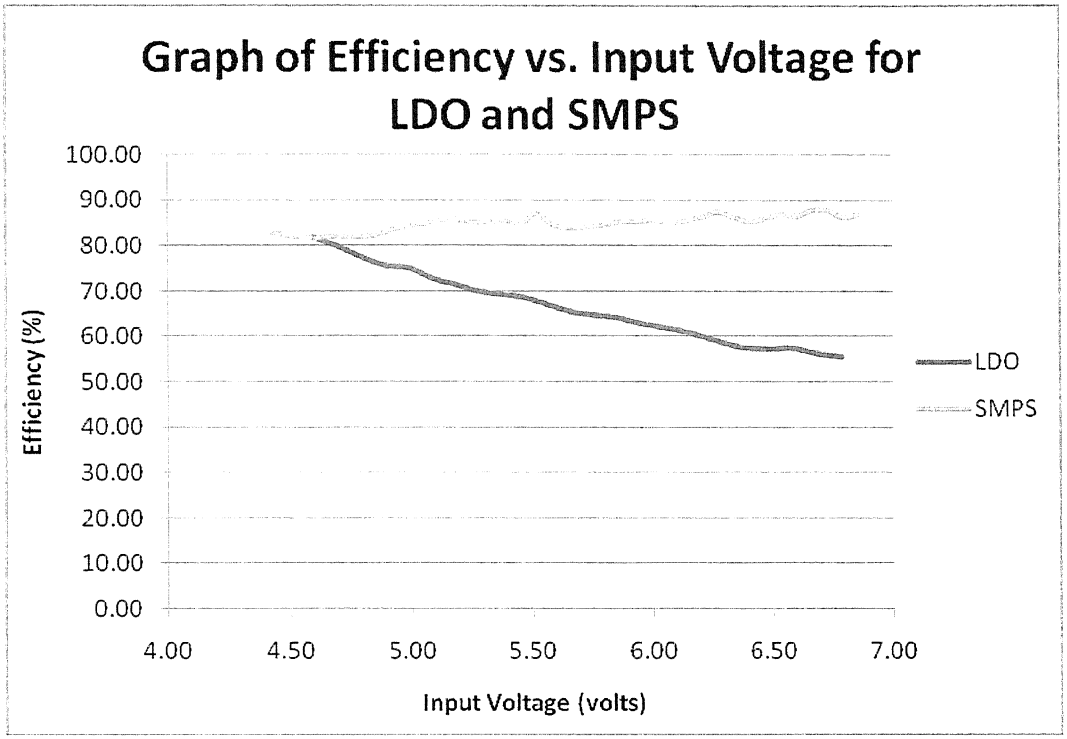

Figure 6.1: Comparison of the efficiency vs. input voltage for the low drop-out regulator and switch mode power supply

6.3 Future Work and Improvements

6.3.1 Data-logger design

The second revision of the data-logger still needs to be tested and programmed for field tests. Until this is done the overall design of the power management system, including the ultra-capacitor storage, cannot be tested properly and the system cannot be judged. This would be the first thing to work on in the future.

However, there are many areas that the data-logger could be improved on. For example, the sensing still does not monitor the full range of environmental parameters and others could be added in future developments, such as lightening strikes, barometric pressure and wind speed.

The sensing of the energizer outputs were limited to a physical, electronic connection to the energizer output that only monitored the output voltage. Future improvements of the data-logger could improve this by designing a contactless

voltage monitoring system, and including a contactless current sensing system also, so the data-logger could be used as a permanent fault finding system on the farm.

Also the sensing elements inside the energizer still rely on a wired connection to operate, so a small opening would be required for the wires to enter through, which unfortunately could change the environment inside the energiser. One way around this could be to use a power and communications system similar to radio frequency identification (RFID) to monitor the inside of the energizer; so research could be done to produce a small RFID powered device that could be used inside the energizer without needing a hole in the energizer enclosure.

6.3.2 Ultra-capacitors

Using ultra-capacitors as power storage needs much more work. The majority of the work needing to be done is to research and design the most efficient way to store the energy in ultra-capacitors, and how to extract the maximum amount of energy from the ultra-capacitor banks as possible.

This includes testing the methods discussed above, like the multiple capacitor banks, against other ideas, like simply using a buck-boost converter in the data-logger to take the maximum amount of energy from the ultra-capacitor bank as possible. An ultra-capacitor comparison also needs to be done, to work out which ultra-capacitor brand and product is best suited for the application. This includes comparing leakage current, ESR, capacitance, voltage, price, and lifetime.

6.3.3 New Power Management System

If a new revision of the data-logger is made it could use the power management system shown in Figure 6.2, where the only part of the circuit powered directly off the main energy storage unit is the microcontroller, which can switch on an individual power supply for any sub-system when it is needed, and the ultra-capacitor bank for each sub-system (UC*n*) could be selected to hold enough energy to power the system for as long as the sub-system needs to be on for. Using this method each sub-system would not need to be as high efficiency because they would only be on for a small percentage of the time.

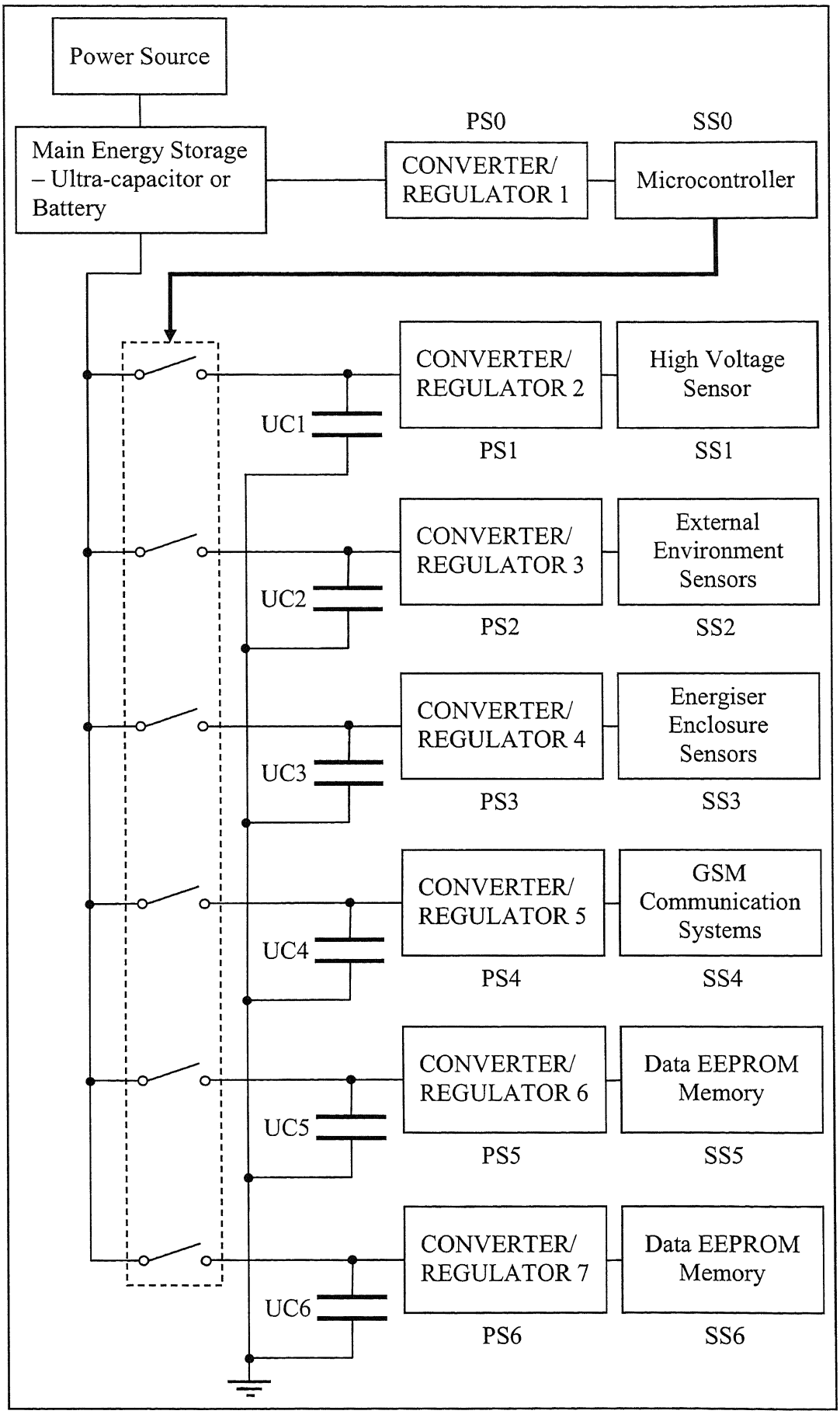

Figure 6.2: Proposed power management system for future designs

The weighted efficiency of each sub-system (SS*n*), its power supply (PS*n*) and ultra-capacitor energy storage (UC*n*) could be found by its efficiency (η_{SSn}) multiplied by the time it would be switched on ($t_{ON,SSn}$), divided by the total time (t_{Total}). The overall efficiency (η_T) of the system could be calculated by averaging all the individual efficiencies, or using the formula:

$$\eta_T = \frac{\sum_{n=0}^{6}\left(\eta_{SSn} \times \frac{t_{ON,SSn}}{t_{Total}}\right)}{n+1} \tag{20}$$

This or a similar power management system could be used in the data logger to make the overall system more efficient; but work needs to be done to refine the technique and find the best combination of component efficiency and on time for each of the sub-systems.

6.3.4 Energy Harvesting

Work can still be done regarding the energy harvesting for the data-logger. This includes both finding the best power output to suit the system, and finding different means of energy extraction that could be more effective in different parts of the world.

For example, a small wind turbine could be designed for those areas that get less sun during winter or in coastal regions, as a solar panel might not provide enough power to keep the data-logger going throughout the year. A hybrid system could also be designed that uses both wind and solar energy to power the data-logger system.

6.4 Conclusion

A data-logger already existed, but had very limited capability for monitoring an energizer, and a new one needed to be designed that could monitor the energizer and the environment around it. Two new data-logger revisions were made to achieve the environmental monitoring goal, the first revision not working properly, and the second revision designed too late to test or program.

Unfortunately the product specifications from chapter one were not entirely met with the second revision of the data-logger, as it had not been put into an

enclosure yet, and the high voltage pulse circuit was designed around ten kilo-volts rather than 20 kilo-volts. The waterproof enclosure specification could still be met as the board was designed to fit into the existing SmartWatch enclosure. The PCB may have to be redesigned to make it possible to work on 20 kilo-volts, as the clearances between components and tracks on the high voltage lines were too small for 20 kilo-volts, or some other plan may be possible that insulates the high voltage lines better.

A lot was discovered about power management systems and ultra-capacitors, however designing them into the circuit could be a lot more challenging. And while powering each sub-circuit off its own power supply may be more efficient overall, the cost of achieving that efficiency in this case was too high; and the circuitry it requires would take up too much board space for this particular data-logger, as space was already very limited. For these reasons the method was not implemented in the data-logger.

While the design of the data logger is not complete and work still needs to be done on programming and testing the second revision, there was still three months of funding remaining after this thesis is due, which was enough time to complete these tasks. For this reason the project outcome will not be known until well after the due date, however at the time of writing this thesis the project was running on time and appeared on time for overall completion of the project.

APPENDICES

Appendix 1: Schematics of Data-logger First Revision

1-a) First Revision Power Supply Schematic

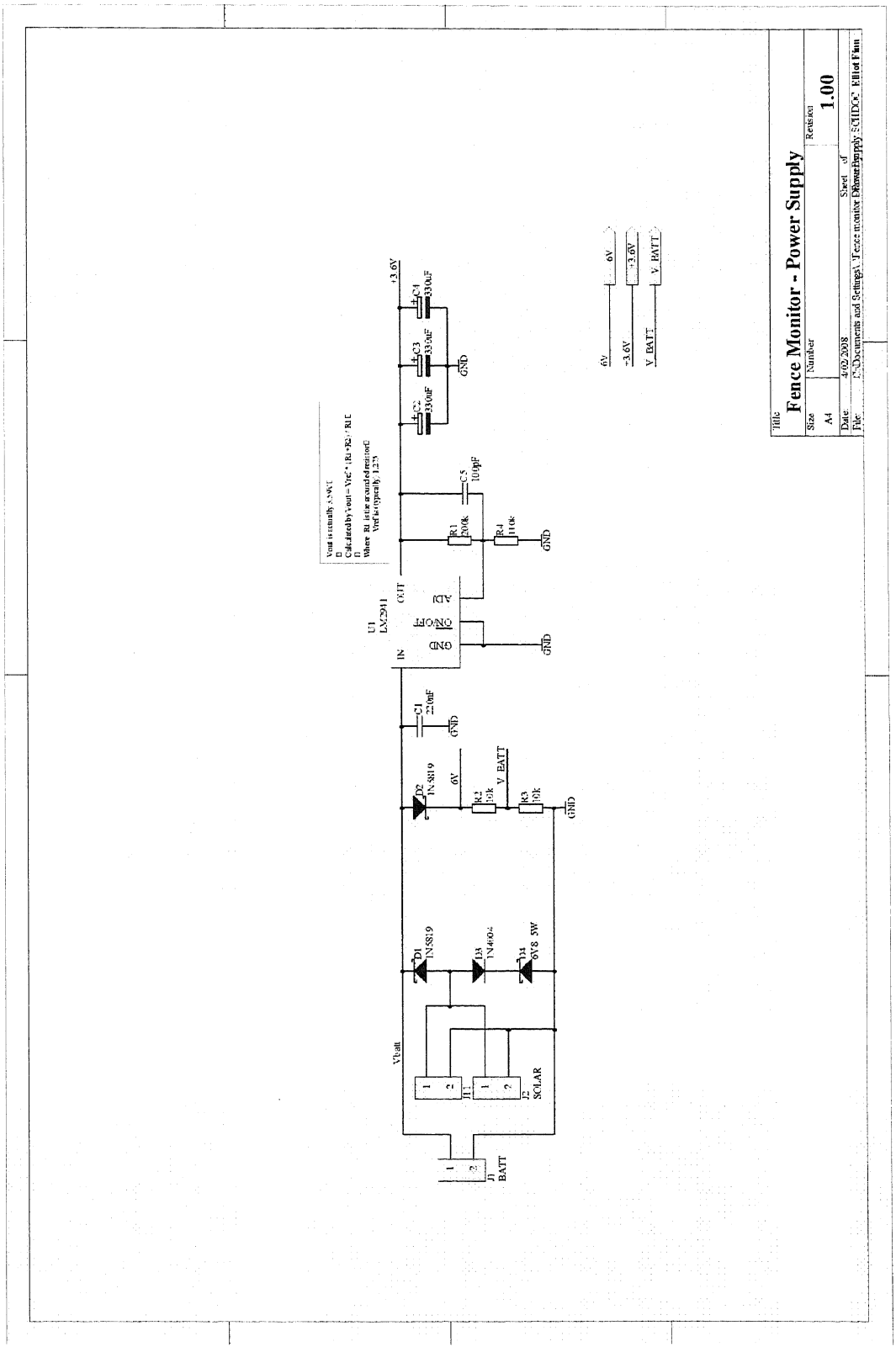

1-b) First Revision Main Schematic

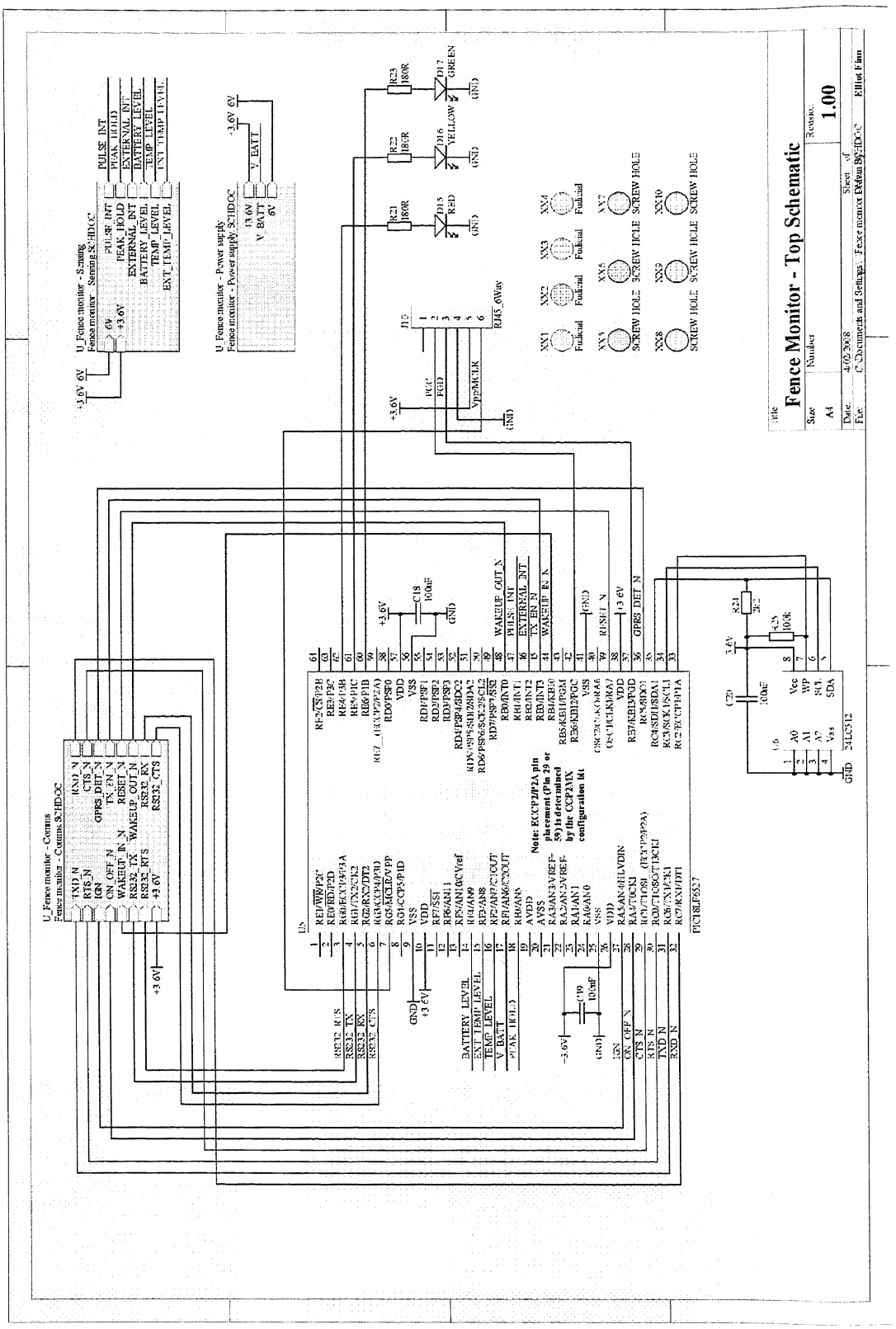

1-c) First Revision Sensing Schematic

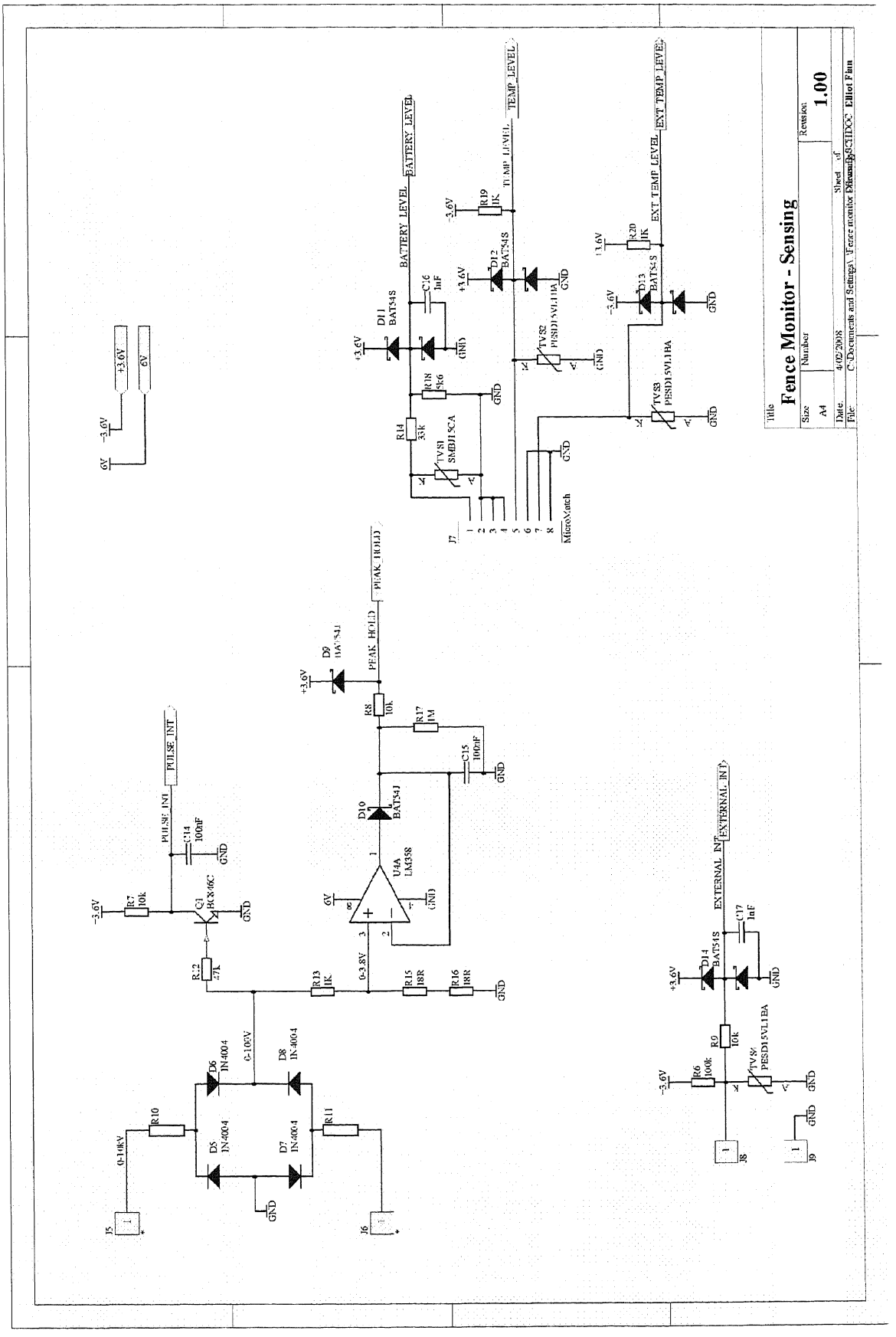

1-d) First Revision Communications Schematic

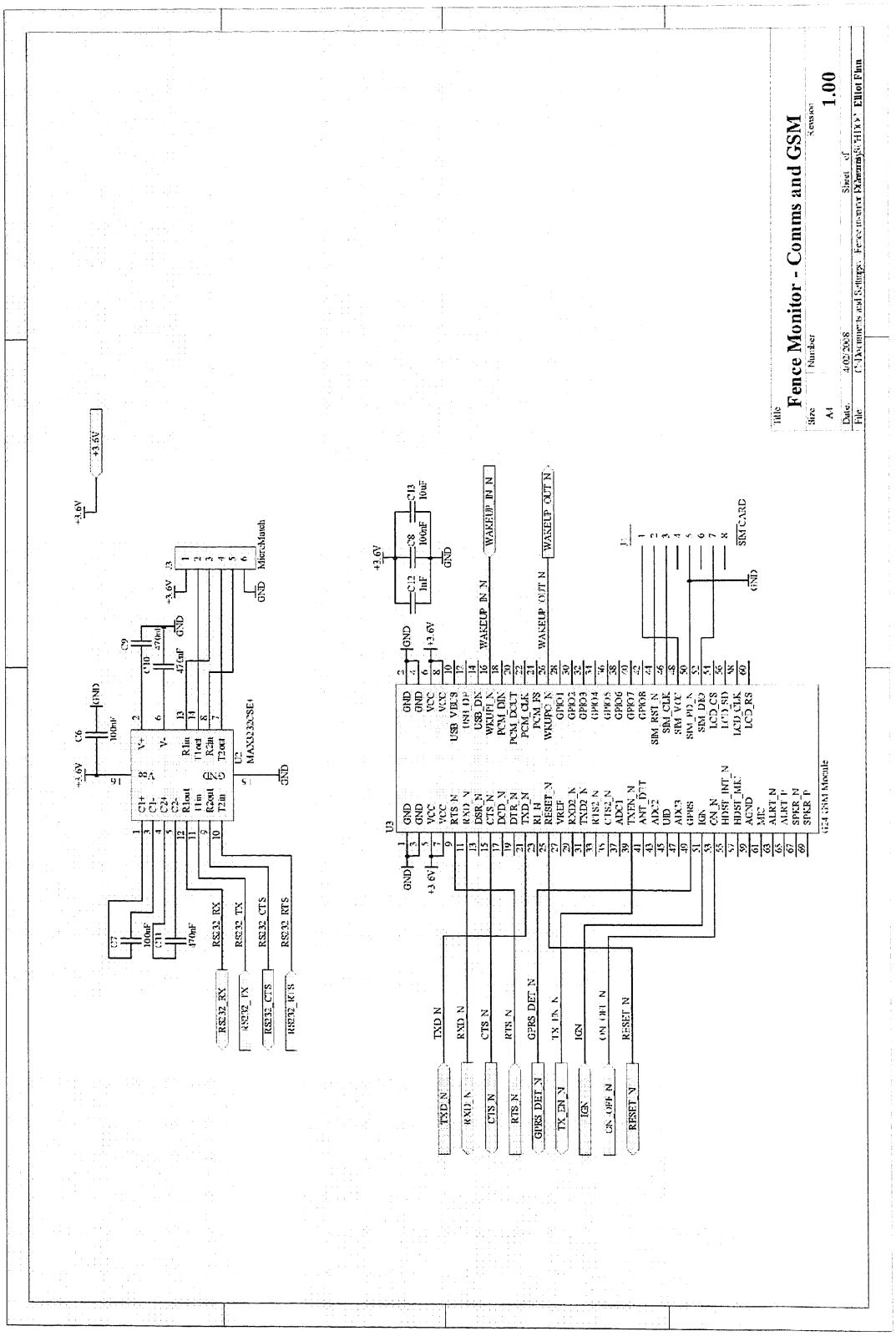

Appendix 2: PCB of the Data-logger First Revision

2-a) Top Layer:

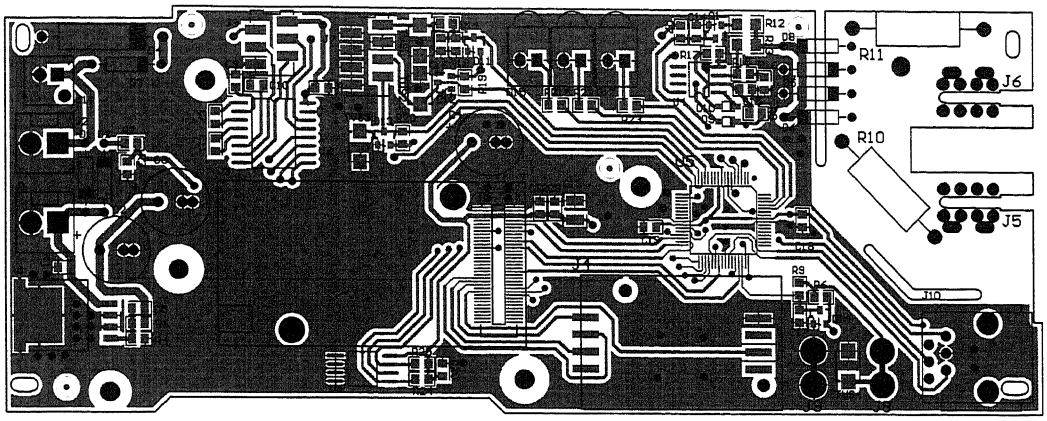

2-b) Bottom Layer:

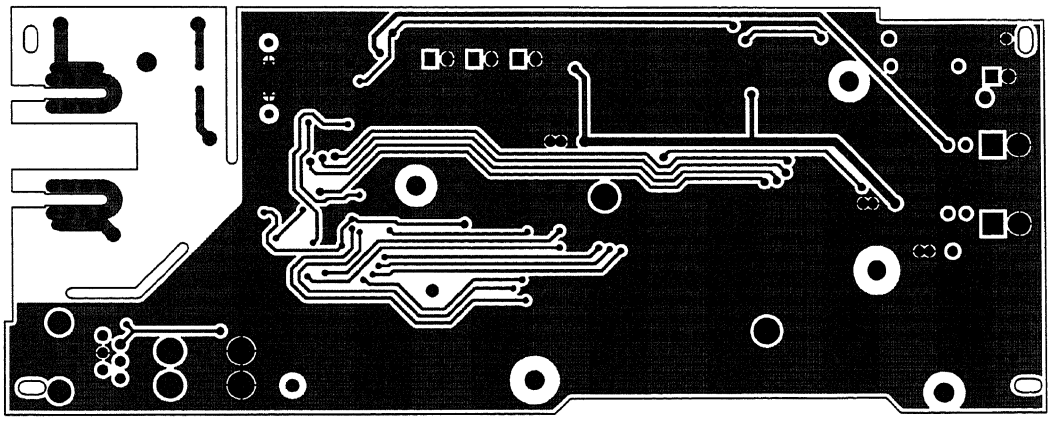

Appendix 3: Microcontroller Code for Testing GSM

```
#include <p18f6527.h>
#include <stdlib.h>
#include <string.h>
#include <i2c.h>
#include "My_defines.h"
#include "Ascii_def.h"
#include "Main.h"
#include "GSM_pins.h"

#pragma config OSC = INTIO7

#define TRUE 1
#define FALSE 0
#define ON 1
#define OFF 0
#define LED_R RE4
#define LED_Y RE5
#define LED_G RE6

char Header[] = "Transmit works";
char Sleep[] = "AT";
unsigned char count = 0;
char BlankStr[] = "                    ";//                    ";
char String[40];
unsigned char strcnt = 0;
char OutString[20];
unsigned char outstrcnt = 0;
char InString[20];
unsigned char instrcnt = 0;
char AT_Command[20];
unsigned char gsm_strcnt = 0;
char inchar1 = 0;
char inchar2 = 0;
unsigned short int Mem_Write_Byte = 0;
unsigned short int Mem_Read_Byte = 0;

/*#########################################################
 #                                                       #
 #  Initialisations                                      #
 #                                                       #
 #########################################################*/

/*********************************************************
      init_adc
      - initialises the adc ready for sampling
 *********************************************************/

void init_adc(void)
{
      TRISF |= 0x1F;

      ADCON1 &= 0xC4;
      ADCON1 |= 0x04;
      ADCON2 &= 0xFF;
      ADCON2 |= 0xBF;
      ADCON0 = 0x01;
      return;
}
```

```
/*********************************************************
      - init_timer0
            initialises timer 0
 *********************************************************/

void init_timer0(void)
{
      T0CON = 0x98;
      TMR0IF = 0;             //clear timer0 int flag
      TMR0IE = 1;
      return;
}


/*********************************************************
      init_interrupts
      - initialises the interrupts registers
 *********************************************************/

void init_interrupts(void)
{
      INTCON &= 0x38;
      RCON &= 0x7F;
      INTCON2 = 0;

      INTCON3 = 0x38;         // set up external interrupts

      PORTB = 0x00;           // set up Port B as peripheral
      LATB = 0x00;            //    (External interrupt) pins
      TRISB = 0xFF;

      INTCON |= 0xC0;         // enable all interrupts
      return;
}

/*************************************************************
      - gsm_init
            initialises the gsm module on Serial port 1 (USART1)
            with interrupts enabled for flow control.

 *************************************************************/

void init_gsm(void)
{
      GSM_WAKEUP_IN = TRUE;    // enable sleep mode
      GSM_IGN = FALSE;  // disable IGN - dont switch on
      GSM_ON_OFF = TRUE;       // disable ON_OFF
      GSM_RTS = TRUE;          // disable GSM Transmitter

      PORTC &= ~Bit7;

      TRISC |= 0xA2;           // Set up port G for USART
      TRISC &= 0xBE;           //          communications
                  // also sets GPRS_DET_N and CTS as inputs and
                  //          RTS as an output

      TRISA |= 0x80;           // set RESET_N as an input
      TRISA &= 0xCF;           // set ON_OFF_N and IGN as outputs
      TRISB |= 0x09;           // set WAKEUP_OUT & TX_EN as inputs
      TRISB &= 0xEF;           // set WAKEUP_IN as an output
```

```
	TXSTA1 = 0x02;			// set up EUSART 1 for GSM module
	RCSTA1 = 0x92;
	BAUDCON1 |= 0x0A;

	TX1IP = TRUE;			// set up EUSART 1 interrupts
	RC1IP = TRUE;
	RC1IF = FALSE;
	RC1IE = TRUE;

	SPBRGH1 = 0x00;
	SPBRG1 = 0x33;			// set baud rate to 9600 (9615)

	return;
}

/*******************************************************
	- init_USART2
		initialises baud rate for the 232 communications

 *******************************************************/

void init_USART2(void)
{
	TRISG |= 0x04;			// Set up port G for USART
	TRISG &= 0xFD;			//		communications

	TXSTA2 = 0x02;			// set up EUSART 2 for Serial port
	RCSTA2 = 0x92;
	BAUDCON2 |= 0x0A;

	TX2IP = TRUE;			// set up EUSART 2 interrupts
	RC2IP = TRUE;
	RC2IF = FALSE;
	RC2IE = TRUE;

	SPBRGH2 = 0x00;
	SPBRG2 = 0x33;			// set baud rate to 9600 (9615)
	return;
}

/*#######################################################
 #                                                     #
 #  Functions and subroutines                          #
 #                                                     #
 #######################################################*/

/*******************************************************
	Delay subroutine
	- delays the program for "time" in milliseconds
 *******************************************************/

void delay(unsigned int time)
{
	unsigned int i;
	for(i = 0; i < time; i++){}
	while (time > 0)
	{
		for(i = 0; i < 62; i++){}
		time++;
		time--;
```

```
            time--;
      }
      return;
}

/*******************************************************
      Sample adc subroutine

      - takes in a char as channel, samples the ADC over
            selected channel and outputs the ADC reading
 *******************************************************/

unsigned int sample_adc(char channel)
{
unsigned int level_input = 0;

ADCON0 = (channel << 2) + 3;  // Start the ADC on 'channel'
while(ADCON0 & 0x02);         // wait for conversion to finish
level_input = ADRES;          // copy result to level_input
return level_input;           // return result to subroutine
}

/*************************************************************
      - gsm_power_up
            powers up the gsm module on Serial port 1 (USART1)
            with interrupts enabled for flow control.

 *************************************************************/

void gsm_power_up(void)
{
      if(GSM_RESET == 0)
      {
            GSM_IGN = TRUE;    // enable the IGN line
                               // - powers up GSM module
            delay(75);
            // wait until the module is powered up
      }
      return;
}

/*************************************************************
      - gsm_power_down
            powers down the gsm module on Serial port 1 (USART1)
            with interrupts enabled for flow control.

 *************************************************************/

void gsm_power_down(void)
{
      if(GSM_RESET) GSM_IGN = FALSE;// disable the IGN line
                                    // -powers down GSM module
      return;
}
```

```
/*************************************************************
      - gsm_power_low
            puts the gsm Module into the low power mode

 *************************************************************/

void gsm_sleep(void)
{
      if(GSM_RESET)
      {
            if (GSM_WAKEUP_IN)
            {
                  gsm_tx_str(Sleep);
                              // give initial sleep command.
            }
            else
            {
                  GSM_WAKEUP_IN = TRUE;          // disable WKUPI_N
                              // forces sleep if sleep mode was
                              // halted by the WKUPI_N pin
            }
      }
      return;
}

/*************************************************************
      - gsm_wake_up
            takes the gsm module out of sleep mode

 *************************************************************/

void gsm_wake_up(void)
{
      if(GSM_RESET == 0)
      {
            gsm_power_up();
      }
      GSM_WAKEUP_IN = FALSE;

      delay(32);
      return;
}

/*************************************************************
      - gsm_tx_str
            initialises the transmitting of the string that is
            passed into it, then leaves the actual transmission
            up to the interrupt routines

 *************************************************************/

void gsm_tx_str(char *tx_str)
{
      gsm_wake_up();

      GSM_RTS = TRUE;

      strcpy(AT_Command, BlankStr);
      strcpy(AT_Command, tx_str);

      while (GSM_CTS);
```

```
      TX1IF = FALSE;
      TX1IE = TRUE;
      TXEN1 = TRUE;
}
/*#########################################################
 #                                                       #
 #    Interrupt vectors                                  #
 #                                                       #
 #########################################################*/

void InterruptHandler(void);
//--------------------------------------------------------
// High priority interrupt vector

#pragma code InterruptVectorHigh = 0x08
void
InterruptVectorHigh (void)
{
  _asm
    goto InterruptHandler //jump to interrupt routine
  _endasm
}

//--------------------------------------------------------
// Low Priority interrupt vector

#pragma code InterruptVectorLow = 0x18
void
InterruptVectorLow (void)
{
  _asm
    goto InterruptHandler //jump to interrupt routine
  _endasm
}

//--------------------------------------------------------
// High priority interrupt routine

#pragma code
#pragma interrupt InterruptHandler

void InterruptHandler(void)
{
      GIE = FALSE;      // disable interrupts

/************************************************
      External (INT2) interrupt routine.
************************************************/

      if(INT2IF)
      {
            INT2IE = FALSE;
            INT2IF = FALSE;

            if (TMR0IE) TMR0IE = 0;
            else TMR0IE = 1;

            INT2IE = TRUE;
      }
```

```
/************************************************
      TMR0 interrupt routine.
************************************************/

      if (TMR0IF)
      {
            TMR0IE = FALSE;
            TMR0IF = FALSE;

            //count++;

            TMR0IE = TRUE;
      }

/************************************************
      USART1 interrupt routine.
************************************************/

      if (TX1IF)
      {
            TX1IE = FALSE;
            TX1IF = FALSE;

            if (TXDONE1)
            {
                  TXDONE1 = FALSE;
                  STRDONE1 = FALSE;
                  while (!TRMT1);
                  TXEN1 = FALSE;
                  GSM_RTS = FALSE;
            }
            else if (STRDONE1)
            {
                  TXREG1 = LF;      // = LF (line feed)
                  TXDONE1 = TRUE;
            }
            else
            {
                  if (AT_Command[gsm_strcnt] == 0)
                  {
                        TXREG1 = CR;// = CR (carriage return)
                        STRDONE1 = TRUE;
                        gsm_strcnt = 0;
                  }
                  else if (AT_Command[gsm_strcnt] == ESC)
                  {
                        TXREG1 = ESC;// = CR (carriage return)
                        TXDONE1 = TRUE;
                        gsm_strcnt = 0;
                  }
                  else
                  {
                        TXREG1 = AT_Command[gsm_strcnt];
                        gsm_strcnt++;
                  }
            }

            TX1IE = TRUE;
      }

      if (RC1IF)
```

```
	{
		RC1IE = FALSE;
		RC1IF = FALSE;

		inchar1 = RCREG1;
		LED_Y = ON;
		if (inchar1 == CR)
		{
			OutString[outstrcnt] = 0;
			RXCR1 = 1;
			outstrcnt = 0;
		}
		else if (inchar1 == LF)
		{
			OutString[outstrcnt] = 0;
		}
		else
		{
			OutString[outstrcnt] = inchar1;
			outstrcnt++;
		}

		RC1IE = TRUE;
	}

/************************************************
	USART2 interrupt routine.
************************************************/

	if (TX2IF)
	{
		TX2IE = FALSE;
		TX2IF = FALSE;

		if (TXDONE1)
		{
			TXDONE1 = FALSE;
			STRDONE1 = FALSE;
			while (!TRMT2);
			TXEN2 = FALSE;
		}
		else if (STRDONE1)
		{
			TXREG2 = LF;		// = LF (line feed)
			TXDONE1 = TRUE;
		}
		else
		{
			if (String[strcnt] != 0)
			{
				TXREG2 = String[strcnt];
				strcnt++;
			}
			else
			{
				//TMR0IE = FALSE;
				TXREG2 = CR;// = CR (carriage return)
				STRDONE1 = TRUE;
				strcnt = 0;
			}
		}
```

```
            TX2IE = TRUE;
      }
      if (RC2IF)
      {
            RC2IE = FALSE;
            RC2IF = FALSE;

            LED_R = ON;
            inchar2 = RCREG2;
            if (inchar2 == CR)
            {
                  RXCR2 = 1;
                  InString[instrcnt] = 0;
                  instrcnt = 0;
            }
            else if (inchar2 == ESC)
            {
                  InString[instrcnt] = inchar2;
                  instrcnt = 0;
                  RXCR2 = 1;
            }
            else if (inchar2 == LF)
            {
                  //do nothing - ignore
            }
            else
            {
                  InString[instrcnt] = inchar2;
                  instrcnt++;
            }

            RC2IE = TRUE;
      }
      if (SSP1IF)
      {
            SSP1IE = FALSE;
            SSP1IF = FALSE;

            flag = 1;

            SSP1IE = TRUE;
      }

      GIE = TRUE;
      return;
}
```

```
/*#########################################################
 #                                                       #
 #  Main program                                         #
 #                                                       #
 #########################################################*/

void main(void)
{
      unsigned int i = 0;
      unsigned int sample;

      OSCCON = 0b01111011; //8Mhz, internal oscillator block
      PORTE = 0x00;
      TRISE = 0x00;

      init_adc();
      init_timer0();
      init_interrupts();
      init_gsm();
      init_USART2();
      delay(500);
      gsm_wake_up();

      while(1)
      {
            if (RXCR2)
            {
                  RXCR2 = FALSE;
                  gsm_tx_str(InString);
            }
            if (RXCR1)
            {
                  RXCR1 = 0;
                  gsm_sleep();
                  TX_str(OutString);
            }
      }
}
```

Appendix 4: Tables of Data from Test Results

4-a) Processed Data for the Constant Current Charge Test

Time (seconds)	V_C (volts)	I_{IN} (amperes)
0.00	0.045	-0.019
1.00	0.033	-0.022
2.00	0.037	-0.022
3.00	0.038	-0.015
4.00	0.034	-0.023
5.00	0.042	-0.022
6.00	0.038	-0.014
7.00	0.047	-0.023
8.00	0.048	-0.013
9.00	0.046	-0.016
10.00	0.050	-0.018
11.00	0.047	-0.019
12.00	0.045	-0.018
13.00	0.049	-0.014
14.00	0.051	-0.021
15.00	0.042	-0.021
16.00	0.048	-0.023
17.00	0.050	-0.021
18.00	0.056	-0.023
19.00	0.050	-0.018
20.00	0.069	0.879
21.00	0.138	1.998
22.00	0.187	1.999
23.00	0.243	2.001
24.00	0.300	1.998
25.00	0.352	1.991
26.00	0.415	1.994
27.00	0.459	1.993
28.00	0.514	1.997
29.00	0.567	1.996
30.00	0.616	1.991
31.00	0.664	1.994
32.00	0.722	1.985
33.00	0.780	1.991
34.00	0.824	1.987
35.00	0.880	1.988
36.00	0.937	1.994
37.00	0.983	1.989
38.00	1.040	1.981
39.00	1.090	1.996
40.00	1.143	1.979
41.00	1.191	1.981
42.00	1.250	1.983
43.00	1.294	1.991
44.00	1.346	1.982
45.00	1.402	1.982

Time (seconds)	V_C (volts)	I_{IN} (amperes)
46.00	1.458	1.985
47.00	1.499	1.991
48.00	1.553	1.985
49.00	1.602	1.984
50.00	1.648	1.982
51.00	1.704	1.978
52.00	1.748	1.978
53.00	1.795	1.983
54.00	1.854	1.981
55.00	1.897	1.976
56.00	1.941	1.977
57.00	1.998	1.973
58.00	2.054	1.982
59.00	2.104	1.972
60.00	2.158	1.970
61.00	2.205	1.966
62.00	2.252	1.978
63.00	2.302	1.971
64.00	2.354	1.978
65.00	2.399	1.981
66.00	2.447	1.973
67.00	2.492	1.974
68.00	2.546	1.970
69.00	2.597	1.967
70.00	2.645	1.978
71.00	2.691	1.970
72.00	2.742	1.965
73.00	2.790	1.969
74.00	2.830	1.974
75.00	2.883	1.965
76.00	2.939	1.967
77.00	2.984	1.962
78.00	3.030	1.966
79.00	3.081	1.975
80.00	3.131	1.969
81.00	3.185	1.976
82.00	3.228	1.970
83.00	3.270	1.970
84.00	3.321	1.964
85.00	3.371	1.966
86.00	3.418	1.974
87.00	3.468	1.963
88.00	3.517	1.958
89.00	3.558	1.964
90.00	3.611	1.966
91.00	3.658	1.966

Time (seconds)	V_C (volts)	I_{IN} (amperes)
92.00	3.702	1.967
93.00	3.749	1.957
94.00	3.807	1.961
95.00	3.854	1.964
96.00	3.891	1.962
97.00	3.942	1.966
98.00	3.993	1.966
99.00	4.034	1.964
100.00	4.078	1.968
101.00	4.126	1.971
102.00	4.171	1.970
103.00	4.227	1.973
104.00	4.266	1.960
105.00	4.318	1.960
106.00	4.366	1.966
107.00	4.408	1.965
108.00	4.454	1.952
109.00	4.503	1.959
110.00	4.548	1.901
111.00	4.593	1.757
112.00	4.627	1.622
113.00	4.663	1.504
114.00	4.695	1.383
115.00	4.718	1.289
116.00	4.750	1.185
117.00	4.771	1.100
118.00	4.793	1.014
119.00	4.810	0.946
120.00	4.825	0.879
121.00	4.844	0.809
122.00	4.862	0.742
123.00	4.882	0.700
124.00	4.890	0.649
125.00	4.905	0.610
126.00	4.915	0.570
127.00	4.921	0.526
128.00	4.928	0.490
129.00	4.945	0.456
130.00	4.952	0.430
131.00	4.958	0.401
132.00	4.967	0.366
133.00	4.974	0.346
134.00	4.980	0.325
135.00	4.988	0.306
136.00	4.987	0.285
137.00	4.998	0.270
138.00	4.999	0.257
139.00	4.999	0.246
140.00	5.001	0.222
141.00	5.010	0.212
142.00	5.018	0.195
143.00	5.014	0.190
144.00	5.022	0.179
145.00	5.015	0.166
146.00	5.018	0.155
147.00	5.026	0.145
148.00	5.035	0.146
149.00	5.030	0.132
150.00	5.038	0.129
151.00	5.031	0.117
152.00	5.037	0.116
153.00	5.044	0.108
154.00	5.043	0.102
155.00	5.038	0.104
156.00	5.050	0.095
157.00	5.038	0.086
158.00	5.045	0.088
159.00	5.046	0.080
160.00	5.046	0.079
161.00	5.052	0.072
162.00	5.054	0.076
163.00	5.050	0.070
164.00	5.047	0.067
165.00	5.054	0.062
166.00	5.054	0.059
167.00	5.051	0.059
168.00	5.046	0.058
169.00	5.054	0.054
170.00	5.053	0.052
171.00	5.054	0.049
172.00	5.058	0.057
173.00	5.049	0.049
174.00	5.055	0.040
175.00	5.050	0.051
176.00	5.055	0.043
177.00	5.058	0.042
178.00	5.053	0.048
179.00	5.049	0.034
180.00	5.059	0.038
181.00	5.066	0.038
182.00	5.062	0.034
183.00	5.056	0.035
184.00	5.057	0.037
185.00	5.055	0.030
186.00	5.066	0.035
187.00	5.061	0.037
188.00	5.056	0.037
189.00	5.054	0.031
190.00	5.067	0.029
191.00	5.060	0.023
192.00	5.058	0.025
193.00	5.053	0.024

Time (seconds)	V_C (volts)	I_{IN} (amperes)
194.00	5.066	0.034
195.00	5.067	0.026
196.00	5.065	0.029
197.00	5.067	0.026

Time (seconds)	V_C (volts)	I_{IN} (amperes)
198.00	5.062	0.020
199.00	5.069	0.022
199.98	5.075	0.026

4-b) Processed Data for the Discharge through Resistor Test

Time (seconds)	V_C (volts)	I_{IN} (amperes)
0.00	5.083	-0.029
1.00	5.072	-0.030
2.00	5.080	-0.030
3.00	5.068	-0.030
4.00	5.076	-0.031
5.00	5.076	-0.033
6.00	5.081	-0.028
7.00	5.078	-0.027
8.00	5.078	-0.022
9.00	5.070	-0.026
10.00	5.074	-0.032
11.00	5.077	-0.021
12.00	5.069	-0.028
13.00	5.080	-0.027
14.00	5.079	-0.025
15.00	5.076	-0.027
16.00	5.075	-0.027
17.00	5.079	-0.029
18.00	5.073	-0.020
19.00	5.073	-0.017
20.00	5.077	-0.011
21.00	4.962	3.292
22.00	4.874	3.307
23.00	4.782	3.245
24.00	4.694	3.182
25.00	4.602	3.128
26.00	4.515	3.072
27.00	4.428	3.019
28.00	4.336	2.964
29.00	4.273	2.912
30.00	4.191	2.868
31.00	4.117	2.816
32.00	4.041	2.765
33.00	3.973	2.718
34.00	3.904	2.668
35.00	3.842	2.626
36.00	3.769	2.585
37.00	3.709	2.537
38.00	3.643	2.502
39.00	3.587	2.467
40.00	3.528	2.421

Time (seconds)	V_C (volts)	I_{IN} (amperes)
41.00	3.468	2.390
42.00	3.406	2.342
43.00	3.352	2.298
44.00	3.299	2.267
45.00	3.246	2.229
46.00	3.200	2.194
47.00	3.141	2.156
48.00	3.085	2.130
49.00	3.037	2.095
50.00	2.986	2.050
51.00	2.946	2.021
52.00	2.887	1.981
53.00	2.850	1.946
54.00	2.806	1.918
55.00	2.753	1.888
56.00	2.711	1.863
57.00	2.666	1.832
58.00	2.627	1.790
59.00	2.592	1.770
60.00	2.540	1.742
61.00	2.507	1.706
62.00	2.463	1.682
63.00	2.422	1.654
64.00	2.382	1.624
65.00	2.350	1.598
66.00	2.307	1.574
67.00	2.263	1.550
68.00	2.245	1.526
69.00	2.207	1.498
70.00	2.178	1.476
71.00	2.135	1.447
72.00	2.105	1.428
73.00	2.081	1.407
74.00	2.036	1.387
75.00	1.999	1.360
76.00	1.966	1.335
77.00	1.942	1.316
78.00	1.914	1.292
79.00	1.874	1.276
80.00	1.847	1.245
81.00	1.822	1.236

Time (seconds)	V_C (volts)	I_{IN} (amperes)
82.00	1.787	1.213
83.00	1.758	1.190
84.00	1.742	1.170
85.00	1.713	1.154
86.00	1.686	1.138
87.00	1.662	1.121
88.00	1.642	1.106
89.00	1.621	1.081
90.00	1.586	1.058
91.00	1.570	1.050
92.00	1.538	1.030
93.00	1.517	1.014
94.00	1.494	1.002
95.00	1.473	0.987
96.00	1.454	0.966
97.00	1.429	0.939
98.00	1.405	0.927
99.00	1.374	0.919
100.00	1.356	0.902
101.00	1.334	0.890
102.00	1.323	0.870
103.00	1.291	0.853
104.00	1.271	0.842
105.00	1.260	0.826
106.00	1.242	0.811
107.00	1.218	0.802
108.00	1.200	0.793
109.00	1.181	0.782
110.00	1.167	0.767
111.00	1.148	0.759
112.00	1.129	0.743
113.00	1.110	0.730
114.00	1.096	0.721
115.00	1.080	0.709
116.00	1.065	0.690
117.00	1.054	0.681
118.00	1.038	0.675
119.00	1.022	0.660
120.00	0.999	0.652
121.00	0.989	0.641
122.00	0.970	0.635
123.00	0.959	0.626
124.00	0.952	0.614
125.00	0.936	0.612
126.00	0.919	0.598
127.00	0.914	0.592
128.00	0.891	0.583
129.00	0.872	0.563
130.00	0.867	0.567
131.00	0.854	0.546
132.00	0.836	0.546
133.00	0.826	0.540
134.00	0.818	0.533
135.00	0.802	0.520
136.00	0.793	0.505
137.00	0.782	0.502
138.00	0.780	0.497
139.00	0.762	0.494
140.00	0.744	0.478
141.00	0.738	0.477
142.00	0.722	0.460
143.00	0.714	0.466
144.00	0.706	0.462
145.00	0.698	0.446
146.00	0.689	0.450
147.00	0.674	0.438
148.00	0.670	0.423
149.00	0.654	0.410
150.00	0.650	0.406
151.00	0.637	0.410
152.00	0.627	0.404
153.00	0.618	0.391
154.00	0.610	0.389
155.00	0.597	0.379
156.00	0.596	0.375
157.00	0.586	0.370
158.00	0.573	0.366
159.00	0.573	0.366
160.00	0.565	0.347
161.00	0.562	0.351
162.00	0.550	0.338
163.00	0.538	0.336
164.00	0.534	0.336
165.00	0.527	0.325
166.00	0.519	0.316
167.00	0.514	0.314
168.00	0.512	0.300
169.00	0.498	0.301
170.00	0.490	0.294
171.00	0.486	0.294
172.00	0.478	0.295
173.00	0.470	0.289
174.00	0.461	0.287
175.00	0.458	0.273
176.00	0.452	0.280
177.00	0.442	0.273
178.00	0.439	0.270
179.00	0.434	0.260
180.00	0.433	0.259
181.00	0.424	0.253
182.00	0.421	0.257
183.00	0.416	0.248

Time (seconds)	V_C (volts)	I_{IN} (amperes)
184.00	0.406	0.247
185.00	0.410	0.244
186.00	0.399	0.242
187.00	0.394	0.236
188.00	0.387	0.224
189.00	0.379	0.219
190.00	0.376	0.230
191.00	0.367	0.222
192.00	0.367	0.214

Time (seconds)	V_C (volts)	I_{IN} (amperes)
193.00	0.358	0.217
194.00	0.354	0.204
195.00	0.357	0.201
196.00	0.346	0.211
197.00	0.346	0.202
198.00	0.328	0.201
199.00	0.333	0.184
199.98	0.326	0.189

4-c) Processed Data for the LDO Efficiency vs. Voltage test

Time (seconds)	Input Voltage (volts)	Input current (amperes)	Output Voltage (volts)	Output current (amperes)	Input Power (watts)	Output Power (watts)	Efficiency (%)
15.00	6.79	1.02	3.60	1.07	6.94	3.85	55.54
17.50	6.68	1.02	3.59	1.07	6.81	3.83	56.33
20.00	6.59	1.03	3.60	1.08	6.75	3.88	57.48
22.50	6.48	1.03	3.59	1.06	6.66	3.81	57.27
25.00	6.37	1.03	3.59	1.06	6.59	3.80	57.64
27.50	6.27	1.03	3.59	1.06	6.45	3.81	59.04
30.00	6.16	1.02	3.59	1.07	6.30	3.83	60.73
32.50	6.06	1.02	3.60	1.07	6.19	3.83	61.88
35.00	5.95	1.03	3.59	1.07	6.10	3.84	62.92
37.50	5.85	1.02	3.59	1.07	5.98	3.84	64.19
40.00	5.77	1.03	3.59	1.07	5.96	3.85	64.66
42.50	5.66	1.03	3.59	1.06	5.81	3.80	65.42
45.00	5.55	1.03	3.59	1.07	5.72	3.85	67.25
47.50	5.45	1.03	3.59	1.07	5.60	3.85	68.73
50.00	5.37	1.03	3.59	1.06	5.50	3.81	69.24
52.50	5.27	1.03	3.59	1.06	5.43	3.80	70.04
55.00	5.18	1.03	3.58	1.07	5.35	3.82	71.42
57.50	5.09	1.03	3.59	1.06	5.22	3.80	72.74
60.00	4.99	1.02	3.59	1.06	5.07	3.81	75.03
62.50	4.89	1.03	3.58	1.06	5.03	3.80	75.62
65.00	4.79	1.03	3.59	1.07	4.95	3.84	77.53
67.50	4.69	1.02	3.59	1.07	4.79	3.83	79.82
70.00	4.59	1.03	3.58	1.07	4.70	3.85	81.81

4-d) Processed Data for the SMPS Efficiency vs. Voltage test

Time (seconds)	Input Voltage (volts)	Input current (amperes)	Output Voltage (volts)	Output current (amperes)	Input Power (watts)	Output Power (watts)	Efficiency (%)
0.00	6.86	0.61	3.47	1.04	4.15	3.61	86.85
2.50	6.79	0.61	3.46	1.03	4.14	3.57	86.29
5.00	6.73	0.61	3.47	1.03	4.08	3.58	87.85
7.50	6.67	0.61	3.46	1.04	4.09	3.59	87.83
10.00	6.60	0.63	3.46	1.03	4.14	3.58	86.55
12.50	6.55	0.63	3.46	1.04	4.15	3.61	86.92
15.00	6.49	0.64	3.47	1.04	4.18	3.61	86.44
17.50	6.42	0.65	3.47	1.03	4.18	3.57	85.41
20.00	6.35	0.66	3.45	1.04	4.17	3.59	86.09
22.50	6.27	0.66	3.46	1.05	4.14	3.62	87.46
25.00	6.21	0.67	3.47	1.04	4.16	3.60	86.42
27.50	6.14	0.68	3.46	1.04	4.19	3.59	85.61
30.00	6.07	0.70	3.46	1.04	4.24	3.60	85.02
32.50	6.00	0.70	3.47	1.04	4.22	3.62	85.75
35.00	5.93	0.71	3.47	1.04	4.23	3.61	85.36
37.50	5.87	0.72	3.47	1.04	4.22	3.60	85.34
40.00	5.80	0.74	3.46	1.04	4.27	3.62	84.75
42.50	5.74	0.74	3.47	1.04	4.28	3.61	84.34
45.00	5.67	0.76	3.47	1.04	4.29	3.60	84.05
47.50	5.59	0.76	3.47	1.03	4.24	3.58	84.54
50.00	5.52	0.76	3.46	1.06	4.20	3.66	87.08
52.50	5.45	0.78	3.46	1.04	4.23	3.59	84.98
55.00	5.38	0.78	3.47	1.04	4.22	3.61	85.66
57.50	5.31	0.80	3.46	1.04	4.23	3.60	85.14
60.00	5.24	0.81	3.46	1.04	4.22	3.60	85.31
62.50	5.16	0.82	3.47	1.05	4.23	3.64	86.01
65.00	5.08	0.84	3.46	1.05	4.26	3.63	85.12
67.50	5.02	0.86	3.46	1.05	4.29	3.64	84.65
70.00	4.94	0.87	3.46	1.05	4.32	3.63	83.96
72.50	4.86	0.90	3.46	1.04	4.36	3.60	82.57
75.00	4.76	0.93	3.47	1.05	4.44	3.64	82.01
77.50	4.69	0.94	3.46	1.05	4.41	3.62	82.24
80.00	4.60	0.96	3.47	1.04	4.43	3.62	81.76
82.50	4.51	0.98	3.47	1.04	4.40	3.62	82.23
85.00	4.42	0.99	3.46	1.05	4.39	3.64	82.96

Appendix 5: Schematics of Data-logger Second Revision

5-a) Second Revision Power Supply Schematic

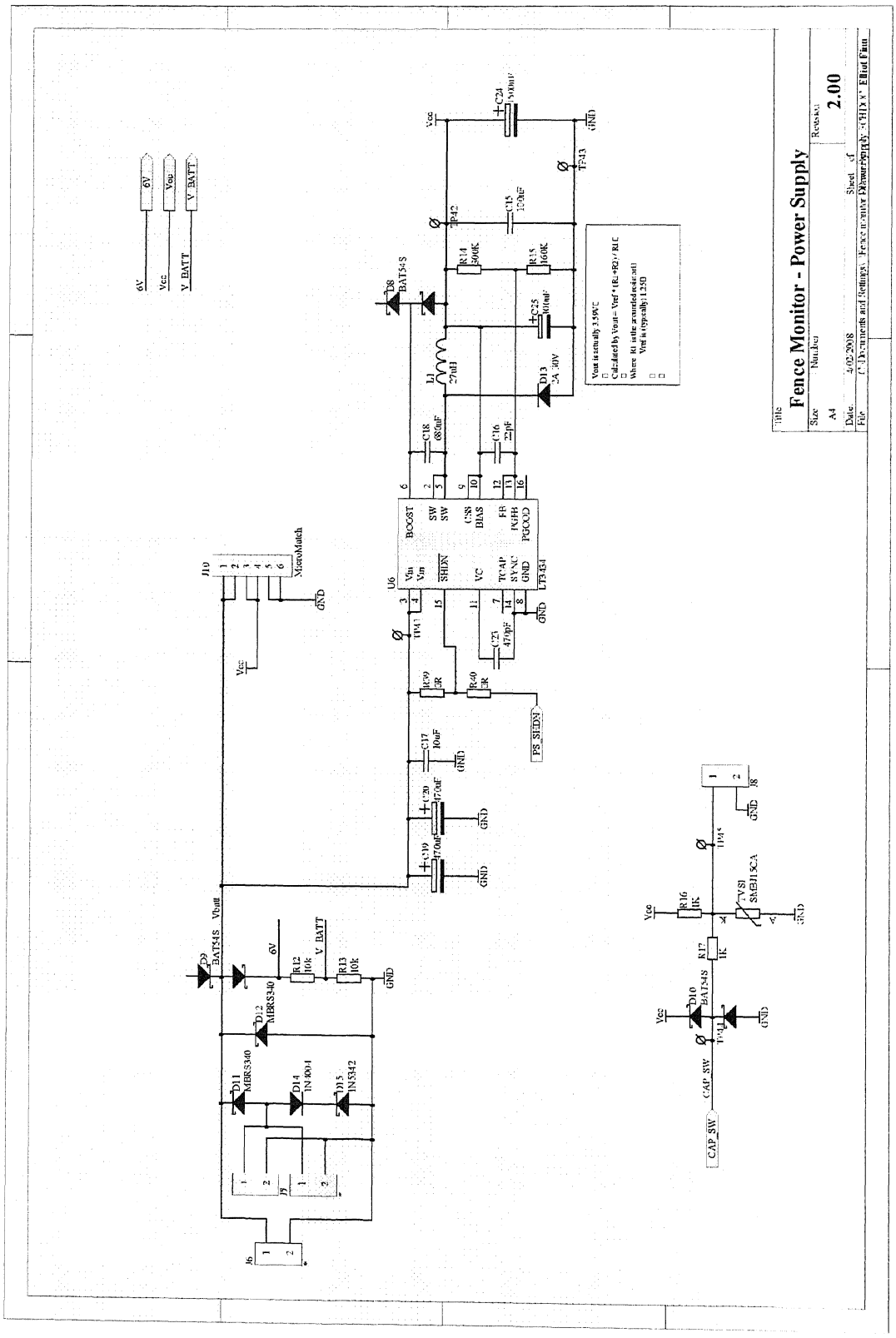

5-b) Second Revision Main Schematic

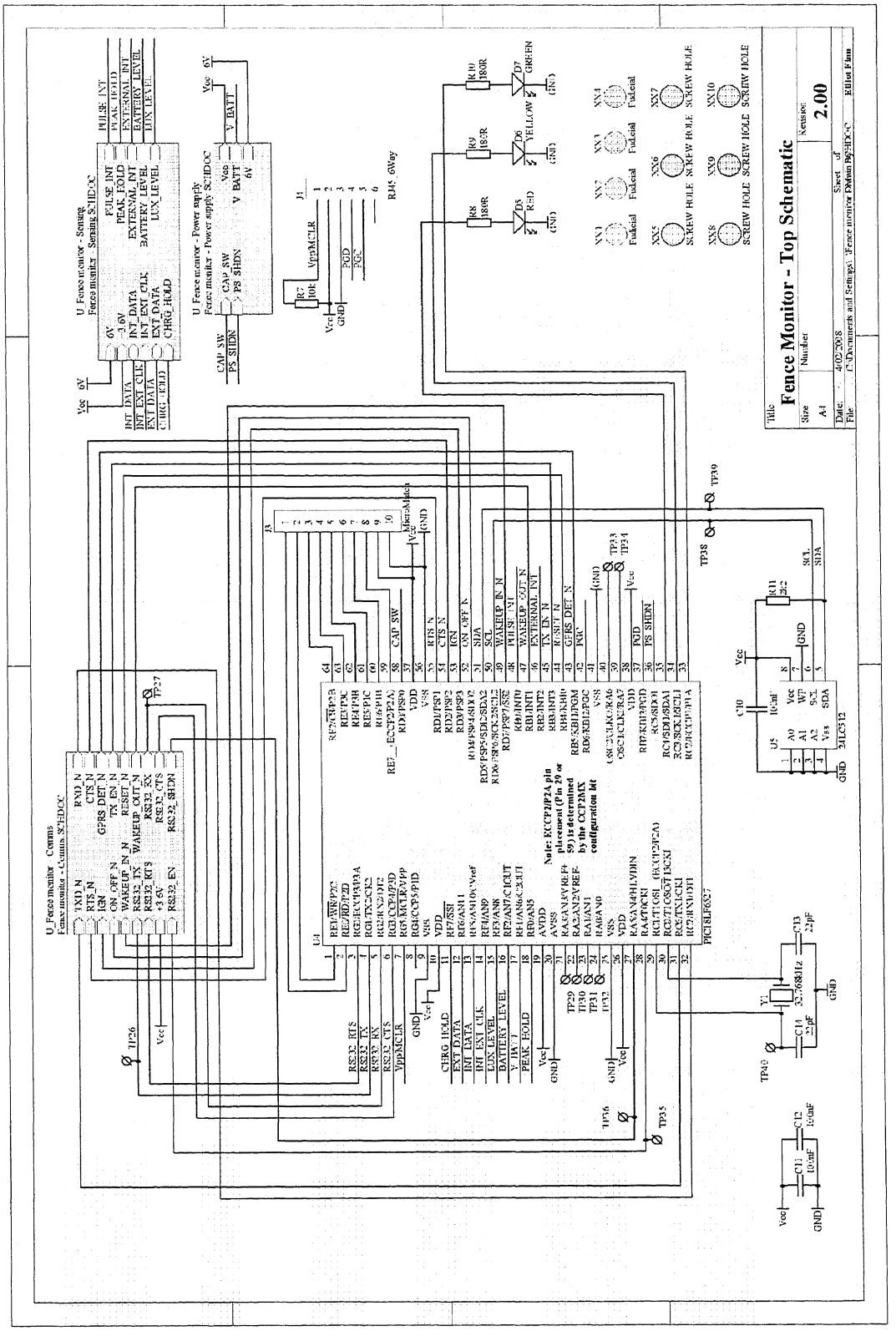

5-c) Second Revision Sensing Schematic

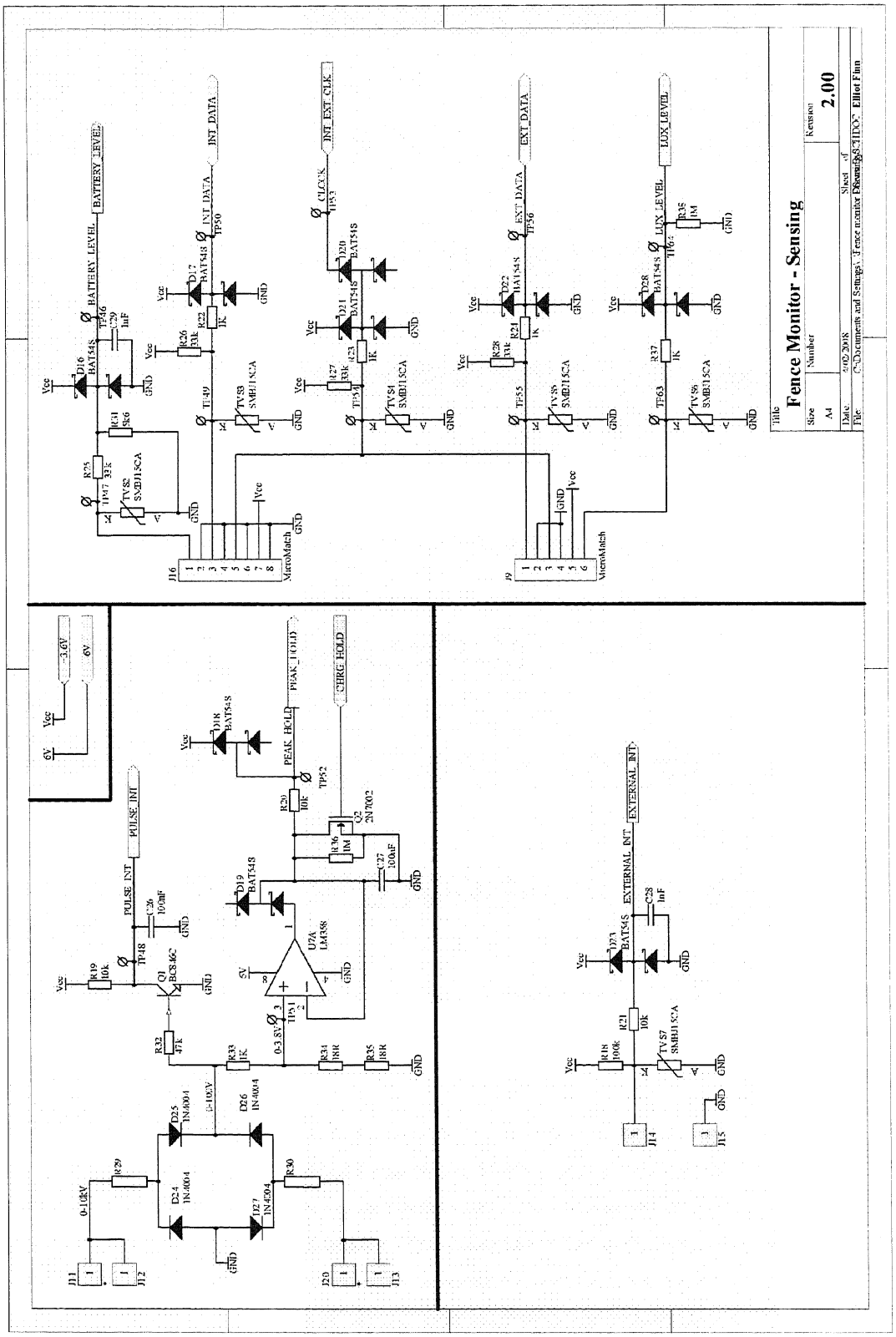

5-d) Second Revision Communications Schematic

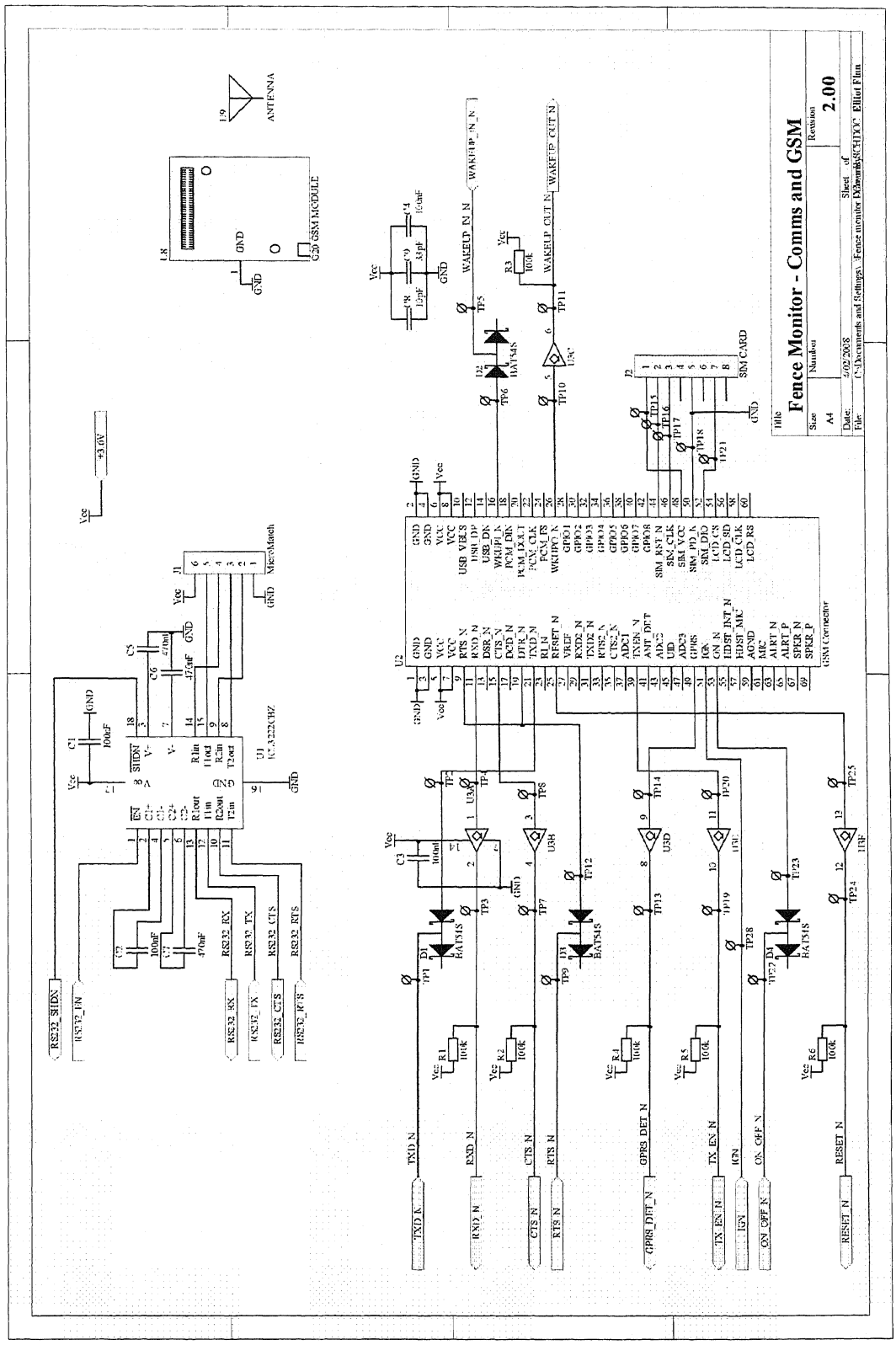

REFERENCES

Becker, H. I. (1957). Low Voltage Electrolytic Capacitor, General Electric Company. U.S. Patent 2,800,616.

Cap-XX Pty limited (2006). Active Voltage Balancing for Supercapacitors Application Note. Australia: Cap-XX Pty limited.

Cap-XX Pty limited (2007). HS206 SUPERCAPACITOR Datasheet Rev 1.0 Data Sheet. Australia: Cap-XX Pty limited.

Gallagher Animal Management Systems. (2007). "About Gallagher." Retrieved 24 Jan, 2008, from http://www.gallagher.co.nz/default.aspx?pageid=505.

Gallagher Group Ltd. (2007). "Gallagher Group :: Gallagher History." Retrieved 24 Jan, 2008, from http://www.gallaghergroup.co.nz/history.aspx.

Gallagher Ltd (2007). Power Fence Weighing & EID Systems Product Brochure. Hamilton: Gallagher Ltd.

Halber, D. (2006). "Researchers fired up over new battery." **2008**(28 Jan.).

Kularatna, N. (2008). Electronic Circuit Design: From Concept to Implementation. Boca Raton, FL, USA, CRC Press.

Linear Technology Corporation (1998). LTC1433/LTC1434 - 450mA, Low Noise Current Mode Step-Down DC/DC Converters Data Sheet. U.S.A.: Linear Technology Corporation.

Linear Technology Corporation (2006). LT3434 - High Voltage 3A, 200kHz Step-Down Switching Regulator with 100μA Quiescent Current Data Sheet. U.S.A.: Linear Technology Corporation.

MAXIM Integrated Products (2002). MAX1953/MAX1954/MAX1957 Low-Cost, High-Frequency, Current-Mode PWM Buck Controller Data Sheet. Sunnyvale: MAXIM Integrated Products.

Microchip Technology Inc (2004a). 24AA512/24LC512/24FC512 Data Sheet Data Sheet. Chandler: Microchip Technology Inc.

Microchip Technology Inc (2004b). PIC18F8722 Family Data Sheet Data Sheet. Chandler: Microchip Technology Inc.

Morrison, D. (2004, May 01). Distributed Power Architectures Evolve and Reconfigure. *Power Electronics Technology*, Retreived from Power Electronics Technology Back issues.

Motorola, Inc. (2005). G24 specsheet 01.eps Specification Sheet. U.S.A.: Motorola, Inc.

Motorola, I. (2006). Motorola G24 Developer's Guide - Module Hardware Description Data Sheet. U.S.A.: Motorola, I.

Nesscap Co. Ltd. (2005). "EDLC Products." Retreived 05 Feb., 2008, from http://www.nesscap.com/products_edlc.htm.

Nesscap Co. Ltd. (2005). "EDLC Products." Retrieved 05 Feb., 2008, from http://www.nesscap.com/products_edlc.htm.

Prophet, G. (2003, January 09). Supercaps for Supercaches. *EDN: Electronics Design, Strategy, News*, Retreived from EDN Archives.

Rush, B. (2000, September 01). Power-supply sequencing for low-voltage power supplies. *EDN: Electronics Design, Strategy, News*, Retreived from EDN Archives.

Schindall, J. (2007, November). The Charge of the Ultra - Capacitors, Nanotechnology takes energy storage beyond batteries. *IEEE Spectrum, 44*, Retreived from IEEE Spectrum Online.

Sensirion, Inc. (2007). SHT1x / SHT7x Humidity & Temperature Sensor Data Sheet. Westlake Village: Sensirion, Inc.

Vrana, G. (2001, June 21). Power down for portables. *EDN: Electronics Design, Strategy, News*, Retreived from EDN Archives.

Weir, R. D. and C. W. Nelson (2006). Electrical-energy-storage unit (EESU) utilising ceramic and integrated-circuit technologies for replacement of electrochemical batteries, Eestor, Inc. U.S. Patent 7,033,406.

Wikipedia, the free encylopedia. (2001, 31 Jan. 2008). "RS-232." Retrieved 01 Feb., 2008, from http://en.wikipedia.org/wiki/RS-232.